Molecular Mechanisms of Sprouting Angiogenesis in the Retina: Crosstalk between Notch and Norrin-Wnt Signaling.

Dissertation

zur

Erlangung der naturwissenschaftlichen Doktorwürde
(Dr. sc. nat.)

vorgelegt der

Mathematisch-naturwissenschaftlichen Fakultät
der
Universität Zürich

von

Jurian Zürcher

aus

Madiswil

Promotionskomitee

Prof. Dr. Wolfgang Berger (Vorsitz und Leitung der Dissertation)
Prof. Dr. Christian Grimm
Prof. Dr. Stephan Neuhauss

Zürich, 2012

Declaration

I declare that the present thesis was composed by myself and that the enclosed experimental work was conducted by myself as indicated in the respective chapters. This dissertation has not been submitted for any other degree or professional qualification except as specified.

Jurian Zürcher, Zurich 2012

Für Marlies & Theodor Zürcher

Abbreviations

αSMA	alpha smooth muscle actin
µl	microliter
A/V	arteriovenous
AAV	adeno associated viruses
ADAM17	ADAM metallopeptidase domain 17
Alk5, TGFBR1	transforming growth factor, beta receptor 1
Amot	angiomotin
Angpt2	*angiopoietin 2*
angiogenesis	vessels sprouting from preexisting vessels
Apj receptor	apelin receptor
BCE	bovine capillary endothelial cells
bHLH	basic helix loop helix
cDNA	complementary DNA
Col IV	collagen IV; a marker for blood vessels
Connexin 40	see GJA5
Cldn5	*claudin 5*
Connexin-37	see GJA4
COUP-TFII	see Nr2f2
csf-1	colony stimulating factor 1
DAPT	*N*-[(3,5-Difluorophenyl)acetyl]-L-alanyl-2-phenyl]glycine-1,1-dimethylethyl ester
Dkk1	*dickkopf1*
ddH_2O	double distilled water
Dll4	delta-like 4
DNA	deoxyribonucleic acid
dNTP	deoxy nucleotide-triphosphate
DRVP	deep retinal vascular plexus
E2F	E2F transcription factor
ECM	extracellular matrix
ECs	vascular endothelial cells
efficacy	the quality of being successful in producing an intended result; effectiveness
eGFP	enhanced green fluorescent protein
EphB4	EPH receptor B4
ER	endoplasmatic reticulum
EVR	exudative vitreoretinopathy
FEVR	familial exudative vitreoretinopathy
Fovea	A depression in the center of the macula of the retina where only cones are present and blood vessels are lacking.
Fz-4	frizzled 4 protein
FZD4	*frizzled 4 gene*
gDNA	genomic deoxyribonucleic acid

GFAP	glial fibrillary acidic protein
GFP	green fluorescent protein
GJA4	gap junction protein, alpha 4
GJA5	gap junction protein, alpha 5
GPR91/SUCNR1	succinate receptor 1
GSK3	glycogen synthase kinase 3
HEK293T cells	human embryonic kidney 293T cells
Hes1	hairy and enhancer of split 1
Hey1	hairy/enhancer-of-split related with YRPW motif 1
HMEC	human microvascular endothelial cells
HMEC-1	human microvascular endothelial cells
hs	Homo sapiens
HUVEC	human umbilical vascular endothelial cells
IB4	Isolectin B4; a marker for blood vessels
IBA1	induction of brown adipocytes 1
IHC	immunohistochemistry
IRVP	intermediate retinal vascular plexus
ISH	in situ hybridisation
Jag1	jagged 1
kb	kilobases
KO	*Ndph*$^{y/-}$ mice
LD_{50}	the amount of a toxic agent (as a poison, virus, or radiation) that is sufficient to kill 50 percent of a population of animals within a certain time
Lfng	lunatic fringe
LiCl	lithium chloride
LIF	leukemia inhibitory factor
LRP5	*low density lipoprotein receptor-related protein 5 gene*
LRP-5	low density lipoprotein receptor-related protein 5 protein
MAE	mouse aortic endothelial cells
MAOA	monoamine Oxidase A
MAOB	monoamine Oxidase B
MAPK	mitogen activated protein kinase
MB	megabases
$MgCl_2$	magnesium chloride
mm	Mus musculus
Monc-1	a immortalized neural crest stem cell line
morpholino	nonionic antisense oligonucleotide analogs with a stable morpholine moiety replacing the pentose ring
MT1-MMP	membrane anchored metalloproteinase MT1
N1ICD	notch1 intracellular domain
NaCl	sodium chloride
ND	Norrie disease
NDP	*Norrie Disease Pseudoglioma gene*
ng	nanogramm
NGF	nerve growth factor
Nr2e1	nuclear receptor subfamily 2, group E, member 1
Nr2f2	nuclear receptor subfamily 2, group F, member 2
Nrp1	neuropilin 1
Nrp2	neuropilin 2
OMIM	Online Mendelian Inheritance in Man; a database of human genes

	and genetic disorders
PCR	polymerase chain reaction
PDGFA	platelet derived growth factor A
PDGFB	platelet derived growth factor B
PDGFRα	platelet derived growth factor receptor alpha
PFA	paraformaldehyde
pTopflash	Wnt reporter luciferase construct
PU.1	spleen focus forming virus proviral integration oncogene spi1
QRT-PCR	quantitative real time polymerase chain reaction
RhoA	ras homolog gene family, member A
RMCs	retinal myeloid cells
RNA	ribonucleic acid
SDS	sodiumdodecylsulfate
sFlt-1	soluble VEGFR1
SMA	smooth muscle actin
Smad5	SMAD family member 5
SMCs	smooth muscle cells
SRF	serum response factor
SRVP	superficial retinal vascular plexus
sVEGFR1	soluble VEGFR1
synteny	conservation of gene order
Syx	syntaxin, mammalian RhoA ortholog
TGFβ	transforming growth factor β
TrkA	tyrosine receptor kinase A
TSPAN12	*tetraspanin 12 gene*
Tspan-12	tetraspanin12 protein
Unc5b	unc-5 homolog B
UPR	unfolded protein response
vasculogenesis	de novo formation of blood vessels
VEGF or VEGF-A	vascular endothelial growth factor
VEGF/VPF	vascular endothelial growth factor / vascular permeability factor
VEGF-A	vascular endothelial growth factor A
VEGFR1	VEGF receptor 1
VEGFR2	VEGF receptor 2
VEGFR3	VEGF receptor 3
WT	wildtype mice

Summary

Norrie disease is an X-linked recessive disorder that presents with congenital blindness, progressive deafness and rarely with mental retardation. It is caused by mutations in the *Norrie Disease Pseudoglioma* (*NDP*) gene, which may also lead to milder diseases like exudative vitreoretinopathy, retinopathy of prematurity or Coats' disease. In the eye, mutations in *NDP* lead to a delayed and incomplete development of the superficial retinal vascular plexus (SRVP) and they prevent the development of the two deep retinal vascular plexuses. This is accompanied with persisting hyaloid vessels around the vitreous. It has been shown that Norrin, the protein product of *NDP*, binds the co-receptor complex consisting of Fz-4, LRP-5 and Tspan-12 which leads to the downstream activation of canonical Wnt signaling.

Despite the phenotypic and molecular knowledge about Norrin, the intrinsic function of Norrin during retinal blood vessel development remains a mystery. This thesis aimed to gain more insight about the role of Norrin during retinal blood vessel development from *Ndph*$^{y/-}$ mice. This work suggests that Norrin-Wnt signaling and Notch signaling may not be directly linked. Further, endomucin was identified as a marker for central thorn-like aligned filopodia in *Ndph*$^{y/-}$ mice and extensive mural cell coverage of the SRVP from *Ndph*$^{y/-}$ retinas was found after P9. Arterial/vein crossing within the SRVP of *Ndph*$^{y/-}$ retinas was described for the first time. This indicates that MAPK signaling might be altered in *Ndph*$^{y/-}$ retinas since knockout mice with altered MAPK signaling also display vessel crossing. Norrin was further identified to be a mitogen for cells of the SRVP which is in concert with *in vitro* data from micro vascular endothelial cells. Finally, equal numbers of hyaloid vascular associated macrophages was found between P7 and P12 in *Ndph*$^{y/-}$ mice, suggesting that hyaloid vessels fail to regress despite the presence of a constant number of macrophages. In sum, it was shown that the loss of Norrin signaling might primarily affect MAPK signaling rather than Notch signaling.

Zusammenfassung

Die Norrie Krankheit, zu deren Hauptanzeichen kongenitale Blindheit, progressiver Höhrverlust und in einigen Fällen mentale Retardierung zählen, wird X chromosomal vererbt. Verursacht wird die Norrie Krankheit durch Mutationen im *Norrie Disease Pseudoglioma (NDP)* Gen. Einige Mutationen im *NDP* Gen können auch zu milderen Phänotypen wie etwa zu Exudativen Vitreoretinopathien, Frühgeborenen Retinopathie oder Morbus Coats führen. Alle bisher bekannten Mutationen im *NDP* Gen führen im Auge zur unvollständigen Entwicklung des oberflächigen retinalen Blutgefässnetzes und ein fehlendes Auswachsen der beiden tiefen retinalen Blutgefässnetzwerke. Weiter verhindern Mutationen im *NDP* Gen die Rückbildung der hyaloiden Blutgefässe des Vitreus. Bisher wurde gezeigt dass Norrin, das vom *NDP* Gen codierte Proteinprodukt, an einen Rezeptorkomplex bestehend aus Fz-4, LRP-5 und Tspan-12 bindet und schliesslich die kanonische Wnt-Signalkaskade aktiviert.

Obwohl man schon länger über ein molekulares und phänotypisches Basiswissen bezüglich Norrin verfügt, blieb die intrinsische Funktion dieses Proteins grösstenteils verborgen. Diese Doktorarbeit hatte zum Ziel, durch systematisches Studium von Norrin-Gendefekt-Mäusen, mehr Wissen über die Funktion von Norrin zu gewinnen. Die Auswertung der generierten Daten lassen folgende Aussagen zu: Die Norrin-Wnt- und Notch-Signalkaskaden sind nicht direkt gekoppelt. Endomucin ist ein molekularer Marker für zentrale dornartig angeordnete Filopodien des oberflächigen retinalen Blutgefässnetzwerks von Norrin-Gendefekt-Mäusen. Die oberflächigen retinalen Blutgefässe von Norrin-Gendefekt-Mäusen sind spätestens neun Tage nach der Geburt übermässig mit Mauerzellen bedeckt. Das Kreuzen von Arterien und Venen bei Norrin-Gendefekt-Mäusen weist auf reduzierte Aktivität der MAPK-Signalkaskade in retinalen Endothelzellen hin. Norrin ist ein Mitogen für Endothelzellen der oberflächlichen retinalen Blutgefässe von Mäusen. Schliesslich wurden konstante Anzahlen von Makrophagen, welche an die hyaloiden Gefässe des Vitreus angelagert sind, zwischen 7 und 12 Tagen nach der Geburt bei Norrin-Gendefekt-Mäusen gefunden. Dies zeigt, dass die fehlende Regression der hyaloiden Blutgefässe bei Norrin-Gendefekt-Mäusen nicht durch eine verminderte Anzahl and Makrophagen verursacht wird. Zusammenfassend wurde gezeigt, dass der Verlust von Norrin, nicht primär zu verändertem Notch Signaling führt, sondern eher verändertes MAPK Signaling verursacht.

Table of content

Abbreviations 4

Summary 7

Zusammenfassung 8

1. Introduction 11

1.1 The Eye 11

1.2 The retina 12

1.3 Norrie Disease and Norrin 13

1.4 The time course of retinal vascularisation in human and mouse 16

1.5 The development of the retinal vasculature 21

1.5.1 Retinal astrocytes form a scaffold for endothelial cells above the ganglion cell layer 21

1.5.2 Vascular growth in the retina 22

1.5.3 Guidance of sprouting angiogenesis and arterial/venous specification 24

1.5.4 Vascular remodeling and maturation 27

1.5.5 Deep retinal vascular plexus development 29

1.5.6 Regression of the hyaloid vasculature 29

1.6 The aim of the thesis 30

2. Material and Methods 32

2.1 Material 32

2.1.1 Cloning constructs for luciferase assays 32

2.1.2 TaqMan analysis of Notch target genes in HEK293T cells 35

2.1.3 Analysis of Notch activity in *Ndph*$^{y/-}$ mice 35

2.2 Methods 37

2.2.1 Cloning and organizing the constructs for luciferase reporter assays 37

2.2.2 Wnt- and Notch-pathway luciferase reporter assays 41

2.2.3 TaqMan analysis of Notch target genes in HEK293T cells 43

2.2.4 Analysis of Notch activity in *Ndph*$^{y/-}$ mice 44

2.2.5 Quantification of retinal parameters 48

3. Results 50

3.1 Norrin stimulates cell proliferation in the SRVP and is pivotal for the recruitment of mural cells 50

3.2 Establishing Calcium phosphate precipitation transfection method 70

3.3 Establishing Wnt reporter assay 70

3.3.1 Wnt reporter assay for transiently Norrin expressing HEK293T cells 70

3.3.2 Wnt reporter assay for stably Norrin expressing HEK293T cells 72
3.4 Analysis of Norrin-Wnt and Norrin-Notch signaling interactions in HEK293T cells 72
3.5 Analysis of Norrin-Notch signaling interaction in mouse retina 73
3.6 Influence of Norrin on TGFβ signaling, ER stress and Estrogen response 74
3.7 Quantification of Notch target genes after Norrin expression in HEK293T cells 74
3.8 Analysis of the retinal vascular phenotype in *Ndph*$^{y/-}$ mice 75
3.8.1 Establishing weight control table for *Ndph*$^{y/-}$ and wildtype littermates 75
3.8.2 Inhibition of Notch signaling partially rescues delayed outgrowth of the SRVP 76
3.8.3 The bulky front of the SRVP from *Ndph*$^{y/-}$ mice shows enhanced Dll4 expression 76
3.8.4 The number of hyaloid vessel-associated macrophages persists between P7 and P12 in *Ndph*$^{y/-}$ retinas 77
3.8.5 LiCl administration does not rescue deep vascular sprouting in *Ndph*$^{y/-}$ mice 78
4. Discussion 80
4.1 Establishing the luciferase assay 80
4.2 Establishing quality control for mice litters 81
4.3 Molecular mechanisms of sprouting angiogenesis in the retina: crosstalk between Notch and Norrin signaling 81
4.3.1 Norrin-Wnt signaling is unlikely to interact with Notch signaling in stalk cells 81
4.3.2 TaqMan analysis of Notch target genes in vitro 82
4.3.3 Extended pathway analysis of Norrin in vitro 83
4.3.4 The number of hyaloid vasculature associated macrophages persists between P7 and P12 in *Ndph*$^{y/-}$ retinas 85
4.3.5 Lithium chloride is toxic for mice pups 87
4.3.6 Outlook and future experiments 87
Acknowledgements 91
References 92
Web links 106
Appendix 1 107
Appendix 2 111
Appendix 3 112
Appendix 4 115
Appendix 5 116
Curriculum vitae 125

1. Introduction

The human eye is a powerful sensory organ that allows catching the moving scene at a glance. When healthy, we are most of the time unaware of the benefit of having functional eyes. Sometimes, e.g. when entering a tunnel by car or being dazzled by the sun, we lose the ability to see for a tick and realize the power of vision. Developmental defects, degenerative diseases or eye injuries can lead to permanent or temporal impaired vision or blindness. Norrie disease is one example of a familial developmental disease, caused by mutations in the *Norrie Disease Pseudoglioma* gene (*NDP*) (Berger et al., 1992). Its gene product, Norrin, binds to a receptor complex consisting of Frizzled4 (Fz-4), Low Density Lipoprotein Receptor-related Protein 5 (LRP-5) (Xu et al., 2004) and the auxiliary membrane protein Tetraspanin12 (Tspan-12) (Junge et al., 2009) and triggers canonical Wnt signaling. A few other eye diseases similar to Norrie disease do exist. These diseases are associated with mutations in *NDP*, *FZD4, LRP5 or TSPAN12* and feature retinal vascular defects. Aberrant signaling of another pathway, the Notch signaling pathway, also causes retinal vascular defects. This thesis aimed to investigate the interplay of Norrin and Notch signaling during blood vessel development in the mouse eye. The activity of both signaling cascades is likely to be altered in developing retinal blood vessels from Norrin deficient mice. Therefore the introduction starts to give a general overview about the eye and its most important structures (e.g. the retina) with later focus on the retinal vascular development and the Norrin-Wnt and Notch signaling cascades.

1.1 The eye

The eye, in the interplay with the brain, is the sensory organ that allows humans to perceive color, shape, and motion and to differentiate between light intensities that may vary about ten orders of magnitude. The structures of the eye develop from all three blastodermic layers. The anterior, non-neuronal, part of the eye develops from the mesoderm, which gives rise to the cornea, sclera and the uveal tunics (iris, ciliary body and choroid). The surface ectoderm gives rise to the lens. The posterior part of the eye descends from the neuroectoderm that gives rise to the diencephalon which in turn forms two optic buds that finally become the retina and its associated pigment cell layer (Figure 1).

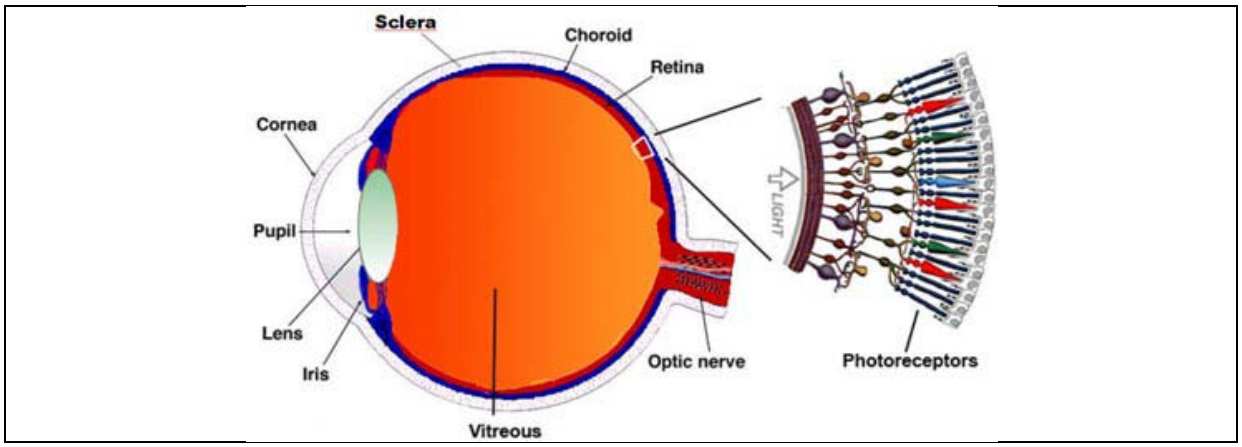

Figure 1: Schematic representation of a mid-sagittal section of the human eye and retina. Anterior structures include the cornea, pupil, lens, iris and the sclera. Posterior structures are the choroid, retina and the optic nerve (adapted from www.webvision.med.utah.edu/imageswv/Sagschem.jpeg).

Light enters trough the cornea, the transparent sector of the otherwise white appearing sclera. The sclera is made of a tough fibrous tissue that shapes the eye and confers stability to the eye globe. The light then passes the pupil, the opening of the iris. The iris is a usually blue, green or brown skin also containing a sphincter muscle that regulates the diameter of the pupil according to perceived light intensity. The light then passes the lens and vitreous before it impinges clearly focused on the retina, where phototransduction, the first step of photo perception, occurs.

1.2 The retina

The retina is located adjacent to the choroid, which is an extensively vascularized tissue that nourishes the retina (Figure 1). The retina itself is organized in three neuronal or nuclear (ONL, INL, GCL) and two synaptic or plexiform (OPL, IPL) layers (Figure 2). The outer nuclear layer (ONL) consists of photoreceptors, which are the light sensing cells. The human retina consists of two different types of photoreceptors: the rods and the cones. The rods absorb dim light and are the major cells involved in scotopic vision. The cones, which are more abundant at the center of the retina, are excited by bright light (photopic vision) and are, in contrast to rods, color sensitive. The photoreceptors project to synapses of bipolar cells (BC) at the outer plexiform layer (OPL). In addition to bipolar cells, the OPL consists also of horizontal and amacrine cell somas (HC, AC). Horizontal and amacrine cells modulate the transduced neuronal signal. The bipolar and amacrine cells project at the inner plexiform layer (IPL) to ganglion cells (GC). The somas of the ganglion cells are located at the ganglion cell layer (GCL). The axons of the ganglion cells leave the retina as the optic nerve and project to brain areas involved in visual processing.

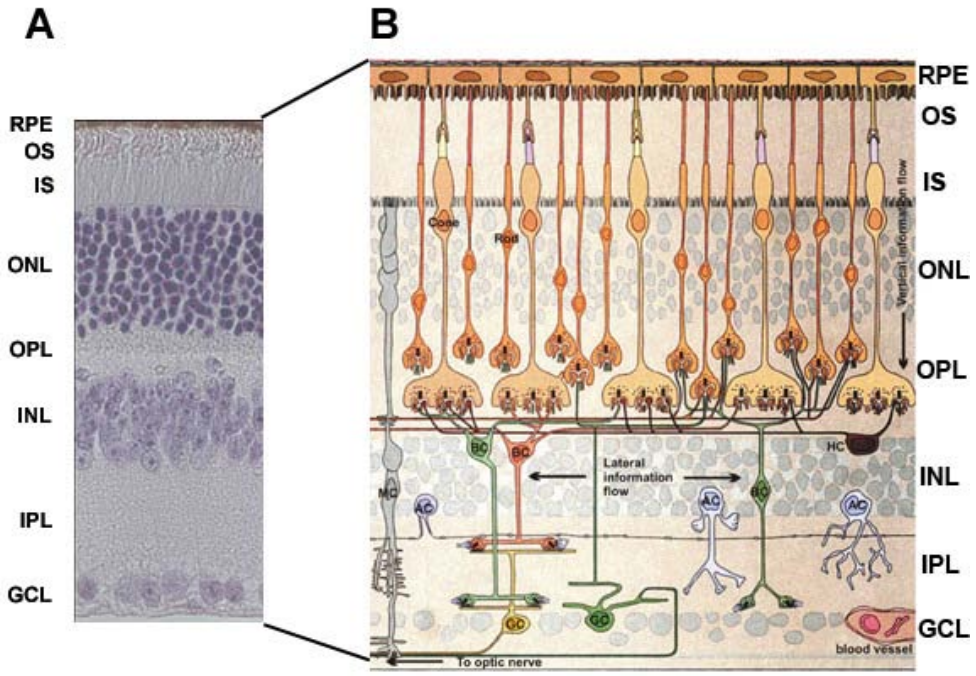

Figure 2: Light micrograph of a vertical section through the human retina (A) with schematic representation of the major retinal layers with their respective cell types (B). Five major layers are observed in retinal sections. The most apical layer is the retinal pigment epithelium (RPE). Adjacent to the RPE is the photoreceptor layer that consists anatomically of the outer segments (OS), inner segments (IS) and the outer nuclear layer (ONL). The synapses of the photoreceptors (rods and cones) connect to synapses of bipolar cells (BC) at the outer plexiform layer (OPL). The cell somas of the bipolar cells are located at the inner nuclear layer (INL). Additionally, the INL hosts the somas of the horizontal (HC) and amacrine cells (AC), which are involved in signal implementation. The bipolar and amacrine cells connect to the ganglion

cells (GC) in the inner plexiform layer. The somas of the ganglion cells are located at the ganglion cell layer (GCL) which represents the innermost layer of the retina. Mueller cells (MC) are glial cells spanning through the entire retina. Adapted from www.anatomy.unimelb.edu.au/researchlabs/rees/images/retina.jpg

The retina has the highest oxygen demand of all human tissues and hence depends on a well-developed blood supply (Yu et al., 2001). The developing retina is nourished by three vascular systems: the hyaloid, retinal and choroid vascular systems. This thesis focuses on the development of the retinal vascular system as well as hyaloid vascular regression, which are both severely altered in Norrin knockout (*Ndph*$^{y/-}$) mice. The following sections describe the characteristic clinical features of Norrie disease and the normal development of human and mouse retinal vasculature.

1.3 Norrie disease and Norrin

Norrie disease (ND, OMIM #310600) is a severe X-linked recessive form of congenital blindness. The locus underlying the disease was first mapped to Xp11.3 and later, by positional cloning, narrowed down to the *Norrie Disease Pseudoglioma* (*NDP*) gene that encodes for the Norrin protein (Berger et al., 1992; Chen et al., 1992; Chen et al., 1993; Sims et al., 1992). The severity of the phenotype caused by mutations in Norrin varies even within a family and includes essentially congenital blindness and progressive hearing loss and sometimes mental retardation. Norrie Disease patients with large gene deletions in Xp11.4 (including *NDP*) often develop additional clinical features, including hypogonadism, epilepsy, microcephaly, immunodeficiency and growth disturbancies (Berger1998).

Cardinal ocular signs of Norrie disease include leukokoria, pseudoglioma and phthysis bulbi (Chynn et al., 1996)(Bergen et al., 1994) (Figure 3). Leukokoria is a condition characterized by a reflective white mass within the eye that gives the appearance of white pupils (Figure 3A). Pseudoglioma is an inflammatory condition of the eye resembling a glioma of the retina and is marked by a circumscribed suppurative inflammation of the vitreous body (Figure 3B). Phthisis bulbi is the progressive atrophy and degeneration of the eye and occurs mainly in older patients (Figure 3C).

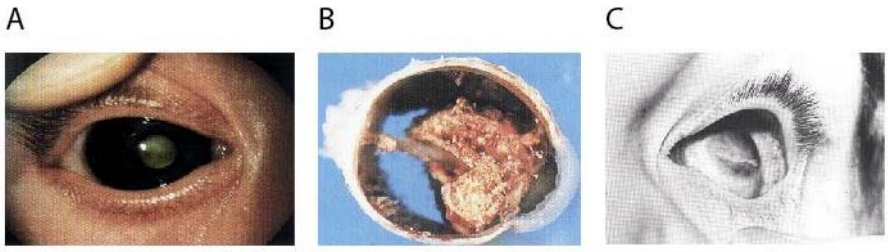

Figure 3: Clinical signs of Norrie Disease. A) Leukokoria B) Pseudoglioma of the enucleated eye from the patient depicted in A. C) Phthisis bulbi of a 77 year old patient (Chynn et al., 1996; Bergen et al., 1994)

The *NDP* gene comprises three exons (Figure 4). Only exons 2 and 3 are partially translated into Norrin. More than 110 distinct *NDP* point mutations have been identified in Norrie disease patients (appendix 1). In addition, several mutations in *NDP* have been identified in patients with familial exudative vitreoretinopathy (FEVR), Coats' disease (CD) and/or retinopathy of prematurity (ROP) (Berger and Ropers, 2001). These Norrin-related diseases are described in the Masterthesis from Jurian Zuercher, Walter Haenseler or Lea Sollfrank and in the PhD Thesis from Nikolaus Schaefer and in Berger et al., 2010 (Berger et al., 2010). A table that summarizes the most prominent features of these syndromes is available in appendix 2. The mouse homologue of *NDP*, *Ndph*, has been cloned and mapped. RNA i*n situ* hybridization studies of *Ndph* revealed transcription in the inner nuclear

layer and ganglion cell layer of the retina, Purkinje cells of the cerebellum and in the olfactory bulb of two-week-old mice (Berger et al., 1996). Ye et al. used a knock-in mouse, which carries the coding sequence of human placental alkaline phosphatase inserted at the *Ndph* locus (*Ndph*^{AP}) and found that *Ndph* is expressed in Müller glia in the retina and Bergman glia in the cerebellum and more widespread by astrocytes in the fore- and midbrain. In the cochlea of the inner ear, *Ndph*^{AP} expression was limited to the stria vascularis and a capillary plexus between the organ of Corti and the spiral ganglion (Ye et al., 2011). Due to the lack of functional Norrin antibodies, no Norrin localization studies based on immunohistochemistry have been published yet. Norrin also confines neuroprotective functions. Loss of retinal ganglion cells has been reported in Norrin-deficient mice (Ohlmann et al., 2005) and vitreal injection of recombinant Norrin protected optic nerve axons and perikarya of surviving retinal ganglion cells after N-methyl-D-aspartate (NMDA) injection in these mice (Seitz et al., 2010). This effect of Norrin could be abolished by additional injection of recombinant Dkk-1 protein, indicating that neuroprotection is mediated by canonical Wnt signaling. Norrin/NMDA treatment led to increased expression of LIF, FGF-2, BDNF, PSIP1 and CNTF in treated eyes. Norrin is also expressed in the luminal and glandular epithelia during the estrus cycle and in the antimesometrial decidual reaction zone at day 7 of gestation in albino rats. This suggests that Norrin regulates decidual and the placental angiogenesis of the luminal and glandular epithelial and decidual cells in rat (Kaloglu et al., 2011). Furthermore, *Ndph*$^{-/-}$ mice are infertile due to defects in vascularization and decidualization during pregnancy from E7 onwards, which results in embryonic loss (Luhmann et al., 2005b).

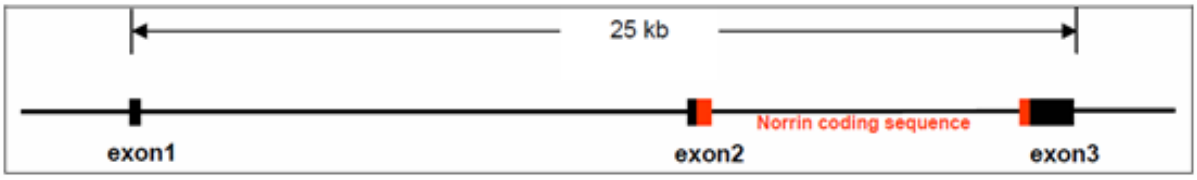

Figure 4: Schematic representation of the *NDP* locus on the short arm of the X chromosome. Transcription involves all three exons. Translation involves only partially exons 2 and 3 (red) which encode for the Norrin protein.

The human Norrin protein consists of 133 amino acids and shows high homology to other species including its cow and mouse orthologue (Figure 5A). The first 24 amino acids are predicted to be a signal peptide, suggesting that Norrin is a secreted protein (Figure 5A+B). Norrin is rich in cysteins and predicted to form a cystine-knot structure reminiscent of mucins, slit, von Willebrand factor and transforming growth factor beta (TGFβ) (Figure 5B+C) (Meindl et al., 1992; Meitinger et al., 1993). This structural relatedness to the TGFβ-family suggests that Norrin might have similar functions and that it is involved in differentiation and cell fate. Norrin is believed to form disulphide-bonded oligomers that are associated with the extracellular matrix (Perez-Vilar et al., 1997).

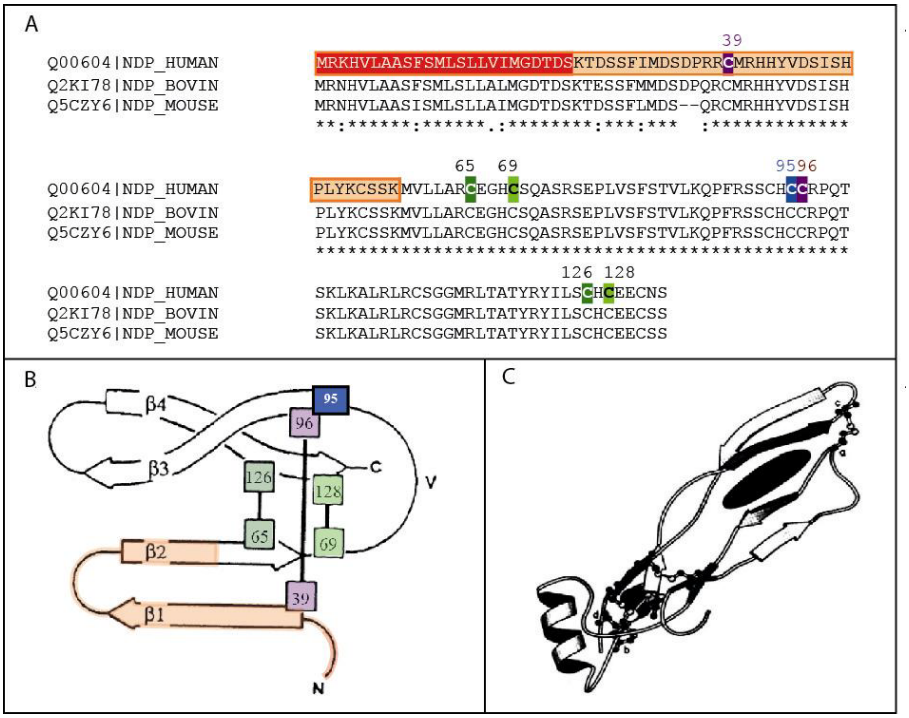

Figure 5: Bioinformatic analysis of the Norrin protein. A) Multiple alignment of human, cow and mouse amino acid sequences of Norrin showing strong conservation among species (CLUSTAL W v1.82). Different colors highlight specific domains: orange frame = amino acids encoded by exon 2; red = signal peptide; green = intramolecular disulfide bridge forming cysteins; magenta = intramolecular disulfide bridge forming cysteins; blue = cysteine putatively involved in dimerisation or oligomerisation B) Schematic drawing of the putative tertiary structure of Norrin representing a cystine-knot (adapted from Meitinger et al., 1993). Color setting is equal to the one used in A. C) 3D model of Norrin as a monomere. An α-helix is shown instead of the v-loop in B (from Meitinger et al., 1993).

Xu et al., 2004 have shown in cell culture assays that Norrin binds to Fz-4 (frizzled-4) and its co-receptor LRP-5 (Low-density lipoprotein receptor-related protein 5) and activates the canonical Wnt pathway (Xu et al., 2004). The same group has shown that Fz-4 is the only Norrin receptor among the existing ten mammalian frizzled receptors (Smallwood et al., 2007). Another protein, Tspan-12 (tetraspanin 12), has recently been reported to be an auxiliary membrane protein during Norrin-Wnt signaling (Junge et al., 2009) (Figure 6). Tspan-12 belongs to the family of tetraspanins which are thought to be organized in specialized microdomains that act as signaling platforms in the plasma membrane (Boucheix et al., 2001; Hemler2005). Junge et al. 2009, showed, using Wnt-reporter luciferase assays and deconvolution microscopic resolved co-stainings, that Tspan-12 significantly regulates Norrin/β-catenin but not Wnt/β-catenin signaling by modulating Fz-4 multimerisation (Figure 6). Interestingly, TSPAN12 expression is restricted to the vasculature in the retina, but Norrin, Fz-4 and LRP-5 show broader expression profiles within the retina (Figueroa et al., 2000; Hartzer et al., 1999; Junge et al., 2009; Wang et al., 2001; Xia et al., 2010). Soon after, mutations in *TSPAN12* were described in FEVR patients with autosomal dominant inheritance (Nikopoulos et al., 2010; Poulter et al., 2010).

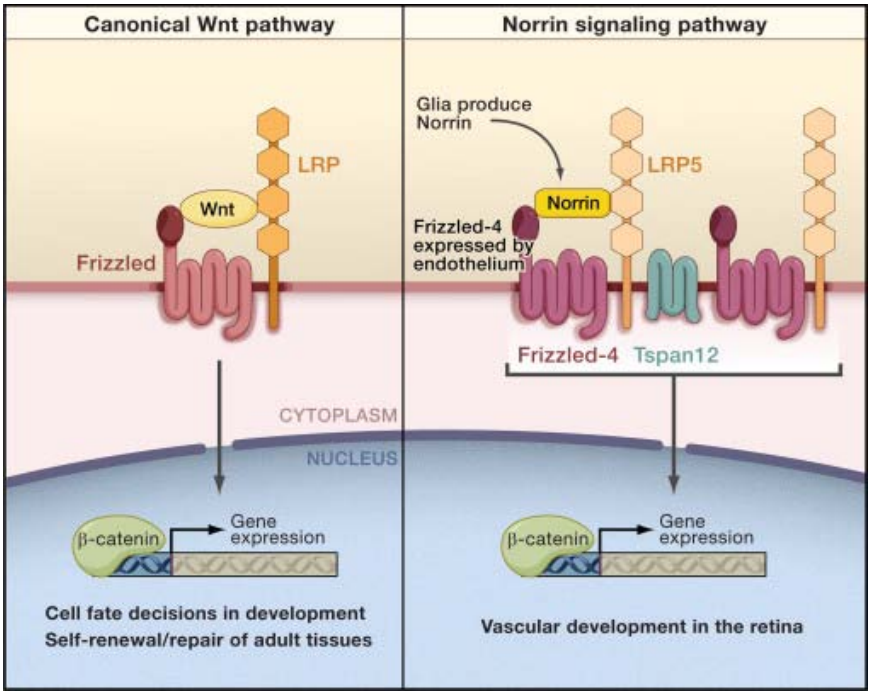

Figure 6: The auxiliary transmembrane protein Tspan12 mediates Norrin-Wnt-signaling. In canonical Wnt-signaling (left) about 20 Wnt ligands bind to any of the 10 frizzled receptors which are associated with LRP5 or LRP6. Binding of canonical Wnt-ligands (e.g. Wnt3A) leads to the accumulation of β-catenin in the nucleus and subsequently to the expression of Wnt target genes that regulate various processes in the embryo and in adult tissues. In the retina, the non-Wnt ligand Norrin binds Fz-4 and LRP-5 on endothelial cells. Tspan-12 facilitates clustering of multiple Fz-4/Lrp-5 complexes (right). This complex also initiates downstream β-catenin signaling, which is required for proper retinal vascularization during development. From Clevers 2009.

Lack of Norrin, Fzd-4, Lrp-5 or Tspan-12 prevents the formation of the deep and intermediate retinal vascular plexuses in mice (Berger et al., 1996; Junge et al., 2009; Richter et al., 1998; Xia et al., 2008; Xu et al., 2004). The time course of retinal vascular development in human and mouse is described in the following sections.

1.4 The time course of retinal vascularization in human and mouse

In humans, the retinal vascularization proceeds completely *in utero*. It starts at approximately 16 weeks of gestational age. During these early stages, vascular supply to the eye is mainly provided by the hyaloid vessels originating from the optic nerve, passing the primitive vitreous towards the anterior segment. The hyaloid vessels regress during retinal vascularization ensuring transparency of the vitreous (Mitchell et al., 1998). Hyaloid regression is usually completed before 34 weeks of gestation when retinal vascularization is already well advanced. The nasal retina is completely vascularized at 36 weeks of gestational age, whereas the temporal vessels reach periphery at ora serrata at approximately week 40. Human term infants are thus born with fully developed retinal vessels and a regressed hyaloid vasculature. In contrast to human, both, retinal vascularization and hyaloid regression occur postnatally in mice (Gyllensten et al., 1954a; Gyllensten et al., 1954b). The time course of retinal vascularization and hyaloid regression described here applies only to C57BL/6J mice, as we use them in our lab, and may slightly vary in other mouse strains. In total, three retinal vascular plexuses are formed in the mouse retina (Figure 7).

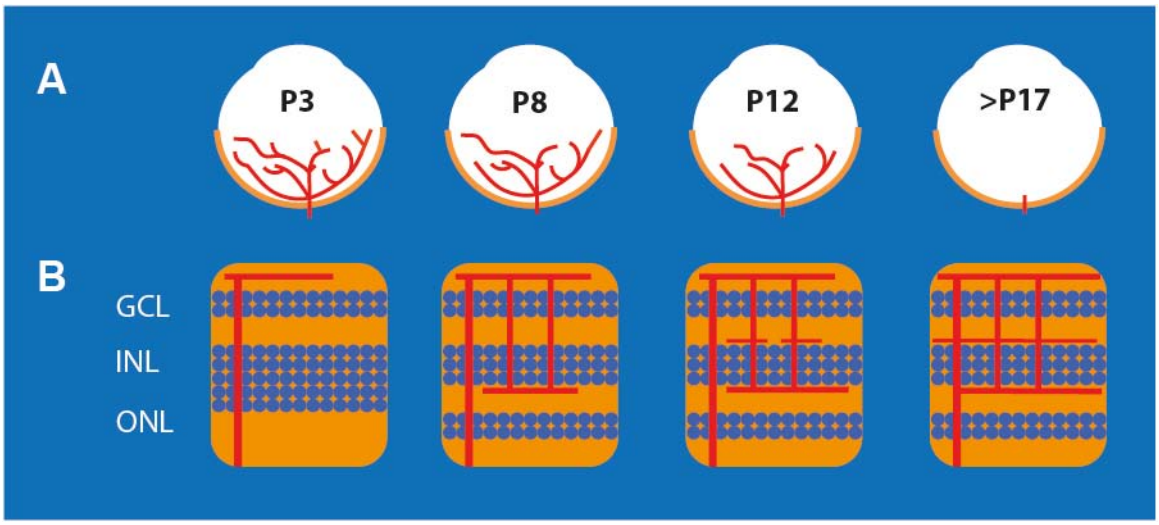

Figure 7: Schematic representation of vascular development in the early postnatal mouse eye A) Temporal cross-sections of the eye showing the hyaloid vessels in red, the retina in orange and the postnatal day (P) in black. B) Cross-section of the central retina showing the development of the superficial (lowest), intermediate (middle) and deep vascular plexuses (upper). ONL = outer nuclear layer; INL = inner nuclear layer; GCL = ganglion cell layer; P = postnatal day. Adapted from Xu et al., 2004.

The superficial vascular plexus, on top of the ganglion cell layer, develops during the first postnatal week by radial outgrowth of vessels, originating from the optic nerve head, reaching the periphery at P7-P8. The superficial capillaries start sprouting vertically from P7 onwards to form first the deep and later the intermediate vascular plexus. The deep plexus develops between P8 and P12 in the outer plexiform layer. The intermediate plexus, later located at the inner plexiform layer, forms between P12 and P15. All vascular plexuses remodel (Figure 8) during the whole development, starting at P3 and are considered mature by the end of the third postnatal week (P18-21) (Hofmann et al., 2007; Stahl et al., 2010).

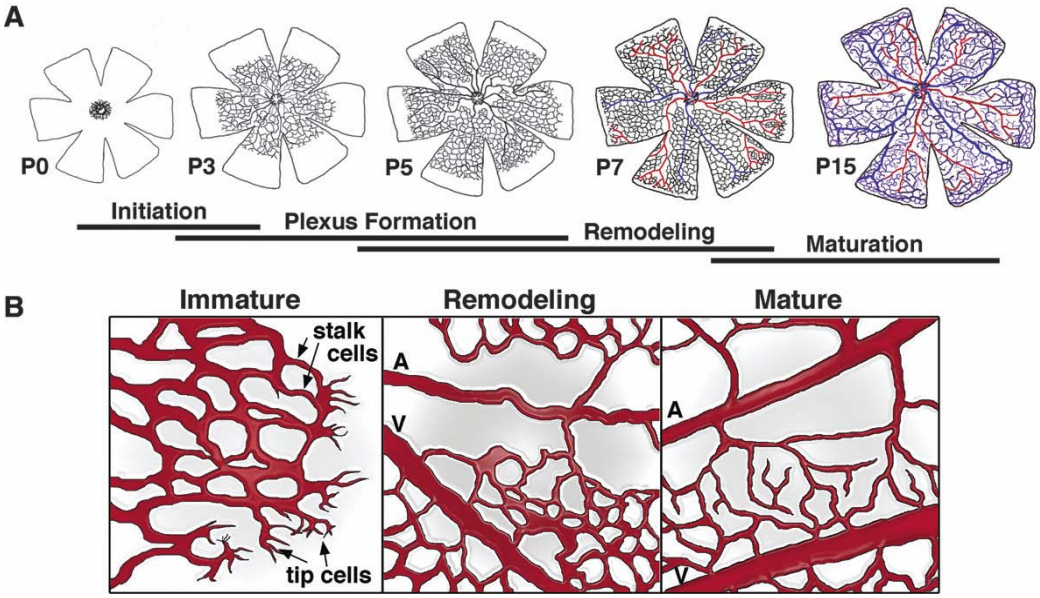

Figure 8: Retinal blood vessel morphogenesis in the mouse during the first 15 postnatal days (P) schematically represented as retinal whole-mounts. A) The development of the superficial retinal vascular plexus (SRVP) begins at P0 when sprouts grow from the optic nerve head towards the periphery. At P3, more mature vessels, next to the optic nerve head, begin to remodel into an alternating radial pattern of arteries and veins interconnected by capillaries. At P7, when the SRVP reaches the retinal front, deep

sprouts grow downwards and form the deep retinal vascular plexus (DRVP) (not shown). At P15, the SRVP and DRVP have matured and the intermediate retinal vascular plexus develops between the two established vascular layers (not shown). B) Guiding tip cells followed by dividing stalk cells ensure the proper development of the immature SRVP. Older vessels behind the leading edge of the SRVP remodel into arteries (A) and veins (V). Note the absence of capillaries at the peri-arterial space (after Hofmann et al., 2007).

Our *Ndph*$^{y/-}$ mice were generated by targeted replacement of the coding sequence of exon 2 by a reverse oriented neomycine cassette. This results in the deletion of the first 56 amino acids of Norrin, including the signal peptide (Berger et al., 1996) and therefore a loss of function of the protein. The ganglion cell layer of *Ndph*$^{y/-}$ retinas is disorganized. Electroretinography from *Ndph*$^{y/-}$ retinas showed a reduced b-wave, indicating a severe involvement of the inner retina, while the a-waves were indistinguishable at low intensities and only became conspicuous with brighter flashes (Ruether et al., 1997). Later it was shown that photoreceptors are degenerated in older *Ndph*$^{y/-}$ mice (Lenzner et al., 2002). More importantly, the development of the superficial retinal vascular plexus (SRVP) is delayed and incomplete and the deep and intermediate retinal vascular plexuses (DRVP, IRVP) do not develop in *Ndph*$^{y/-}$ mice (Figure 9). The hyaloid vessel regression is also delayed and incomplete in *Ndph*$^{y/-}$ retinas (Luhmann et al., 2005a). Our group suggested a biphasic disease progression in *Ndph*$^{y/-}$ mice: In the early phase, the lack of Norrin causes a sprouting angiogenesis defect of retinal endothelial cells which leads to the delayed outgrowth of the superficial vessels and prevents the formation of the deep capillary networks in the retina. In the later phase, the lack of the deep vascular plexuses leads to inner retinal hypoxia, which in turn leads to HIF1 mediated upregulation of VEGF-A. The high VEGF-A levels may also contribute to vessel leakiness (Luhmann et al., 2005a; Schafer et al., 2009). Hearing loss in *Ndph*$^{y/-}$ mice starts at 3-4 months with the loss of high frequencies and it progresses to a loss of all frequencies till 15 month of age. The hearing loss is caused by enlarged vessels of the stria vascularis that decrease progressively in their numbers finally resulting in the loss of outer hair cells and in the loss of spiral ganglion neurons (Rehm et al., 2002).

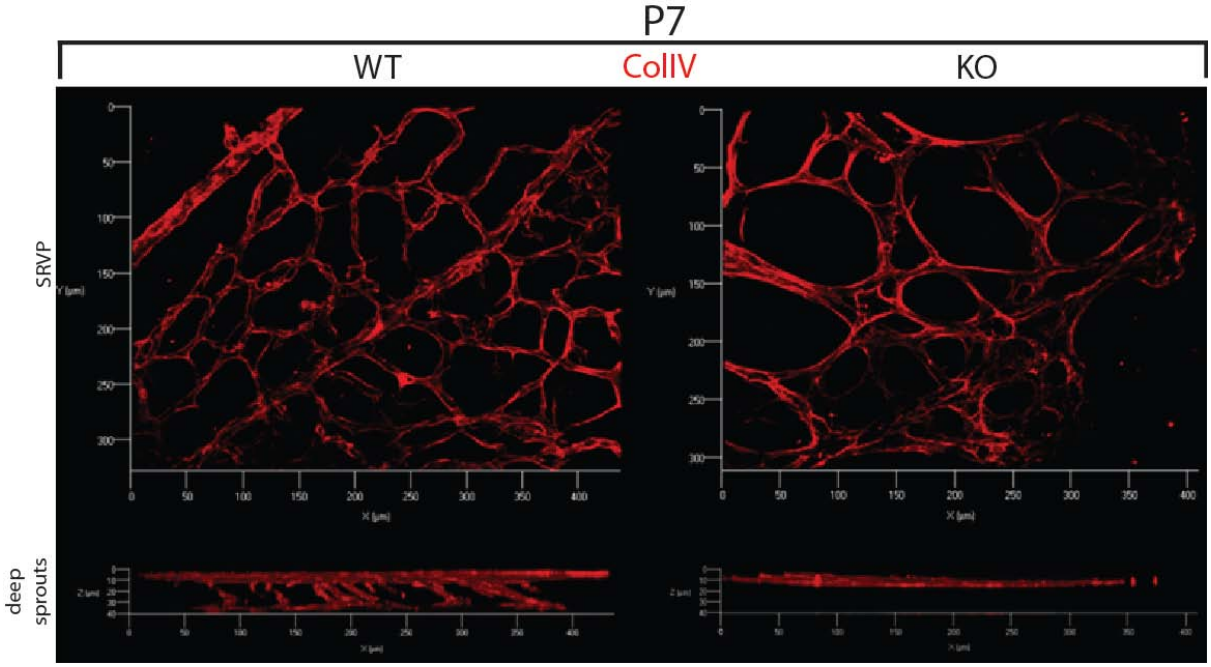

Figure 9: *Ndph*$^{y/-}$ mice do not develop the deep and intermediate retinal vascular plexuses (DRVP, IRVP). Sections of wildtype (WT, left) and *Ndph*$^{y/-}$ (KO, right) retinal whole-mounts from mice at postnatal day 7 (P7) are shown. Retinas were stained against collagen IV which labels the basement membrane that

underlies the retinal blood vessels (red). Top row: The basement membrane of the superficial retinal vascular plexus (SRVP) from wildtype retinas (left) appears denser and more organized compared to *Ndph*$^{y/-}$ mice (right). The diameter of the basement membrane sleeves seems to be enlarged in *Ndph*$^{y/-}$ retinas. Bottom row: z-stacks of the respective sections from above are shown. Deep sprouts grow downwards to form the DRVP at P7 in wildtype (left) but not in *Ndph*$^{y/-}$ retinas (right). Pictures were taken by Nikolaus Schaefer.

Similarly, knockout mice for *Fzd4*, *Lrp5*, *Tspan12* and *Angpt2* also fail to develop the DRVP and IRVP. An overview about the respective phenotypes of these knockout mice is given below (Table 1).

Table 1: Overview about knockout mice that lack the DRVP and IRVP

	Ndph$^{-/y}$	*FZD4*$^{-/-}$	*LRP5*$^{-/-}$	*TSPAN12*$^{-/-}$	*Angpt2*$^{-/-}$
Chromosome	Xp11.4	11q14-q21	11q13.4	7q31	8p33
OMIM	#310600	#133780	#601813	#613310	*601922
Locus name	EVR2	EVR1	EVR4	EVR5	-
Knockout	complete*	endothelial*	complete*	complete*	complete*
complete knockout embryonic lethal	no*/**	Yes	no	no	no*/**
Natural dead of mice	n.a.	n.a.	n.a.	n.a.	2 weeks**
Vascular plexuses present	superficial**/******	superficial*	superficial*	superficial*	superficial*
Expression	Müller cells*****		Müller cells within the INL at p42****		hyaloid vessels and outer boarder of INL plus smooth muscle cells of large arteries*/**
Microaneurisms extending from NFL	present**	n.a.	n.a.	present*	n.a.
MECA-32/Plvap staining	present***/*****	present**/***	present***	present*	n.a.
Slc38a5	downregulated at p7***		downregulated at p21 ****		n.a.
Delayed hyaloid vessel regression	present**	present*	present**	present*	present*
Focal hemorrhage	n.a.	present*	n.a.	present*	n.a.
Retinal glial cell activation	present**	n.a.	n.a.	present*	n.a.
Ischemia-induced retinal neovascularisation	yes*******	yes ***	n.a.	n.a.	no*
Vessel enlargement in the stria vascularis of the inner ear	present****	present*	n.a.	present*	n.a.
ERG	diminished oscillatory potentials and reduced b-wave; confirmed retinal hypoxia**	n.a.	b-wave amplitude reduced****	n.a.	n.a.
References	*Berger et al., 1996 **Luhmann et al., 2005 ***Schäfer et al., 2009 ****Rehm et al., 2002 *****Junge et al., 2009 ******Richter et al., 1998 *******Luhmann, manuscript in progress	*Xu et al., 2004 **Ye et al., 2009 ***Paes et al., 2011 (a)	*Xia et al., 2008 **Lobov et al., 2005 ***Junge et al., 2009 ****Xia et al., 2010	*Junge et al., 2009	* Hackett et al., 2002 **Gale et al., 2001

n.a. = not available; (a) no FZD4$^{-/-}$ mice were used in this publication, but mice were treated with anti-Fz-4 antibody;

It is clear that Norrin-mediated Wnt signaling is essential to initiate deep sprouting (Ye et al., 2010) according to the phenotypic data gained from knockout mice in Table 1. However, to date it is not clear how Angpt2 and Wnt signaling are connected in this regard. The following sections cover knowledge about molecular mechanisms in angiogenesis including sprouting angiogenesis and blood vessel maturation.

1.5 The development of the retinal vasculature

1.5.1 Retinal astrocytes form a scaffold for endothelial cells above the ganglion cell layer

The retinal vascularization is energy dependent. It has been shown that succinate, a Krebs cycle metabolite, activates expression of proangiogenic factors upon binding to its receptor GPR91/Sucnr1 in retinal ganglion cells (Sapieha et al., 2008). This seems to be an initial step that links tissue energy demand and initiation of angiogenesis. Development of the retinal vasculature is preceded by an invasion of astrocytes, migrating from the optic nerve head (Watanabe et al., 1988) in a radial fashion across the inner surface of the retina to form an astrocytic network above the retinal ganglion cells. The astrocyte migration and network formation occurs during the first postnatal days (Fruttiger et al., 1996; Ling et al., 1988). The presence of the astrocytic network seems to be essential for the development of retinal blood vessels, since the avascular retinas from the possum, avascular areas in horse, rabbit, primates and the avascular fovea in humans all lack the astrocytic network (Stone et al., 1987). But, in contrast, all vascularized areas in these retinas possess an astrocytic network. These observations suggest that the retinal astrocyte network and the retinal vasculature are developmentally linked. The retinal astrocytes differentiate from an astrocyte precursor lineage at the optic nerve by expression of the Pax2 transcription factor (Chu et al., 2001; Mi et al., 1999). The exact mechanism of differentiation is unknown, but, the earliest marker that distinguishes retinal astrocytes from all other populations of astrocytes is PDGFRα (platelet derived growth factor receptor alpha). PDGFRα is expressed by retinal astrocytes in the optic nerve, several days before they start to invade the retina. Plateled derived growth factor A (PDGFA) is secreted by retinal ganglion cells, that already cover the developing retina, and serves as a mitogen for retinal astrocytes (Fruttiger et al., 2000; Mudhar et al., 1993). Immature retinal astrocytes have a spindle shaped (elongated and bipolar) morphology during migration across the retina. They establish a mesh-like network as soon as they reach the retina, expressing low levels of GFAP (glial fibrillary acidic protein) and high levels of vimentin (Chu et al., 2001). Retinal astrocytes then experience hypoxia and start strongly to express VEGF-A (vascular endothelial growth factor A), which has been shown to be the key stimulus for retinal angiogenesis (Pierce et al., 1996; Stone et al., 1995; West et al., 2005). However, a more recent study questions this dogma by the finding that mice with retinal astrocytes that lack the expression of VEGF develop normal retinal vascular plexuses (Scott et al., 2010). As the vascular network expands, the vascular endothelial cell covered retinal astrocytes acquire a more mature state. The mature state of astrocytes is induced by endothelial cell derived LIF (leukemia inhibitory factor) which induces GFAP expression and downregulates vimentin and VEGF expression, leading to a stellate-like appearance (Chu et al., 2001; Kubota et al., 2009a; West et al., 2005). The maturation of astrocytes is suggested to create a negative-feedback loop that limits both, astrocyte and blood vessel numbers (West et al., 2005). The key component to regulate the number of astrocytes is the orphan receptor Nr2e1 (nuclear receptor subfamily 2, group E, member 1 or Tlx), which is strongly expressed by immature retinal astrocytes. Nr2e1 expression is downregulated in retinal astrocytes as they mature (Miyawaki et al., 2004). In Nr2E1 mutant mice,

retinal astrocytes fail to acquire the mature stellate morphology and remain highly elongated. They proliferate slowly, express high levels of GFAP and retinal vascularization is severely delayed (Miyawaki et al., 2004). It is not clear from the literature if the deep and intermediate vascular plexus develop in Nr2E1 mutant mice.

1.5.2 Vascular growth in the retina

To date, formation of the retinal vasculature in humans is believed to occur by vasculogenesis (de novo formation of vasculature) and angiogenesis (branching and growth of the vasculature from existing vessels) (McLeod et al., 2006). In mice, only angiogenesis seems to contribute to the formation of the retinal vasculature. Endothelial cells are the key proliferating cells during angiogenesis. They are among the least proliferating cell types, with about one per 10'000 cells entering the cell cycle in the adult stage (Hobson et al., 1984). This quiescence is rapidly inverted during angiogenesis by the virtue of acting growth factors. As previously described, retinal blood vessels of the superficial plexus grow from the optic nerve head (central) towards the periphery of the retina (peripheral). Vessels at the growing periphery of the retinal vasculature are less mature than the more central ones. Therefore different stages of vascular differentiation in a peripheral to central gradient are observed during the investigation of the superficial retinal plexus (Fruttiger2007). Endothelial cells of the leading edge from the growing retinal superficial vascular plexus represent a specialized subclass of vascular endothelial cells, designated tip cells. The tip cells extend numerous long filopodia (Kurz et al., 1996; Marin-Padilla et al., 1989; Ruhrberg et al., 2002), similar to axonal growth cones, and are responsible for the guidance of the growing blood vessels according to guidance cues (e.g. VEGF-A) from the environment (e.g. extracellular matrix, ECM) (Eichmann et al., 2005). Adjacent stalk cells divide ensuring proliferation of the endothelial cells (Figure 8). Delta/Jagged-Notch signaling (Figure 10) plays a crucial role in tip versus stalk cell fate (Figure 11). In general, the Delta/Jagged-Notch pathway enables cell-cell communication influencing proliferation, differentiation or apoptosis. Delta and Jagged are single pass transmembrane ligands for single pass transmembrane Notch receptors. Notch receptors are proteolytically cleaved upon binding of an activating ligand leading to the intracellular separation of the Notch intracellular domain (NICD) which migrates to the nucleus and activates the transcription of Notch target genes (Figure 10) (reviewed in Thurston et al., 2007).

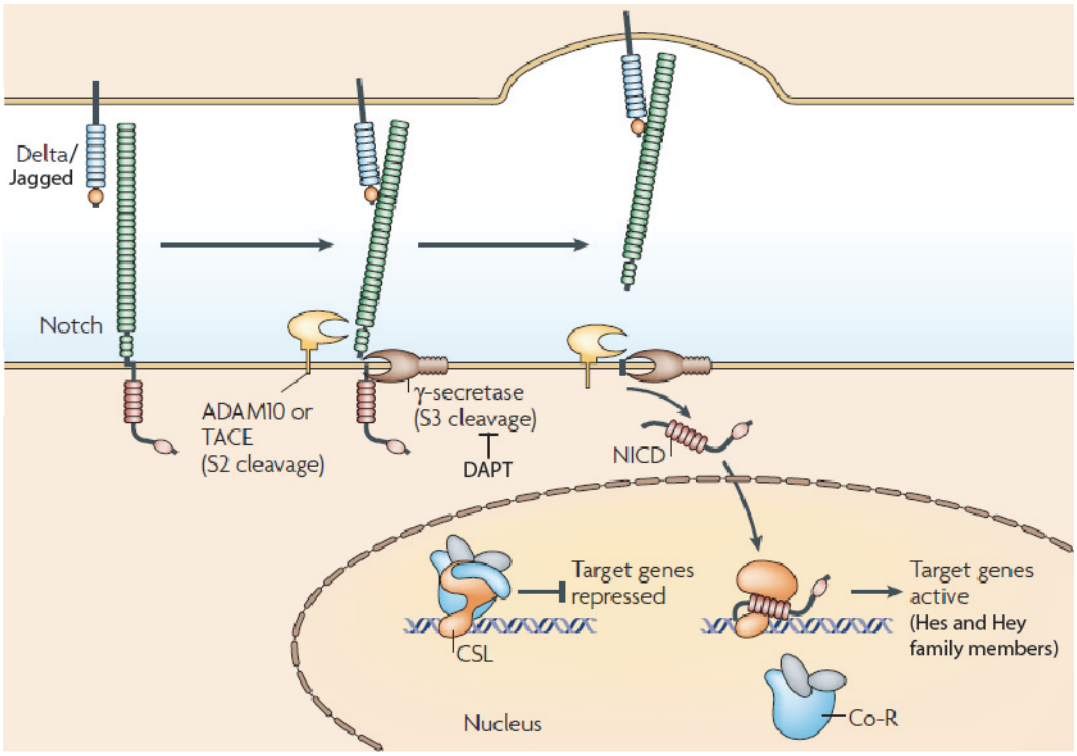

Figure 10: The mechanism of intracellular Delta/Jagged-Notch signaling. The Notch receptor undergoes a series of proteolytic cleavages (S2 and S3 cleavage) upon binding of Delta or Jagged ligands. S3 cleavage is mediated by the enzyme γ-secretase, which can be inhibited by DAPT. The S3 cleavage leads to the release of the Notch intracellular domain (NICD), which translocates to the cell nucleus. Once in the nucleus, the NICD interacts with CBF1, Su(H) and CSL family transcription factors helping to convert the co-repressor (Co-R) complex into an activator complex, inducing the expression of Notch target genes of the Hey and Hes families. Modified from Thurston et al., 2007.

The gene expression of tip cells is distinct from endothelial cells at other positions of the vascular plexus. Notch1-ligand Dll4 (delta like 4), PDGFB (platelet derived growth factor B), apelin, VEGFR2 (VEGF receptor 2), Nrp1 (neuropilin 1), Unc5b (unc-5 homolog B) and membrane anchored metalloproteinase MT1 (MT1-MMP) are upregulated in tip cells of the vascular plexus (Claxton et al., 2004; Gerhardt et al., 2003; Lu et al., 2004; Saint-Geniez et al., 2002; Yana et al., 2007). Jagged1, another Notch1-ligand and Lfng (lunatic fringe) are upregulated in stalk cells. In zebrafish tip cells, Dll4 is upregulated upon VEGF-A-VEGFR2 signaling which leads to a transient disassembly of the Tel/CtBP repressor complex (Roukens et al., 2010). Tip cell-derived Dll4 subsequently activates Notch1 signaling in adjacent stalk cells suppressing their ability to sprout. Accordingly, impaired Dll4-Notch1 signaling leads to excessive non-productive sprouting visible by an elevated number of tip cell filopodia (Hellstrom et al., 2007b; Lobov et al., 2007; Thurston et al., 2007). In contrast, Jag1 levels are high in stalk cells and antagonize the more potent Dll4. As a consequence, Jag1 is hardly able to activate Notch1 signaling in adjacent tip cells. This interaction regulates the number of tip versus stalk cells in the developing vascular plexus. Further, Notch1 is modified by the glucosaminyltransferase Lfng. This amplifies the Dll4-Notch1 signaling in stalk cells but reduces Notch1 activity upon binding of Jag1, rendering Jag1 to act as a Dll4 antagonist (Benedito et al., 2009) (Figure 11a). Notch-regulated ankyrin-repeat protein (Nrarp), a Notch target gene in stalk cells, destabilizes N1ICD and induces Lef-1 dependent Wnt signaling which helps stabilizing the stalk cell phenotype and prevents EC retraction (Phng et al., 2009). Furthermore, VEGF induces PlexinD1 expression on tip cells which interacts with retinal ganglion cell derived Sema3E. This Sema3E-

PlexinD1 signaling negatively regulates VEGF-induced Dll4 expression on tip cells and influences tip/stalk cell balance, Dll4 distribution and lowers vascular density (Figure 11b) (Kim et al., 2011).

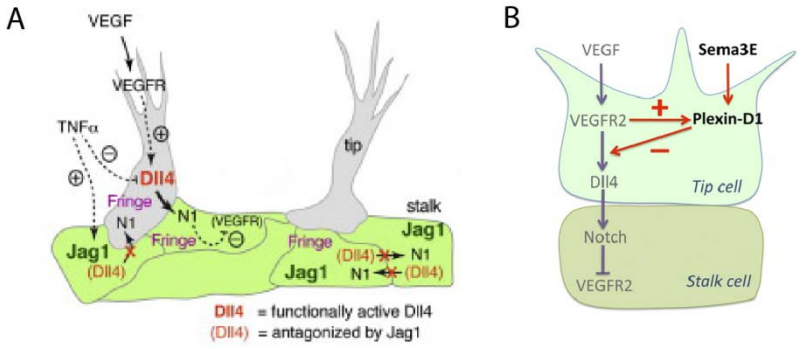

Figure 11: Balanced tip versus stalk cell selection during retinal vascular development in mice. (A) Notch1 (N1) signaling by Jagged1 (left) and alterations in the Jag1 and Lfng mutant vasculature (right). VEGF-A/VEGFR2 signaling in tip cells (grey) enhances (+) the expression of Dll4. Fringe modification of Notch1 in stalk ECs (green) enhances Notch signaling induced by Dll4-presenting tip cells, reducing VEGFR2 expression and maintaining the stalk cell phenotype. Dll4 is antagonized by Jagged1, which promotes angiogenesis and increases tip cell numbers by decreasing Notch activation levels in tip cells, while VEGF-A/VEGFR2 signaling is enhanced. Adapted from Benedito et al., 2009. (B) Sema3E–Plexin-D1 modulates Dll4–Notch signaling via a VEGF-induced negative feedback loop. VEGF induces Plexin-D1 expression leading to Plexin-D1 accumulation in tip cells. Sema3E–Plexin-D1 signaling then modulates VEGF-induced Dll4 expression in these tip cells and, subsequently, Notch activity in stalk cells. Notch activity controls the level of VEGFR2 in stalk cells. From Kim et al., 2011.

Thus, peripheral Dll4-Jag1-Notch1 signaling in tip and adjacent stalk cells tightly regulate the number of tip versus stalk cells. Once tip cells have formed, they guide the growing vascular plexus from the center to the periphery of the retina. It is important to note that tip and stalk cells are transient phenotypes and not stable cell fates (Jakobsson et al., 2009; Jakobsson et al., 2010). These cells undergo iterative cycles leading to transitions between tip and stalk cell phenotypes (Eilken et al., 2010; Phng et al., 2009; Potente et al., 2011).

1.5.3 Guidance of sprouting angiogenesis and arterial/venous specification

The distinct identity of endothelial stalk and tip cells allows different responses of these cells to their environment, facilitating vascular growth and guidance. Stalk cells mainly contribute to vascular growth by extensively proliferating, whereas proliferation is rare in tip cells (Gerhardt et al., 2003). In contrast, only tip cells form extensive bundles of filopodia in the direction of vascular growth. These filopodia depend on signaling via VEGFR2, that detects environmental gradients of VEGF-A, and mediates migration towards higher concentration of VEGF-A. VEGF mRNA expression is high in the non-vascularized, peripheral retina, and low in vascularized retinal regions. Despite a protein gradient has not yet been shown, there is evidence for its existence. Firstly, excessive injection of VEGFA protein floods the endogenous VEGF gradient and slows retinal vascular growth (van Eys et al., 2007) and secondly, three mutant mouse strains, that selectively express only one VEGF-A isoform (120, 164 or 188), which differ in their ability to bind the ECM, show different vascular growth behavior (Davis et al., 1996; Sato et al., 1995; van Eys et al., 2007). The splicing of VEGF-A isoforms has been nicely reviewed in Ladomery et al., 2007. In brief, mice possessing only the VEGF-A120 isoform, which does not bind to the ECM, have a flattened VEGF gradient and a slowed vascular growth in the retina. Mice possessing only the ECM associated VEGF-A188 isoform have a strict VEGF gradient leading to extensive retinal vascular branching (Figure 12).

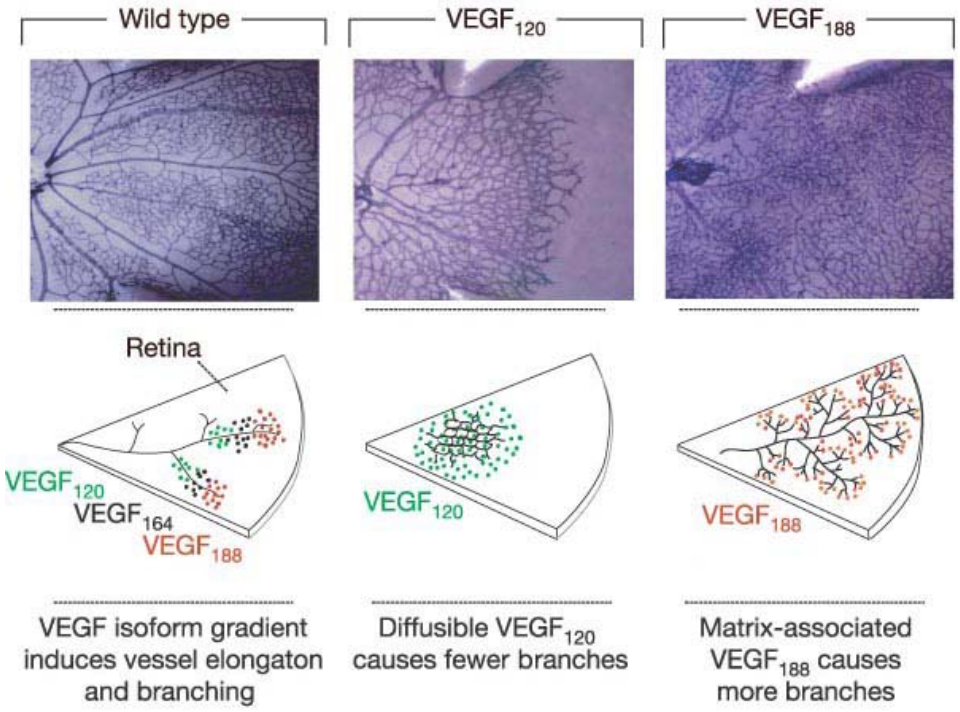

Figure 12: Blood vessel branching in the mouse retina is determined by a VEGF-A gradient. Top row: retinal whole-mounts from neonatal wildtype (left), VEGF-A120 (middle) and VEGF-A188 (right) expressing mice. Proper branching and elongation of blood vessels are determined by a spatial gradient of the different VEGF-A isoforms (middle panel). Matrix associated VEGF188 (red) localizes closer to VEGF-A producing astrocytes whereas soluble VEGF-A120 diffuses after secretion (green). VEGF-A164 (black) has intermediate properties. A proper VEGF-A gradient including all isoforms controls ramification from larger into smaller vessels. Vessels in VEGF-A120 (middle) mice are larger and less ramified than in wildtype littermates (left). Vessels in VEGF-A188 mice (right) are smaller and more extensively branched compared to wildtype littermates (left). From Carmeliet et al., 2005.

Today, the VEGF family of growth factors is the best characterized growth factor family regarding its effects on angiogenesis. This family is large, including VEGF-A to VEGF-E isoforms and PlGF (Almodovar et al., 2009). Alternative splicing of *VEGFA* can additionally generate several variants of the growth factor, including also the so-called b isoforms that differ in the last six C-terminal amino-acid residues and have anti-angiogenic properties (Ladomery et al., 2007). The anti-angiogenic VEGF-A165b isoform has been shown to be downregulated in diabetic retinopathy which facilitates neovascular proliferation (Magnussen et al., 2010). Interestingly, the authors could show that bevacizumab (Avastin, Roche), a monoclonal antibody against VEGF-A, did interact with VEGF-A165b, but pegaptanid (Macugen, Pfizer), another VEGF inhibitor, does not. This highlights the importance for better understanding of the role of the different members of the VEGF family of growth factors to improve the development of novel drugs. The important and central role of VEGF in vascular development is indisputable. Interestingly, miR-132 has recently been identified to act as an angiogenic switch. miR-132 has been shown to be upregulated by VEGF in HUVECs, initiating proliferation, tube formation and angiogenesis of HUVECs. Similarly, anti-miR-132 inhibited angiogenesis in wildtype but not in mice defective of p120Ras-GAP. Thus, miR-132 is believed to impede p120RasGAP, an inhibitor of cell cycle protein Ras, in ECs (Anand et al., 2010). VEGF-A165 has also been shown to prevent extrinsic apoptosis by Nrp1-dependent upregulation of PHACTR-1 which then prevents the expression of apoptosis death receptors DR4, DR5 and FAS. Furthermore, PHACTR-1 depletion decreases PP1 (protein phosphatase 1) activity and thereby disrupts fine-tuning of actin polymerization and impairs lamellipodia dynamics (Allain et al., 2012; Jarray et al., 2011).

However, the existence of VEGF alone cannot account for complex patterning of the retinal blood vessels and in the meanwhile, many proteins involved in the fine tuning of retinal blood vessel growth have been described. A group around Friedlander reported that injection of anti-R-cadherin into P2 mice perturbed the formation of the retinal superficial vascular plexus (Dorrell et al., 2002). It was suggested that R-cadherin would mediate the interaction between the astrocyte template and the growing blood vessels. But, R-cadherin deficient mice do not have retinal vascular defects (Fruttiger 2007).

EphB4 (Eph receptor B4) and ephrinB2, two other well known axon guidance molecules, are of importance during retinal vascular patterning. EphB4 is strongly expressed on veins and ephrinB2 on arteries. Therefore this ligand/receptor pair has been linked to the demarcation of venous versus arterial fate (Adams et al., 1999; Wang et al., 1998). In addition, the same molecules are important in endothelial cell proliferation and migration (Kertesz et al., 2006; Kim et al., 2002; Steinle et al., 2002; Steinle et al., 2003). Arteries express ephrinB2, Connexin-37, Connexin-40, Dll4, and Nrp1. In contrast, veins express EphB4, Nrp2, VEGFR3, COUP-TFII and the Apj receptor (Figure 13). However, it is not known how these arterial/venous (AV) markers interact and specify arterial and venous differentiation of endothelial cells in detail (Rocha et al., 2009).

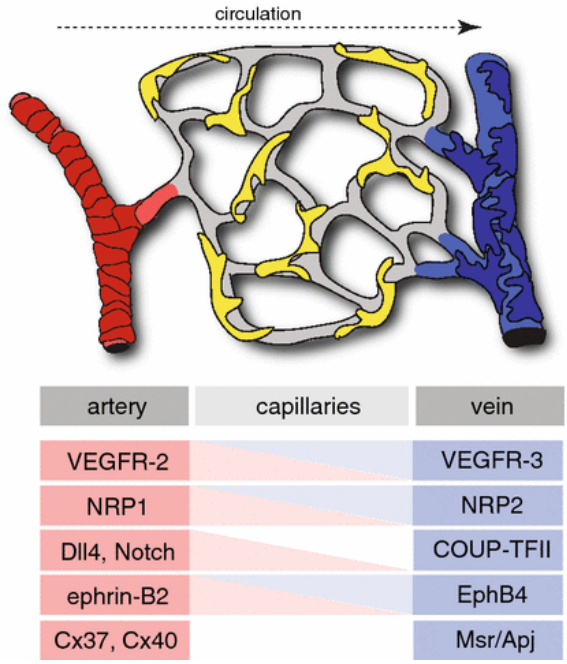

Figure 13: Artery- and vein-specific markers. Vascular smooth muscle cells on blood vessels (red/blue) as well as pericytes (yellow) covering capillaries (grey) are illustrated. Bottom row: Arterial (red) and venous (blue) specific markers are depicted. From Rocha et al., 2009.

It is believed that A/V specification arises already during primitive vascular plexus formation in the yolk sac (Wang et al., 1998). Hong et al, 2006 have shown that VEGF-A signaling inhibits arterial fate in cells committed to venous differentiation (Hong et al., 2006). The mode of action might be depending on VEGF receptor expression. VEGFR2 is expressed on arteries and veins, but VEGFR3 expression is restricted to veins. Also binding affinities of the respective VEGF isoforms differ. VEGF-A is able to bind VEGFR1 and VEGFR2, while VEGF-C and D have higher affinities for VEGFR3. VEGF-A mediates PKC-γ/ERK (=MAPK) signaling, while VEGF-D induces PI3K/Akt pathways. VEGF-C is able to induce both pathways (Jia et al., 2004). PKC-γ/ERK signaling induces arterial fate (Covassin et al.,

2006; Lawson et al., 2003; Takahashi et al., 2001) while PI3K/Akt signaling inhibits PKC-γ/MAPK activation in zebrafish and in vitro (Hong et al., 2006). Neuropilins (Nrp1, Nrp2) are modifiers of VEGF signaling. Nrp1 forms a receptor complex with VEGFR2, which only interacts with VEGF-A164. Endothelial specific deletion of VEGF-A164 co-receptor Nrp1 leads to loss of arterial markers such as connexin40 or ephrinB2. Thus, Nrp1 binding isoforms of VEGF preferentially induce arterial markers (Mukouyama et al., 2005). Further, deletion of the cytoplasmatic domain of Nrp1 leads to A/V crossing in the mouse retinas (Fantin et al., 2011). Deletion of Nrp2 impairs lymphangiogenesis but not vascular development. Apart from VEGF signaling, Notch signaling plays a pivotal role during arterial specification (Duarte et al., 2004; Gale et al., 2004; Krebs et al., 2000; Krebs et al., 2004; Lawson et al., 2001). Notch signaling acts downstream of VEGF signaling (Lawson et al., 2002) which induces expression of Dll4 and Notch1 (Liu et al., 2003; Lobov et al., 2007). COUP-TFII is a transcription factor exclusively expressed in veins and it is thought to be the initial regulator of venous endothelial identity (You et al., 2005). Little is known about the mode of action from COUP-TFII, but its negative effect on Dll4 and Nrp1 expression is believed to underlie the regulation of venous differentiation (Rocha et al., 2009). Norrie patients display venous insufficiency (Rehm et al., 2002). AV specification in the mouse retina is visible from P3 onwards (Figure 14). These processes, that start at P3 in the retina and finally end with mature blood vessels are termed vascular remodeling and maturation and summarized in the next chapter.

1.5.4 Vascular remodeling and maturation

As mentioned in the section *´Vascular growth in the retina´*, vessels at the periphery of the growing retinal vasculature are less mature than the more central ones. This implicates that the initially established primitive superficial vascular plexus is remodeled ending up as an organized vascular tree (Figure 14).

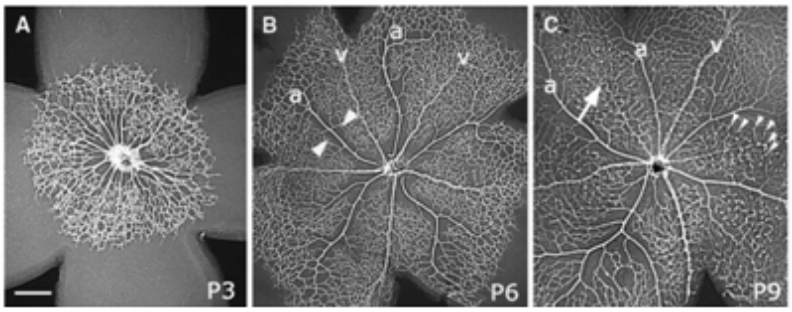

Figure 14: Remodeling of the superficial retinal vascular plexus in mice. A) A primitive but uniform vascular plexus has formed at P3. B) The growing vascular plexus already reached a higher hierarchy of organization where arteries (a) and veins (v) can be distinguished. C) The remodeled primary plexus has reached the periphery of the retina and vessels start to sprout in a perpendicular manner into the deeper neural layers of the retina to form the deep plexus (arrowheads). Some veins start to disappear from the plexus (arrow). Scale bar = 200 µm. From Fruttiger 2007.

Differences in vessel diameters and capillary free zones around arteries emerge, allowing distinguishing between arteries and veins. Some capillaries are strengthened, while others are pruned. The latter is evident in the vicinity of arteries and can occur via migration and re-localization of endothelial cells (Hughes et al., 2000) or by endothelial cell apoptosis (Ishida et al., 2003). Apoptosis of endothelial cells is mediated by CD2+/CD25+ leukocytes that adhere the capillaries through CD18 activating Fas ligand that induces endothelial cell death. Similarly, both, blockade of CD18 or Fas ligand with antibodies increases vascular density. In the opposite, depletion of

macrophages by intraocular injection of clodronate liposomes reduces vascular density (Checchin et al., 2006). This shows that immune cells can have diverse and sometimes opposite roles during vascular development. A possible mediator that causes capillary pruning could be VEGF-A120. It has been shown in vitro that the VEGF concentration in the medium directly influences the diameter of newly forming vascular sprouts (Nakatsu et al., 2003) and, more importantly, it has been shown that capillary pruning is defective in VEGF-A120 mice and that major retinal blood vessels are of larger diameter in these mice (Figure 12). TGFβ signaling is also involved in diameter control of blood vessels possibly by activating its downstream target SRF. SRF mediates also SMC recruitment to the dorsal aorta (Miano et al., 2004; Niu et al., 2005; Parlakian et al., 2004) and myocardin and Elk-1 compete for the same docking site in SRF, modulating SMC-specific gene expression (Franco et al., 2009). However, *Elk1/Sap1* double knockout mice do not display retinal vascular defects. But *Srf* or *Mrtf-a/b* (*Mkl-1/2*) double knockout mice show delayed and incomplete development of the SRVP and lack DRVP and IRVP development (Alfred Nordheim, personal communication). SRF and δEF1 promote the expression of α-SMA (Nishimura et al., 2006). The systemic deficiency of Norrin, which has a similar structure as TGFβ, has also been reported to lead to dilated retinal blood vessels in mice (Luhmann et al., 2005a) and hence is another candiadate to be involved in the regulation of vessel diameter. However, it is not clear if blood vessels are dilated in N*dph*$^{y/-}$ mice. It seems that blood vessels, stained with isolectinB4, have about the same diameter, but that the basal membranes around the vessels, stained with collagen IV, are enlarged (Figure 9, Schaefer et al., 2009). The state of maturation of the superficial retinal vascular plexus can be assessed by the Oxygen-Induced Retinopathy Model (OIR model) (Connor et al., 2009; Stahl et al., 2010). There, P7 mice litters are exposed to 80% of oxygen for five days. Subsequently, litters are euthanized at P12. The exposure of mice to the elevated oxygen levels leads to vasobliteration during the exposure period peaking at P12. The obliteration primarily affects central retinal capillaries around arteries. It was suggested that direct oxidative damage to endothelial cells by reactive oxygen species (Gu et al., 2003) and/or oxygen mediated downregulation of VEGF-A account for this effect (Pierce et al., 1996). Capillaries in the vicinity of arteries are mostly affected, because areas around arteries contain the highest oxygen concentrations (Riva et al., 1986) and the lowest VEGF-A level (Claxton et al., 2003). The effects caused by hyperoxia may be exaggerative, but similar to the processes that lead to the formation of capillary free zones adjacent to arteries during normal development. Vessel coverage by pericytes and vascular smooth muscle cells provides resistance to hyperoxia (Chan-Ling et al., 2004). The cell-cell signaling between mural and endothelial cells is reciprocal. Endothelial cells recruit mural cells by secreting PDGFB, which acts via PDGFRβ on mural cells (Hellstrom et al., 1999). Mural cells in turn express angiopoietin1 (Ang1) that acts on Tie2 receptor on endothelial cells (Nishishita et al., 2004; Satchell et al., 2001; Suri et al., 1996). Injection of soluble PDGFB causes mural cell detachment and potentiates hyperoxia-mediated vaso-obliteration (Benjamin et al., 1998). Likewise, injection of an anti-PDGFRβ antibody impedes vascular remodeling by inhibiting mural cell recruitment (Uemura et al., 2002). TGFβ signaling is also involved in the recruitment of smooth muscle cells. Smad5 knockout mouse embryos display enlarged blood vessels ensheathed by decreased numbers of smooth muscle cells, suggesting that the Alk1-Smad1/5 pathway is essential during this process (Bertolino et al., 2005). Two other remodeling or maturation steps that can be observed in the retina are the formation of the blood-brain (BBB) and of the blood-retina barrier (BRB). The formation of the BBB is better understood than the formation of the BRB. However, it is known that normally developed retinal blood vessels at P10 are impermeable to FITC-dextran. In contrast, vessels of *Ndph*$^{y/-}$ mice are permeable for indocyanine green dye at P14 and at P21

(Luhmann et al., 2005a) which could be an indication for remodeling defects. Another explanation for the permeability of *Ndph*$^{y/-}$ blood vessels could be the upregulation of Meca-32/Plvap which may lead to fenestration of the blood vessels (Schafer et al., 2009). It is likely that both is true. Furthermore, our group has shown that claudin-5 mRNA is downregulated in *Ndph*$^{y/-}$ retinas at P7. Claudin-5 as well as two other tight junction proteins, occludin and zonula occludens-1 (ZO-1) are expressed by adult retinal blood vessels. Elevated occludin expression levels are linked to tightness of endothelial monolayers in cell culture (Kevil et al., 1998; Wong et al., 1997) and protein extravasation into the retina correlates with reduced membrane occludin levels in the retinal vasculature of diabetic rats (Antonetti et al., 1998; Barber et al., 2000; Barber et al., 2003). Regarding the SRVP, this could be mediated by astrocytes that regulate vascular permeability there (Barber et al., 2000; Gardner et al., 1997). It has been established recently that Slit2-Robo4 signaling counteracts VEGF induced vascular permeability (London et al., 2009). Regarding the deeper plexuses, Müller cells are good candidates to induce barrier properties (Tout et al., 1993), possibly via secretion of Norrin (Ye et al., 2009) which might promote the maintenance of the BRB via Fz-4 (Paes et al., 2011).

1.5.5 Deep retinal vascular plexus development

The deep vascular plexus of the retina develops by sprouting from the superficial plexus starting at P7 in mice (Figure 14C) (Stahl et al., 2010). The sprouts emerge exclusively from veins, venules and capillaries in the vicinity of veins (Figure 14C). This sprouting starts at the center of the retina and expands towards the periphery. It is preceded by transient VEGF-A mRNA expression in the inner nuclear layer (Stone et al., 1995). The vascular sprouts grow along Müller cell processes into the retina. They turn sideways when they reach the inner and outer boarder of the inner nuclear layer, leading to the formation of the DRVP and IRVP (Figure 7). Müller cells are also suspected to express Norrin in the retina (Ye et al., 2009). This could explain the lack of both deeper vascular plexuses in *Ndph*$^{y/-}$ mice. It has been shown that overexpression of Norrin in the vitreous rescues the *Ndph*$^{y/-}$ phenotype (Ohlmann et al., 2005). This suggests that Norrin acts as a general switch to activate DRVP formation rather that it acts as a morphogen during DRVP formation (Ye et al., 2010). As mentioned earlier, Fz-4, LRP-5, Tspan-12, Angpt2, SRF and Mrtf-a/b are essential for deep plexus formation (Caprara et al., 2011; Gale et al., 2002; Hackett et al., 2002; Junge et al., 2009; Luhmann et al., 2005a; Xia et al., 2008; Xia et al., 2010; Xu et al., 2004).

1.5.6 Regression of the hyaloid vasculature

In mice, hyaloid regression starts when retinal vascular blood vessels start to grow, but it most extensively progresses between P9 and P12 when deep sprouting occurs. Mutants that lack deep retinal plexus development (*Ndph*$^{y/-}$, *FZD4*$^{-/-}$, *LRP5*$^{-/-}$, *TSPAN12*$^{-/-}$, *Angpt2*$^{-/-}$) have delayed or incomplete hyaloid regression (Hackett et al., 2002; Junge et al., 2009; Lobov et al., 2005; Luhmann et al., 2005a; Xu et al., 2004). It has been shown that hyaloid regression can be inhibited by ablating macrophages (Diez-Roux et al., 1997; Lang et al., 1993). Macrophages have been shown to induce hyaloid regression by Wnt7b expression that acts via Fz-4 and LRP-5 on hyaloid vessels (Lobov et al., 2005). Wnt7b-independent FZ-4 activation might play a role as well in hyaloid regression, because *Ndph*$^{y/-}$ mice also show persistent hyaloid vessels (Fruttiger 2007). Persistence of hyaloid vessels in *Angpt2*$^{-/-}$ mice implicate that Tie2 receptor signaling might play a role in hyaloid regression (Hackett et al., 2002). Macrophages are rare or absent in BMP4$^{+/-}$ mice and hyaloid regression also fails in BMP4$^{+/-}$ mice. However, it is not clear if deep retinal vascular plexus development is affected in these mice (Chang et al., 2001).

1.6 The aim of the thesis

Back in 1992 it was found that mutations in *NDP* lead to Norrie disease in men. Despite some knowledge about the binding receptors of Norrin has been gained, its molecular function remains a mystery.

This thesis addresses the function of Norrin using cell culture assays and the *Ndph*$^{y/-}$ mouse model. The aim was to elucidate if Norrin-Wnt signaling is linked to Notch signaling - either within a single cell, across neighboring cells (Figure 15) or not at all.

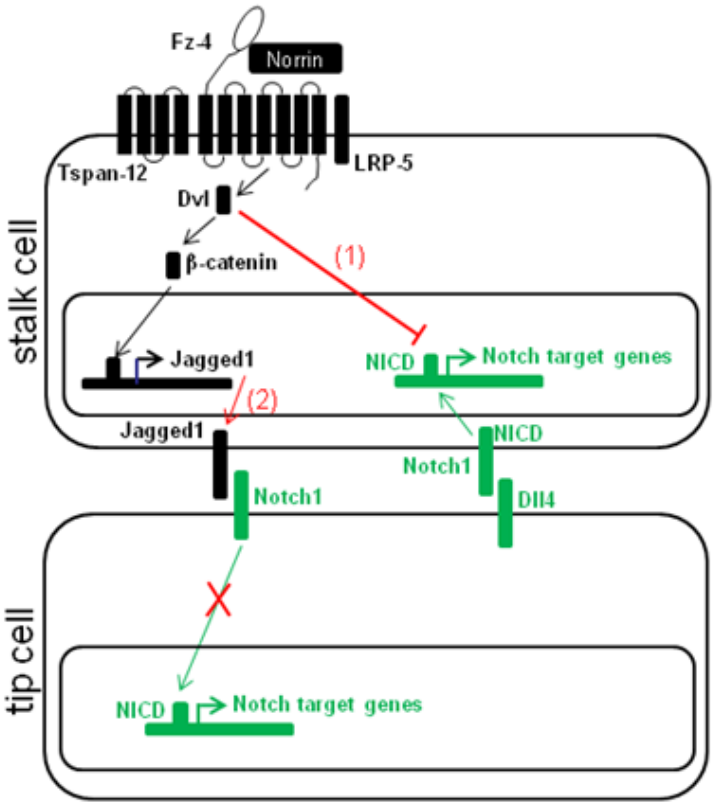

Figure 15: Possible modes of interaction between Norrin-Wnt and Notch signaling. Binding of Norrin to the co-receptor complex consisting of Frizzled4 (Fz-4), low density lipoprotein related receptor 5 (LRP-5) and Tetraspanin 12 (Tspan-12) activates canonical Wnt signaling. The activation starts by phosphorylation of disheveled (Dvl) which, over several steps, leads to stabilization of β-catenin that migrates to the nucleus and activates Wnt-target gene expression (possibly Jagged1) (black). Notch signaling in stalk cells is activated by binding of delta like 4 (Dll4) from tip cells. This leads to cleavage of Notch1 with subsequent migration of the Notch intracellular domain (NICD) to the nucleus and to the expression of Notch target genes (green). Two possible modes of interaction were investigated in this thesis. (1) Is Dvl capable of inhibiting Notch signaling by binding and inactivating NICD? (2) Is Jagged1 a Norrin-Wnt target gene that is not anymore expressed in *Ndph*$^{y/-}$ mice? (red).

Several lines of evidence suggested a role of Norrin as a negative regulator of Notch1 signaling: (a) the vascular phenotypes are similar in Norrin knockout mice and mice haploinsufficient for Notch1 or Dll4, (b) Norrin is a ligand of Fz-4/LRP-5/Tspan-12 and triggers canonical Wnt signaling, (c) Dishevelled (Dvl1), a downstream effector of Wnt, directly interacts with cleaved Notch1, (d) despite of high VEGF levels, neovascularization has never been observed in Norrin knockout mice, (e) the Notch1/Hes1/Hes2 axis promotes glial cell differentiation, which also fits the Norrin phenotype. Thus, we hypothesized that a putative Norrin-Notch signaling interaction could occur in two ways (Figure 15): (1) Any of the three mammalian Dvls might be capable of inhibiting Notch signaling by

binding and inactivating NICD in stalk cells (2) Jagged1 a putative Norrin-Wnt target gene in stalk cells could not anymore be expressed in *Ndph*$^{y/-}$ mice and thus fail to inpede Notch signaling in adjacent tip cells.

To resolve this issue we conducted the following experiments:

- Dvl1,2,3 – N1ICD interaction and their influence on Wnt- and Notch signaling were investigated by luciferase reporter assays.
- Differential Notch target gene expression of Hes1, Hes2, Hes5, Hey1 and Hey2 from HEK293T cells that were stably transfected with a wildtype Norrin or an empty construct was analyzed by qPCR.
- Immunohistochemistry on retinal whole-mounts was done to elucidate the expression of Notch1 ligands Jag1 and Dll4.
- Immunohistochemistry on retinal whole-mounts against the arterial marker a-SMA and against the venous markers EphB4 and Apj were conducted, since Notch signaling is also involved in the regulation of arterial versus venous faith.
- *Ndph*$^{y/-}$ mice were crossed with the Notch reporter mice (TNR1 mice) to monitor Notch activity within the SRVP during its development.
- DAPT, a Notch pathway inhibitor, was injected into *Ndph*$^{y/-}$ and wildtype mice to investigate the influence of Notch inhibition on the development of the SRVP.

Additionally, the following experiments were conducted:

- An extensive morphometric analysis of the SRVP in which I compared the vascular phenotype from *Ndph*$^{y/-}$ with other knockout mice.
- The proliferation of the SRVP from *Ndph*$^{y/-}$ and wildtype mice was compared after BrdU injection.
- The vascular remodeling of the SRVP from *Ndph*$^{y/-}$ and wildtype mice was compared by co-staining the plexus with isolectin B4 and collagen IV.
- Artery and vein crossing of the SRVP from *Ndph*$^{y/-}$ mice was described and linked to MAPK signaling by phenotypic comparison between different mice and by monitoring MAPK activity of wildtype and p.C95R Norrin expressing cells using a MAPK specific luciferase reporter assay.
- Immunohistochemistry of the SRVP from *Ndph*$^{y/-}$ and wildtype mice against endomucin was conducted.
- An additional goal was to describe the Norrie Disease phenotype in *Ndph*$^{y/-}$ mice in more detail and to test whether postnatal administrated sub-lethal doses of LiCl could rescue the Norrie phenotype in mouse pups, because LiCl is known to activate Wnt signaling.
- The number of hyaloid associated macrophages from the SRVP from *Ndph*$^{y/-}$ and wildtype mice was quantified on retinal wholemounts after applying immunohistochemistry against Iba1 and co-staining with isolectin B4.
- Finally, luciferase reporter assays were used to measure the impact of Norrin on TGFβ signaling, ER stress and estrogen response.

2. Material and Methods

2.1 Material

2.1.1 Cloning constructs for luciferase assays

Cloning primers are listed as forward followed by reverse primers. Sequencing primers are always forward oriented.

Subcloning Kits and competent cells

TOPO TA cloning Kit	Invitrogen, Carlsbad, USA
pJET1.2 cloning Kit	Fermentas, St. Leon-Rot, D
TOP10 *E. coli* cells	Invitrogen, Carlsbad, USA
INV110 *E. coli* cells	Invitrogen, Carlsbad, USA

***LRP5* sequencing primers**

CCACCGTGCCAACCTGG	Microsynth, Balgach, CH
CTGTGAGGAGGACAATGGC	Microsynth, Balgach, CH
TGCAGG TGG ACG ACATCC	Microsynth, Balgach, CH
GTGTGCCAACTTGGATGGG	Microsynth, Balgach, CH
CTTCACACCCCACGCAACC	Microsynth, Balgach, CH
GCAAGTCCTCGTGTGGAG	Microsynth, Balgach, CH
AGGGCCATCGTCGTCAAC	Microsynth, Balgach, CH
GATGATCGAGCGTGTGGAG	Microsynth, Balgach, CH
TGCTGACCTGTGGAGAGCC	Microsynth, Balgach, CH
GTGTCTATTTTGTGTGCCG	Microsynth, Balgach, CH
CTCCCTGTACAACATGGAC	Microsynth, Balgach, CH
CGCTGGTGGACAAGGTG	Microsynth, Balgach, CH
TGACTGTATGCACAACAACG	Microsynth, Balgach, CH
TGTTTTGACCTCTCTGAGCC	Microsynth, Balgach, CH

***FZD4* sequencing primers**

GCCAATGGGGATGTTGATCT	Microsynth, Balgach, CH
GCACATGGAGATGCGGATG	Microsynth, Balgach, CH
TGGGAACCAATTCTG ATCAG	Microsynth, Balgach, CH
GTATAAGCCAGCATCATAGC	Microsynth, Balgach, CH
CTTAAGAACACAGGATGTGC	Microsynth, Balgach, CH
GAGTGTCAGAATAACCCACC	Microsynth, Balgach, CH
G ACTGATGGTCAAGATTGGG	Microsynth, Balgach, CH
CAGGCAATCACACACGTTGC	Microsynth, Balgach, CH

Sequencing primer for pTopflash and pFopflash

CTAGCAAAATAGGCTGTCCC	Microsynth, Balgach, CH

Sequencing primer for pJH23a and pJH25a

GGAAGACGCCAAAAACATAAAG	Microsynth, Balgach, CH

Cloning Primers *hs*Dl14

TCTAGAATGGCGGCAGCGTCCCGG	Microsynth, Balgach, CH
TCTAGACTACATTACAGATC CTCTTCTGAGATGAGTTT TTGTTC ATATACCTCCGTGGCAATGACAC	Microsynth, Balgach, CH

Sequencing primers for *hs*Dll4

CACCAGATGCACTCATCAGC	Microsynth, Balgach, CH
TGCAGCAAGCCAGCAGAGTG	Microsynth, Balgach, CH
AACACAGCACCTTGAGCTGC	Microsynth, Balgach, CH
GACATCCATCGATGCCTGTG	Microsynth, Balgach, CH
CAGAAGGACAACCTGATTCC	Microsynth, Balgach, CH

Primers for *hs*FZD4:

CTGGGGTTGCTCCTGCAGTTGCTGCTGCTCCTGGGGC CGGCGCGGGGCTTCGGGGACGAGGAAGAGCGGC	Microsynth, Balgach, CH
AAGCTTATGGCCTGGCGGGGCGCAGGGCCGAGC GTCCCGGGGGCGCCCGGGGGCGTCGGTCTCAGT CTGGGGTTGCTCCTGCAGTTGC	Microsynth, Balgach, CH
AAGCTTTTACAGATCCTCTTCTGAGATGAGTTTTTG TTCATATACCACAGTCTCACTGCCTTTTCC	Microsynth, Balgach, CH

Cloning Primers *mm*Dvl1

AAGCTTATGGAACAAAAACTCATCTCAGAAGAGGATC TGGCGGAGACCAAAATCATCTACC	Microsynth, Balgach, CH
AAGCTTCTATTATCACATGATGTCCACAAAGAACT	Microsynth, Balgach, CH

Sequencing primers *mm*Dvl1

ACAATGAGACAGGCACAGAG	Microsynth, Balgach, CH
TCAACATGGAGAGGCACCAC	Microsynth, Balgach, CH
ACTGGCTGTACACACACGTG	Microsynth, Balgach, CH
AGTGAAGGGAGCAAGAGCAG	Microsynth, Balgach, CH
GCAATGACGACGCTGTACGG	Microsynth, Balgach, CH

Cloning primers *mm*Dvl2

AAGCTTAAGCTTATGGCGGGCAGCAGCG	Microsynth, Balgach, CH
AAGCTTTCATTACTACAGATCCTCTTCTGAGATGAGTT TTTGTTCCATAACATCCACAAAAAACTC	Microsynth, Balgach, CH

Sequencing primers *mm*Dvl2

GGTTGTCTCCTGGCTTGTG	Microsynth, Balgach, CH
GTACCAGCCTAGGAGACTC	Microsynth, Balgach, CH
CAACGACGATGCTGTACGAG	Microsynth, Balgach, CH
AAGATCACCATCCCAAACGC	Microsynth, Balgach, CH
ACGAGCTTTCTTCGTACACC	Microsynth, Balgach, CH
GGTAGTTATGATGCCTCCAC	Microsynth, Balgach, CH
GCTGGATGGGCTCATTTCG	Microsynth, Balgach, CH
CCACGCTCGTTACTTTGGC	Microsynth, Balgach, CH
CTCACAGCCACCACTGAGG	Microsynth, Balgach, CH
CGAAATGAGCCCATCCAGC	Microsynth, Balgach, CH
GGAGACATGCTTTTGCAGG	Microsynth, Balgach, CH

Cloning primers *mm*Dvl3

AAGCTTAAGCTTATGGGCGAGACCAAGATC	Microsynth, Balgach, CH
AAGCTTCTATTATCACAGATCCTCTTCTGAGATGAGTT TTTGTTCCATCACATCCACAAAGAACTC	Microsynth, Balgach, CH

Sequencing primers *mm*Dvl3

CGCACAGGAGGCATTGGG	Microsynth, Balgach, CH
CTTTCAGCAGCATCACAGAC	Microsynth, Balgach, CH
CGGCTGCTTCACATTACCC	Microsynth, Balgach, CH
AGTATGCTAGCAACCTGCTG	Microsynth, Balgach, CH
GAGAAGGACCCAAAAGCTGG	Microsynth, Balgach, CH
CCGATGCTGATGATGACC	Microsynth, Balgach, CH

Cloning primers *hs*TSPAN12

AAGCTTAAGCTTATGGCCAGAGAAGATTCCGTG	Microsynth, Balgach, CH
AAGCTTAAGCTTTCACTATTAGGTGCTATCCAGGCCCAGCAGCGGGTTCGGAATCGGTTTGCCTAACTCCTCCATCTCAAAGTG	Microsynth, Balgach, CH

Sequencing Primers *hs*TSPAN12

TTTAACTGCAGAAACGAGGG	Microsynth, Balgach, CH
GGTGGCTTACTCATGCTTGG	Microsynth, Balgach, CH
TCCTGGCCATGATTCTCACC	Microsynth, Balgach, CH
ATGACCGGATGAACCACAGG	Microsynth, Balgach, CH
CCACAATATCCTAACATCCC	Microsynth, Balgach, CH
CAGATTTCTTTTCACCGTTCCAC	Microsynth, Balgach, CH

Constructs

clone	purpose	cloned	purchased	donation
pTopflash	Wnt-activity luciferase reporter		a	
pFopflash	Wnt-activity luciferase reporter		a	
pWnt3A	Wnt-reporter assay; pos. control			c
pNDP_wt_myc	Wnt/Notch-activity measurement	x		
pNDP_P.C95R_myc	Wnt/Notch-activity measurement	x		
pNDP_wt	Wnt/Notch-activity measurement	x		
pNDP_P.C95R	Wnt/Notch-activity measurement	x		
pDvl1	Wnt-activity assay; pos. control	x		
pDvl2	Wnt-activity assay; pos. control	x		
pDvl3	Wnt-activity assay; pos. control	x		
pJH23a	Notch-reporter luciferase construct			d
pJH25a	Notch-reporter luciferase construct			d
pN1ICD	Notch reporter assay; pos. control			e
pDll4	Notch reporter assay; pos. control	x		
pE2F	Cell cycle reporter assay		b	
pERSE	ER stress reporter assay		b	
pSRF	MAPK reporter assay		b	
pSMAD	TGFβ reporter assay		b	
pERE	Estrogen response reporter assay		b	

a) the constructs were purchased from Addgene. b) the constructs were purchased from SABioseciences, now a Qiagen Company. c) the pWnt3A construct was a donation from Konrad Basler from the University of Zurich, Switzerland. d) the constructs were a donation from Diane Hayward from the John Hopkins University, USA. e) the construct was a donation from Raphael Kopan from the Washington University, USA.

HeBS 2x solution

32.7 g Sodium chloride (Fluka, Buchs, CH), 23.8 g N-2-hydroxyethylpiperazine-N'-2-2-ethanesolfonic acid (HEPES) (Fluka, Buchs, CH) and 0.4 g Disodiumhydrogenphosphate (Fluka, Buchs, CH) were dissolved in 1.8 liters of water. pH was adjusted to 7.05 using a 5N Sodiumhydroxyde solution. ddH_2O was added to a final volume of 2 liters. Sterile 50 ml aliquots were made and stored at -20°C.

2.5 M Calciumchloride solution

183.8 g Calcium chloride dihydrate (Fluka, Buchs, CH) were dissolved in 500 ml ddH_2O under stirring. Sterile 10 ml aliquots were made and stored at -20°C.

Sequencing reagents

Sequencing buffer	Applied Biosystems, Foster City, USA
BigDye	Applied Biosystems, Foster City, USA
Primer	Microsynth, Balgach, CH
ddH_2O	
Sephadex G-50	Sigma-Aldrich, Buchs, CH

2.1.2 TaqMan analysis of Notch target genes in HEK293T cells

RNA isolation and cDNA synthesis

Qiashredder Kit	Qiagen, Hilden, DE
RNeasy Kit	Qiagen, Hilden, DE
RNA Nano Chips	Agilent, Waldbronn, DE
Superscript III Reverse Transcriptase Kit	Invitrogen, Carlsbad, USA

TaqMan Sonden

	Assay ID		
HEY1	Hs01114113_m1	human	ABI, Foster City, USA
HEY2	Hs01012058_m1	human	ABI, Foster City, USA
HES1	Hs00172878_m1	human	ABI, Foster City, USA
HES2	Hs00219505_m1	human	ABI, Foster City, USA
HES5	Hs01387464_g1	human	ABI, Foster City, USA

TaqMan internal controls

S18 RNA		human/mouse	ABI, Foster City, USA
GAPD		human/mouse	ABI, Foster City, USA

TaqMan PCR Kit

TaqMan 2x Universal PCR Master Mix	ABI, Foster City, USA

2.1.3 Analysis of Notch activity in *Ndph*$^{y/-}$ mice

Norrie mice genotyping primers

CTA TCG CCT TCT TGA CGA GTT	Microsynth, Balgach, CH; SL105
GGC CTG GGT GGA GAG GCT TTT T	Microsynth, Balgach, CH, SL106
GTA TTG CAT CCA TAT TTC TTG G	Microsynth, Balgach, CH; SL107
CTC TCC ATC CCC TGA CAA GGA	Microsynth, Balgach, CH; SL108
TTC AGC CCT ACA GCC ACA TGA	Microsynth, Balgach, CH; SL120
ATG TGG GTT CCT GTC CCA CTG	Microsynth, Balgach, CH; SL121

Notch reporter mice genotyping primers

AAG TTC ATC TGC ACC ACC G	Microsynth, Balgach, CH
TCC TTG AAG AAG ATG GTG CG	Microsynth, Balgach, CH
CTA GGC CAC AGA ATT GAA AGA TCT	Microsynth, Balgach, CH
GTA GGT GGA AAT TCT AGC ATC ATC C	Microsynth, Balgach, CH

Proteinase K mix for digestion of tail biopsies

390 µl	ddH_2O	
50 µl	Tris*HCl pH 7.5, c=1 mol/l	Merck, Darmstadt, DE

5 µl	EDTA pH 8.0, c=0.5 mol/l	Merck, Darmstadt, DE
10 µl	SDS 10%	Merck, Darmstadt, DE
20 µl	NaCl c=5 mol/l	Merck, Darmstadt, DE
25 µl	Proteinase K, βi=10 mg/l	Roche, Basel, CH

PBS 1x

1 Tablette	PBS	Invitrogen, Carlsbad, USA
1000 ml	ddH_2O	

PBST 1x

9998 ml	PBS	Invitrogen, Carlsbad, USA
2 ml	Tween 20	Carl Roth GMBH, Karlsruhe, Germany

PFA 4%

4 g	Paraformaldehyd (PFA, P6148)	Sigma-Aldrich, Steinheim, DE
100 ml	ddH_2O	

Preheat water to 70°C, add PFA and heat in water bath at 67°C till it dissolves; filter PFA solution into 12 ml Falcon tubes and store them at -20°C. Use the aliquots within a month.

Mouse body weight

Sartorius Balance CP2202S	Sartorius, Göttingen, DE

Primary antibodies used for retinal wholemount staining

Name	Company	Product number	Source	Fixation 4% PFA	Dilution used
Jagged1	Santa Cruz	SC8303	Rabbit	3 hours	1:200
Dll4	R&D Systems	AF1389	Goat	1 hour	1:200
Collagen IV	AbD serotec	2150-1470	Rabbit	1-24 hours	1:300
IsolectinB4-FITC	Sigma	L2895	Griffonia simplicifolia	1-24 hours	1:500
IsolectinB4-AlexaFluor568	Invitrogen	I21412	Griffonia simplicifolia	1-24 hours	1:500
SMA-Cy3	Sigma	C6198	mouse	24 hours	1:500
GFP	Abcam	AB290	Rabbit	24 hours	1:500
PDGFRα	R&D	AF1062	Goat	3 hours	1:200
Iba1	Abcam	AB5076	Goat	24 hours	1:200
Endomucin	R&D	AF4666	Goat	24 hours	1:200

Secondary antibodies used for retinal wholemount staining

Name	Company	Product number	Dilution used
anti-goat-Cy3	Sigma	C2821	1:500
anti-rabbit-Cy3	Dianova	111-165-003	1:500
anti-rat-FITC	Invitrogen	A11006	1:500
DyLight 488 Streptavidin	Vector Laboratories	SA-5488	1:500
Anti-goat-AlexaFluor568	Invitrogen	A11057	1:500
Anti-rabbit-AlexaFluor568	Invitrogen	A11011	1:500

Antibodies that did not work on retinal wholemounts

Name	Company	Product number
Jagged1	Santa Cruz	SC6011
Nrp1	Calbiochem	PC343
EphrinB2	Santa Cruz	SC1010

Cleaved Notch1	Cell Signaling Technology	2421
Norrin	Santa Cruz	SC49311
ADAM10	Calbiochem	PC528
Hey1	Chemicon	AB5714
Desmin	Abcam	AB8592
Integrinβ1	Millipore	MAN1997
Phalloidin-TRITC	Sigma	P1951
Ki67	Abcam	Ab883-500
Girdin	IBL-Hamburg	JP18979
Girdin-phosphate	IBL-Hamburg	JP28067
EphB4	R&D Systems	AF446
Desmin	Abcam	AB8592
APJ	Abcam	AB66218

DAPT injection

DAPT	Sigma-Aldrich, Steinheim, DE
Peanut oil	Sigma-Aldrich, Steinheim, DE
Ethanol (100%)	Merck, Darmstadt, DE
Precision syringe	Merck, Darmstadt, DE
$30^{G1/2"}$ needle	Merck, Darmstadt, DE
2 ml screw top vial with septum	Sigma-Aldrich, Steinheim, DE

BrdU injection

BrdU	Sigma-Aldrich, Steinheim, DE
Precision syringe	Merck, Darmstadt, DE
$30^{G1/2"}$ needle	Merck, Darmstadt, DE
2 ml screw top vial with septum	Sigma-Aldrich, Steinheim, DE
Anti BrdU Antibody	BD Biosciences, Allschwil, CH,

LiCl injection

Lithiumchloride (LiCl)	Sigma-Aldrich, Steinheim, DE
PBS	Invitrogen, Carlsbad, USA
Precision syringe	Merck, Darmstadt, DE
$30^{G1/2"}$ needle	Merck, Darmstadt, DE
2 ml screw top vial with septum	Sigma-Aldrich, Steinheim, DE

2.2 Methods

2.2.1 Cloning and organizing constructs for luciferase reporter assays

New clones were necessary to conduct pathway reporter assays. Clones were either produced by myself, donated from other labs or purchased from commercial suppliers.

2.2.1.1 Cloning of mmDvl1, mmDvl2, mmDvl3 and hsDll4

The following PCR and cycling conditions were used to amplify *mmDvl1*, *mmDvl2*, *mmDvl3* and *hsDll4* (*mm = mus musculus, hs = homo sapiens*).

	µl	°C	min	
Pfu buffer 10x	2.5	95	2	
dNTPs (20 mM)	0.25	95	1	
Primer Fwd (1µM)	0.25	65	0.5	35 x
Primer Rev (1µM)	0.25	72	5	
DNA (EST plasmid, 100 ng/µl)	2	72	5	
ddH_2O	17.5			
Pfu Polymerase	0.25			
$MgSO_4$ (25 mM)	2			

The cloning strategies and encoded products are described below.

2.2.1.2 Cloning of the hsDll4 construct

hsDll4 was amplified from the EST (#IRAMp995K2414Q) from ImaGenes (Berlin, DE). The PCR product was subcloned into pJet2.1 (Fermentas, St. Leon-Rot, DE) and correct sequence was confirmed by Sanger sequencing on an ABI Prism 3100 DNA sequencer. The pJet1.2_*hs*Dll4 was digested using XbaI and subsequently shuttled into pBUDCE4.1 destination vector. A construct encoding for the following protein was obtained (green = myc-tag):

*hs*Dll4	MAAASRSASGWALLLLVALWQQRAAGSGVFQLQLQEFINERGVLASGRPCEPGCRTFFRVCLKHFQ AVVSPGPCTFGTVSTPVLGTNSFAVRDDSSGGGRNPLQLPFNFTWPGTFSLIIEAWHAPGDDLRPE ALPPDALISKIAIQGSLAVGQNWLLDEQTSTLTRLRYSYRVICSDNYYGDNCSRLCKKRNDHFGHY VCQPDGNLSCLPGWTGEYCQQPICLSGCHEQNGYCSKPAECLCRPGWQGRLCNECIPHNGCRHGTC STPWQCTCDEGWGGLFCDQDLNYCTHHSPCKNGATCSNSGQRSYTCTCRPGYTGVDCELELSECDS NPCRNGGSCKDQEDGYHCLCPPGYYGLHCEHSTLSCADSPCFNGGSCRERNQGANYACECPPNFTG SNCEKKVDRCTSNPCANGGQCLNRGPSRMCRCRPGFTGTYCELHVSDCARNPCAHGGTCHDLENGL MCTCPAGFSGRRCEVRTSIDACASSPCFNRATCYTDLSTDTFVCNCPYGFVGSRCEFPVGLPPSFP WVAVSLGVGLAVLLVLLGMVAVAVRQLRLRRPDDGSREAMNNLSDFQKDNLIPAAQLKNTNQKKEL EVDCGLDKSNCGKQQNHTLDYNLAPGPLGRGTMPGKFPHSDKSLGEKAPLRLHSEKPECRISAICS PRDSMYQSVCLISEERNECVIATEVY**EQKLISEEDL**

2.2.1.3 Cloning of the mmDvl1, mmDvl2 and mmDvl3 constructs

The mouse *Dvl1, 2 and 3* were amplified from the EST (#F630221L20), EST (#IRAVp968B01112D) and EST (#OCACo5052G078D), all purchased from ImaGenes (Berlin, DE). PCR products were subcloned into pJet2.1 (Fermentas, St. Leon-Rot, DE) and correct sequence was confirmed by Sanger sequencing on an ABI Prism 3100 DNA sequencer. Amplicons were shuttled into pBUD CE4.1 after HindIII digestion. Three constructs encoding the following proteins were obtained (green = myc-tag):

*mm*Dvl1	M**EQKLISEEDL**AETKIIYHMDEEETPYLVKLPVAPERVTLADFKNVLSNRPVHAYKFFFKSMDQDF GVVKEEIFDDNAKLPCFNGRVVSWLVLAEGAHSDAGSQGTDSHTDLPPPLERTGGIGDSRPPSFHP NVASSRDGMDNETGTESMVSHRRERARRRNRDEAARTNGHPRGDRRRDLGLPPDSASTVLSSELES SSFIDSDEEDNTSRLSSSTEQSTSSRLVRKHKCRRRKQRLRQTDRASSFSSITDSTMSLNIITVTL NMERHHFLGISIVGQSNDRGDGGIYIGSIMKGGAVAADGRIEPGDMLLQVNDVNFENMSNDDAVRV LREIVSQTGPISLTVAKCWDPTPRSYFTIPRADPVRPIDPAAWLSHTAALTGALPRYGTSPCSSAI TRTSSSSLTSSVPGAPQLEEAPLTVKSDMSAIVRVMQLPDSGLEIRDRMWLKITIANAVIGADVVD WLYTHVEGFKERREARKYASSMLKHGFLRHTVNKITFSEQCYYVFGDLCSNLASLNLNSGSSGASD QDTLAPLPHPSVPWPLGQGYPYQYPGPPPCFPPAYQDPGFSCGSGSAGSQQSEGSKSSGSTRSSHR TPGREERRATGAGGSGSESDHTVPSGSGSTGWWERPVSQLSRGSSPRSQASAVAPGLPPLHPLTKA YAVVGGPPGGPPVRELAAVPPELTGSRQSFQKAMGNPCEFFVDIM
*mm*Dvl2	MAGSSAGGGGVGETKVIYHLDEEETPYLVKIPVPAERITLGDFKSVLQRPAGAKYFFKSMDQDFGV VKEEISDDNARLPCFNGRVVSWLVSSDTPQPEVAPPAHESRTELVPPPPPLPPLPPERTSGIGDSR PPSFHPNVSSSHENLEPETETESVVSLRRDRPRRRDSSEHGAGGHRPGGPSRLERHLAGYESSSTL MTSELESTSLGDSDEDDTMSRFSSSTEQSSASRLLKRHRRRRKQRPPRMERTSSFSSVTDSTMSLN

	IITVTLNMEKYNFLGISIVGQSNERGDGGIYIGSIMKGGAVAADGRIEPGDMLLQVNDMNFENMSN DDAVRVLRDIVHKPGPIVLTVAKCWDPSPQAYFTLPRNEPIQPIDPAAWVSHSAALTGAFPAYPGS SSMSTITSGSSLPDGCEGRGLSVHMDMASVTKAMAAPESGLEVRDRMWLKITIPNAFLGSDVVDWL YHHVEGFPERREARKYASGLLKAGLIRHTVNKITFSEQCYYVFGDLSGGCESYLVNLSLNDNDGSS GASDQDTLAPLPGATPWPLLPTFSYQYPAPHPYSPQPPPYHELSSYTYGGGSASSQHSEGSRSSGS TRSDGGAGRTGRPEERAPESKSGSGSESELSSRGGSLRRGGEPGGTGDGGPPPSRGSTGAPPNLRA LPGLHPYGAPSGMALPYNPMMVVMMPPPPPPVSTAVQPPGAPPVRDLGSVPPELTASRQSFHMAMG NPSEFFVDVMEQKLISEEDL
*mm*Dvl3	MGETKIIYHLDGQETPYLVKLPLPAERVTLADFKGVLQRPSYKFFFKSMDDDFGVVKEEISDDNAK LPCFNGRVVSWLVSAEGSHPEPAPFCADNPSELPPSMERTGGIGDSRPPSFHPHASGGSQENLDND TETDSLVSAQRERPRRRDGPEHAARLNGTTKGERRREPGGYDSSSTLMSSELETTSFFDSDEDDST SRFSSSTEQSSASRLMRRHKRRRRKQKVSRIERSSSFSSITDSTMSLNIITVTLNMEKYNFLGISI VGQSNERGDGGIYIGSIMKGGAVAADGRIEPGDMLLQVNEINFENMSNDDAVRVLREIVHKPGPIT LTVAKCWDPSPRGCFTLPRSEPIRPIDPAAWVSHTAAMTGTFPAYGMSPSLSTITSTSSSITSSIP DTERLDDFHLSIHSDMAAIVKAMASPESGLEVRDRMWLKITIPNAFIGSDVVDWLYHNVEGFTDRR EARKYASNLLKAGFIRHTVNKITFSEQCYYIFGDLCGNMANLSLHDHDGSSGASDQDTLAPLPHPG AAPWPMAFPYQYPPPPHPYNPHPGFPELGYSYGGGSASSQHSEGSRSSGSNRSGSDRRKEKDPKAG DSKSGGSGSESDHTTRSSLRGPRERAPSERSGPAASEHSHRSHHSLTSSLRSHHTHPSYGPPGVPP LYGPPMLMMTPPPAAMGPPGAPPGRDLASVPPELTASRQSFRMAMGNPSEFFVDVMEQKLISEEDL

2.2.1.4 Cloning of the hsTSPAN12

A human Tspan12 clone (Origene, SC112659) was used as PCR template. The following PCR conditions were used for amplification:

	µl	°C	seconds	
Pfu Buffer 10x	5	95	120	
H_2O	31	94	60	40x
dNTPs (20 mM)	0.5	50	30	
Primer F/R (10 mM each)	6	72	150	
$MgCl_2$	4	72	300	
DNA (50 ng/µl)	3	10	eternal	
Pfu Polymerase	0.5			

The amplicon was subloned into pJet vector, sequenced, *Hin*dIII digested and shuttled into pBUD CE4.1 vector. The pBud_hsTSPAN12 clone features a V5 tag and was used for Wnt reporter assay. The isolated construct encodes the following protein (green = V5-tag):

*hs*TSPAN12	MAREDSVKCLRCLLYALNLLFWLMSISVLAVSAWMRDYLNNVLTLTAETRVEEAVILTYFPV VHPVMIAVCCFLIIVGMLGYCGTVKRNLLLLAWYFGSLLVIFCVELACGVWTYEQELMVPVQ WSDMVTLKARMTNYGLPRYRWLTHAWNFFQREFKCCGVVYFTDWLEMTEMDWPPDSCCVREF PGCSKQAHQEDLSDLYQEGCGKKMYSFLRGTKQLQVLRFLGISIGVTQILAMILTITLLWAL YYDRREPGTDQMMSLKNDNSQHLSCPSVELLKPSLSRIFEHTSMANSFNTHFEMEELGKPIP NPLLGLDST

2.2.1.5 Clones donated from other labs

The following clones are donations from people of other labs.

Clone name	Donator	Affiliation
pTopflash	Konrad Basler	University of Zurich, CH
pFopflash	Konrad Basler	University of Zurich, CH
pWnt3A	Konrad Basler	University of Zurich, CH
pJH23A	Diane Hayward	John Hopkins University, USA
pJH25a	Diane Hayward	John Hopkins University, USA

pN1ICD	Raphael Kopan	Washington University, USA
pFZD4	Wei Chen	Duke University, USA
pLRP5	He Xi, Bryan MacDonald	Harvard Medical School, USA
pDkk1	He Xi, Bryan MacDonald	Harvard Medical School, USA

2.2.1.6 Adaption of the FZD4 construct

The FLAG-tagged human FZD4 construct, obtained from Wei Chen from the Duke University, USA, revealed altered N-terminal coding sequence during quality control. Therefore the construct was repaired by conducting two subsequent PCRs using up to 88 bp oligonucleotides as primers. In addition, the construct was myc tagged and cloned into pBud CE4.1 vector.

First PCR:

	µl
Pfu Buffer	2.5
dNTP (20 mM each)	0.25
Primer F	0.25
Primer R	0.25
DNA (50 ng/ul)	2.5
ddH_2O	17
Pfu Pol	0.25
$MgSO_4$ (25 mM)	2

°C	min	
95	2	
95	1	35 x
55-65	30	
72	4	
72	5	
10	eternal	

Second PCR:

	µl
Pfu Buffer	2.5
dNTPs (20 mM each)	0.25
Primer F	0.25
Primer R	0.25
DNA (50 ng/ul)	3
ddH_2O	16.5
Pfu Pol	0.25
$MgSO_4$ (25 mM)	2
	25

°C	min	
95	2	
95	1	35 x
55-65	30	
72	4	
72	5	
10	eternal	

A construct encoding the following protein was isolated (green = myc tag):

*hs*FZD4	MAWRGAGPSVPGAPGGVGLSLGLLLQLLLLLGPARGFGDEEERRCDPIRISMCQNLGYNVTKMPNL VGHELQTDAELQLTTFTPLIQYGCSSQLQFFLCSVYVPMCTEKINIPIGPCGGMCLSVKRRCEPVL KEFGFAWPESLNCSKFPPQNDHNHMCMEGPGDEEVPLPHKTPIQPGEECHSVGTNSDQYIWVKRSL NCVLKCGYDAGLYSRSAKEFTDIWMAVWASLCFISTAFTVLTFLIDSSRFSYPERPIIFLSMCYNI YSIAYIVRLTVGRERISCDFEEAAEPVLIQEGLKNTGCAIIFLLMYFFGMASSIWWVILTLTWFLA AGLKWGHEAIEMHSSYFHIAAWAIPAVKTIVILIMRLVDADELTGLCYVGNQNLDALTGFVVAPLF TYLVIGTLFIAAGLVALFKIRSNLQKDGTKTDKLERLMVKIGVFSVLYTVPATCVIACYFYEISNW ALFRYSADDSNMAVEMLKIFMSLLVGITSGMWIWSAKTLHTWQKCSNRLVNSGKVKREKRGNGWVK PGKGSETVVEQKLISEEDL

2.2.1.7 Quality control of Wnt luciferase and Notch luciferase reporter constructs

To monitor canonical Wnt/β-catenin signaling, two constructs harboring either six wildtype (pTopflash) or mutant (pFopflash) TCF/LEF binding sites upstream the firefly luciferase gene were obtained from Konrad Basler and George Hausmann from the University of Zurich, Switzerland.

Sequencing using pRVprimer3 that binds to the backbone vector pTA-Luc (Clonetech) revealed no sequence alterations (data not shown).

To monitor Notch signaling activity, two constructs harboring either four wildtype (pJH23a) or mutant (pJH25a) CBF1 binding sites upstream the firefly luciferase gene were obtained from Diana S. Hayward from The Johns Hopkins University, USA. The backbone vector is pGL2pro (Promega, Madison WI, USA). Reporter sequences are listed below. Inserts that alter the proper recognition site are printed in bold letters.

pJH23a: GAT CTG GTG TAA CAC GCC GTG GGA AAA AAT TTA TG

pJH25a: GAT CTG GTG TAA **A**CAC GGG CT**T** GGA AAA AAT TTA TG

2.2.1.8 Commercially purchased pathway luciferase reporter constructs

The luciferase reporter constructs pE2F, pERSE, pSRF and pSMAD were ordered from SABiosciences (Frederick, USA) and obtained as 1:40 mix with pRenilla. *E. coli* were transformed using the construct mix and plated on LB plated containing ampicillin. Single colonies of luciferase reporter constructs were isolated and sequenced using the RVprimer3. The respective binding sites of the luciferase constructs are given in the table below. All constructs have a pTA-Luc backbone.

pE2F	GTGCCAGNAACATTTCTCTGGCCTAACTGGCCGGTACCTGAGCTCGCTAGCCTCGAGGGATCC**TTTCGCGGG AAA*TTTCGCGGGAAA*TTTCGCGGGAAATTTCGCGGGAAA*TTTCGCGGGAAA***AAGCTTA GACACTAGAGGGTATATAATGGA
pERSE	TGAGNCTCGCTAGCCTCGAGGGATCCCCTTCA**CCAAT*CGGCGGCCT*CCACG**ACGGCCTTCA**CCAAT*CGGCG GCCT*CCACG**ACGGCCTTCA**CCAAT*CGGCGGCCT*CCACG**ACGGCCTTCA**CCAAT*CGGCGGCCT*CCACG**ACGGAAGCTTAGACACTAGAGGGTATATAATGGA
pSRF	TAACTGGCCGGTACCTGAGCTCGCTAGCCTCGAGGGATCCCA**GGATGTCCATATTAGGA**CACA**GGATGTCC ATATTAGGA**CACA**GGATGTCCATATTAGGA**CACA**GGATGTCCATATTAG GA**CACA**GGATGTCCATATTAGGA**CAAAGCTTAGACACTAGAGGGTATATAATGGA
pSMAD	GGCCTAACTGGCCGGTACCTGAGCTCGCT**AGCCAGCCAGACAAAGCCAGACAAAGCCAGACAAAAGCCA GACAAAGCCAGACAAAAGCCAGAC**AA**AGCCAGACAAAAGCCAGACAAAGCCAGACAAAAGCCAGACAA AGCCAGACAAAAGCCAGACAAAGCCAGACA**AAAGCTTAGACACTAGAGGGTATATAATGGA

Bold/bold italic letters indicate transcription factor binding sites, underlined letters highlight the TA promoter.

2.2.1.9 Sequencing of clones

Sequencing conditions were the same for all clones:

	µl	°C	sec	
Buffer5x	1.5	96	60	
Primer	1.0	96	20	
Plasmid DNA (50 ng/ul)	1.0	50	10	35 x
ddH_2O	5.7	60	3	
BigDye	0.8	10	eternal	

Sequencing reactions were purified using Sephadex filtration columns and analyzed on an ABI Prism 3100 Genetic Analyzer. Electropherograms were analyzed using Sequencer software (GeneCodes, Ann Arbor, USA).

2.2.2 Wnt- and Notch-pathway luciferase reporter assays

Eukaryotic gene expression is regulated by endogenous and environmental stimuli. Initially, an extracellular signaling molecule binds its receptor, triggering a series of molecular cascades, which activate or deactivate specific transcription factors (TFs) that regulate gene expression. The interaction of multiple TFs control the expression of any given gene. The TFs in turn are modulated

by multiple signal transduction pathways. Many transduction pathways converge at transcription factors that bind specific transcriptional response elements (TREs) in promoters of various genes. Therefore, reporter constructs that express a reporter gene (e.g. luciferase) controlled by a promoter consisting of specific TREs (e.g. TCF/LEF for Wnt signaling, CBF1 for Notch signaling) are widely used to monitor respective pathway activity. We delivered these plasmid based reporter constructs (pTopflash to monitor Wnt signaling and pJH23a to monitor Notch signaling) by transient transfection to the nucleus of HEK293T cells. The readout was done using the commercially available Dual Glo™ Luciferase Kit (Promega). Statistical analysis was done with SPSS 19.

2.2.2.1 Calcium phosphate precipitation for transient transfection of HEK293T cells

$4*10^5$ HEK293T cells per well were seeded in a 24-well plate and incubated for 24 hours at 37°C under 5% CO_2. Subsequently, the cells were transfected using the Ca^{2+}-precipitation method. Therefore a total of 3 µg plasmid DNA mix was added to yield in a total volume of 30 µl ddH_2O/DNA solution. 3 µl calcium chloride (c=2.5 mol/l) and 30 µl 2.5x HeBS solution were added. The solution was mixed by pipetting up and down and incubated for 20 minutes at ambient temperature. 60 µl solution were pipetted dropwise into a well of a 24-well plate. The plate was incubated for 24 to 72 hours prior to conduction of the luciferase readouts. Three technical replicas were done per measurement. Each experiment was repeated twice.

2.2.2.2 Transient Wnt reporter assay

Wildtype HEK293T cells were used and treated according to the transfection protocol above to measure Wnt activity of transiently expressed wildtype or mutant Norrin. The ratios of transiently transfected constructs were as follows: pTopflash : pWnt3A : pFZD4 : pLRP5 : pRL = 1:1:1:1:100 or pTopflash : pNDP* : pFZD4 : pLRP5 : pRL = 1:1:1:1:100. pNDP* can be any wildtype or mutant Norrin construct. The medium was replaced with 100 µl of fresh medium after 72 hours. The luciferase activity was measured using the Dual-Glo™ Luciferase Assay System (Promega, Madison, USA). For that, 75 µl/well Dual Glo™ Luciferase Substrate solution was added. The plates were incubated for 5 minutes at ambient temperature under light protection. After measuring the Firefly activity using an Luminoskan Ascent reader (ThermoLabsystems, Helsinki, Finnland), 50 µl Dual-Glo™ Stop and Glo Substrate solution were added. Following 10 minutes of incubation at ambient temperature at dark, the renilla luciferase activity was measured. Statistical analysis was performed as described below.

2.2.2.3 Stable Wnt reporter assay

HEK293T cells stably expressing wildtype, mutant or no Norrin were used and treated according to the transfection protocol above to measure Wnt activity. The ratios of transiently transfected constructs were as follows: pTopflash : pFZD4 : pLRP5 : pRL = 1:1:1:100. 25 mM LiCl and 25 mM NaCl were used as positive and negative control, respectively. The medium was replaced with 100 µl of fresh medium after 48 hours of incubation. The luciferase activity was measured using the Dual-Glo™ Luciferase Assay System (Promega, Madison, USA). Therefore, 75 µl/well Dual Glo™ Luciferase Substrate solution was added. The plates were incubated for 5 minutes at ambient temperature under light protection. After measuring the Firefly activity using a Luminoskan Ascent reader (ThermoLabsystems, Helsinki, Finnland), 50 µl Dual-Glo™ Stop and Glo Substrate solution were added. Following 10 minutes of incubation at ambient temperature at dark, the renilla luciferase activity was measured. Statistical analysis was performed as described below.

2.2.2.4 Conditions to perform the Notch reporter assay

HEK293T cells stably expressing wildtype or mutant (p.C95R) Norrin were used and treated according to the transfection protocol above to measure Notch activity. The ratios of transiently transfected constructs were as follows: pJH23a : pN1ICD : pFZD4 : pLRP5 : pRL = 1:1:1:1:20. After 24 to 72 hours, the medium was replaced with 100 µl of fresh medium. The luciferase activity was measured using the Dual-Glo^{TM} Luciferase Assay System (Promega, Madison, USA). Therefore, 75 µl/well Dual Glo^{TM} Luciferase Substrate solution was added. The plates were incubated for 5 minutes at ambient temperature under light protection. After measuring the Firefly activity using a Luminoskan Ascent reader (ThermoLabsystems, Helsinki, Finnland), 50 µl Dual-GloTM Stop and Glo Substrate solution were added. Following 10 minutes of incubation at ambient temperature at dark, the renilla luciferase activity was measured. Statistical analysis was performed as described below.

2.2.2.5 Statistical analysis of reporter assays

Readouts of reporter assays were only analyzed if the following criteria were met:

- cells were adherent, looked viable and had a normal morphology before measurement
- the cell culture medium was red but not orange or yellow before exchange with fresh medium
- the renilla values of the readout were at least three standard deviations above the average of values from empty measured wells

Readouts that met these criteria were analyzed in SPSS 19 (IBM, New York, USA) using independent samples T-test (two-tailed). Average and confidence intervals are displayed in graphs. P-values below α=0.05 were considered statistically significant.

2.2.3 TaqMan analysis of Notch target genes in HEK293T cells

2.2.3.1 Sample preparation for the quantification of Notch target genes after Norrin expression in HEK293T cells

We assessed the influence of Norrin on the expression of Notch target genes, including Hes1, Hes2, Hes5, Hey1 and Hey2 in HEK293T cells. For that, 10^6 HEK293T cells that stably express wildtype (Norrin) or none Norrin (MOCK) were seeded in 75 cm^2 T-bottles in 12 ml DMEM medium and incubated over night at 37°C, 5% CO_2. 2500 ng pFZD4 and 2500 ng pLRP5 were dissolved in 1120 µl ddH_2O, 125 µl $CaCl_2$ and 1250 µl 2xHeBS buffer and incubated 20 minutes at ambient temperature. The transfection mix was transferred onto the cells and regularly distributed by briefly rotating the T-bottle. Cells were incubated 72 hours at 37°C, 5% CO_2 and harvested. RNA was extracted using RNAShredder columns and RNAEasy Kit (both from Qiagen, Hilden, DE) using standard protocols provided from Qiagen. Quality control and quantification of extracted RNA was done using RNA Nano chip (Agilent, Waldbronn, DE). 2000 ng RNA were used for cDNA synthesis with Superscript III reverse transcriptase Kit (Invitrogen, Carlsbad, USA) according to manufacturers´ protocol. 10 ng cDNA per reaction were used for target gene analysis and 100 pg per reaction for 18S rRNA or GAPDH control analysis. Six technical replicas of four different transfected T-bottles per target and control gene were measured in an ABI PRISM® 7900T (Applied Biosystems, Foster City, USA) using standard conditions for cycling. All Ct values were between 25-30 since ct values below 35 may randomly occur.

2.2.3.2 Analysis of TaqMan data

Relative expression was calculated using the cycle threshold method (ΔΔct). First, target gene expression was normalized to the endogenous control (18s RNA or GAPDH): $Ct_{target\ gene} - Ct_{endogenous\ control}$. Normalized target gene expression was then normalized to an arbitrary calibrator sample, which was the average of all ΔCt from Norrin or non-Norrin expressing cell samples: $\Delta Ct_{sample} - \Delta ct_{calibrator\ sample} = \Delta\Delta Ct$. The fold change expression difference was then calculated with the formula: $2^{-\Delta\Delta Ct}$. Upper and lower confidence intervals were calculated separately using Student's t-test at a significance level of 95% based on ΔΔCt-values, since confidence intervals cannot be plotted linear on the fold change scale. Calculations were done in Excel (Microsoft, Redmont, USA).

2.2.4 Analysis of Notch activity in *Ndph*$^{y/-}$ mice

2.2.4.1 Breeding of Norrin knockout mice (*Ndph*$^{y/-}$)

The coding sequence for the 56 N-terminal amino acids of the murine *Ndph* gene was replaced by a neomycin cassette in the 129/Ola mouse strain (Berger et al., 1996). The obtained *Ndph*$^{y/-}$mice were backcrossed to the C57BL/6J strain. To avoid genetic drift, male *Ndph*$^{y/-}$mice and wildtype female C57BL/6J(Fue) mice were bred and their heterozygous female offspring were mated with wildtype male C57BL/6J(Fue) mice. All male offspring was used to conduct experiments.

2.2.4.2 Breeding of Notch Reporter mice (*Ndph*$^{y/-}$ x *Tg(Cp-EGFP)25Gaia/J*)

To detect Notch signaling in vivo, heterozygous female *Ndph*$^{y/-}$ mice were crossed with homozygous Notch reporter mouse (*Tg(Cp-EGFP)25Gaia/J*, Jackson Laboratory, Main, USA; Hellstrom et al. 2007). Experiments were conducted using wildtype or *Ndph*$^{y/-}$ male offspring harboring the Notch reporter cassette.

2.2.4.3 Health and weight monitoring of mice

Health was monitored by visual inspection of the mice skin or coat (depending on the age of the pups) and hygienic appearance of the animals. Animals with a weight that differed for 3 standard deviations from the average of their litter were excluded from experiments.

2.2.4.4 DNA extraction from mouse tail biopsies

5 mm mouse tail biopsies were digested 1 h at 55°C at 1200 rpm in 500 µl proteinase K mix (see table below). Samples were centrifuged for 5 min at 4°C at 13000 rpm and DNA of the supernatant was precipitated using 500 µl 2-propanol. Samples were centrifuged 2 min at 4°C and 13000 rpm. The pellet was washed with 200 µl 70% ethanol and dried 10 min at 65°C. DNA was dissolved in 500 µl ddH_2O. 1 µl of extracted DNA was used for genotyping.

2.2.4.5 Genotyping of *Ndph*$^{y/-}$ mice

A multiplex PCR was used to determine the genotype of the mice. Primers SL 107 and SL 108 flank exon 2 of the *Ndph* gene and amplify a 527 bp product from the wild type allele. Primers SL 105 and SL 106 bind inside the neomycin cassette of the *Ndph* knockout allele and yield 3 smaller PCR products in combination with primers SL 105 and SL 106: a 133 bp and a 204 bp product (SL 106 with SL 108), and an amplicon of 271 bp (SL 105 with SL 107) (Figure 16).

The *Sry* gene on the Y chromosome was amplified to identify male mice. For that, the primers SL 120 and SL 121 were used. If male mouse DNA is provided the amplicon size generated is 406 bp.

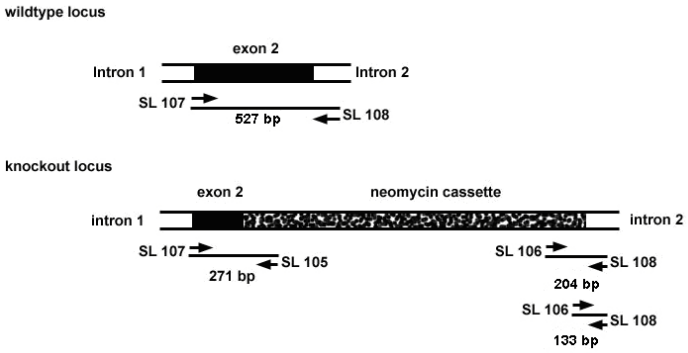

Figure 16: *Ndph* genotyping strategy: Amplification of the endogenous wild type locus with two intron primers results in a fragment of 527 bp, while three fragments of 133, 204 and 271 bp are amplified from the knockout locus (modified after Berger et al., 1996).

Sry genotyping:

	µl
ddH_2O	16.0
Buffer B (10x)	2.5
$MgCl_2$ (25 mM)	3.0
dNTPs (20 mM)	0.25
Primer SL188 (10 µM)	1.0
Primer SL189 (10 µM)	1.0
Hot Fire Polymerase	0.25
DNA from mouse tails extract	1

°C	min	
95	15	
95	1	35 x
56	1	
72	2	
72	10	

Ndph genotyping:

	µl
ddH_2O	12.75
Buffer B (10x)	2.5
$MgCl_2$ (25 mM)	6.0
dNTPs (20 mM)	0.25
DTT (100 mM)	1.25
Primer SL105 (10 µM)	0.25
Primer SL106 (10 µM)	0.25
Primer SL107 (10 µM)	0.25
Primer SL108 (10 µM)	0.25
Hot Fire Polymerase	0.25
DNA from mouse tails	1

°C	min	
95	15	
95	1	35 x
62	1	
72	2	
72	10	

PCR products are analyzed on a 1.5 % agarose gel using 0.5 µg/ml ethidium bromide for staining. 1 kb DNA ladder (Fermentas, St. Leon-Rot, DE) served as size marker. Interpretation of the amplicons are as follows:

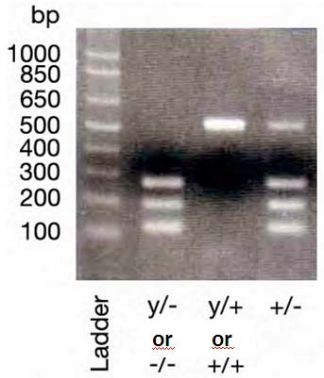

Ndph genotyping on an agarose gel: The presence of the 133 bp, 204 bp and 271 bands is specific for *NDPh*$^{y/-}$ animals. The presence of 527 bp fragment is specific wildtype animals.

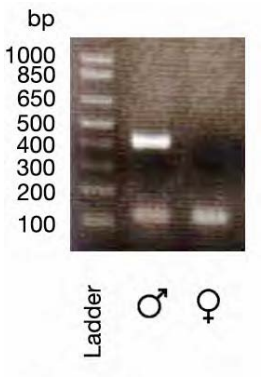

Sry genotyping in an agarose gel: The presence of the 406 bp band is specific for male mice.

2.2.4.6 Genotyping of Notch reporter mice

In addition to *Sry* and *Ndph* genotyping, the presence of the Notch reporter in *Ndph*$^{y/-}$ x *Tg(Cp-EGFP)25Gaia/J*$^{-}$ mice was genotyped using the following PCR conditions.

	µl
ddH_2O	14.95
Puffer B	2.5
$MgCl_2$ (25 mM)	2.0
dNTPs (20 mM)	0.25
20 µM primer #637	1.0
20 µM primer #638	1.0
20 µM primer #635	1.0
20 µM primer #636	1.0
Taq DNA Polymerase	0.3
DNA (50ng/µl)	1.00

°C	min	
95	15	
95	1	35x
60	1	
72	1	
72	10	
10	hold	

PCR products are analyzed on a 2 % agarose gel using 0.5 µg/ml ethidium bromide for staining. 1 kb DNA ladder (Fermentas, St. Leon-Rot, DE) served as size marker. Interpretation of the amplicons are as follows:

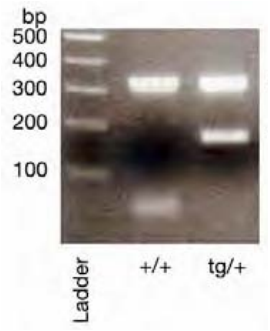

Notch reporter PCR: The 324 bp band serves as positive control for the PCR reaction. The presence of the 174 bp band indicates the presence of the Notch reporter cassette in the animal. The original protocol was derived from Jackson Laboratories (Main, USA; www.jax.org). Jackson Laboratories did not indicate the nature of the produced amplicons in detail.

2.2.4.7 BrdU treatment

BrdU treatment was performed according to a *Nature* protocol (Pitulescu et al., 2010).

2.2.4.8 DAPT treatment

N-[(3,5-Difluorophenyl)acetyl]-L-alanyl-2-phenyl]glycine-1,1-dimethylethyl ester (DAPT) inhibits Notch1 signaling by inhibiting Notch1 cleavage enzyme γ-secretase. We used the following protocol to inject *Ndph*$^{y/-}$ and wildtype littermates:

Day 1 (mice stage P5):

Health status of animals was evaluated by visual inspection of their skin or coat and by weight monitoring.
5 mg DAPT were dissolved in a 2 ml screw top vial with septum in 100 µl ethanol puriss p.a. and subsequently 450 µl peanut oil were added.
The suspension was vortexed before every injection to ensure optimal emulsion properties of the injective.
50 µl DAPT emulsion were injected subcutaneously at the neck using a 30 G$^{1/2''}$ needle and a 100 µl syringe.

Day 2 (mice stage P6):

The procedure from day 1 was repeated.

Day 3 (mice stage P7):

Eyes of euthanized animals were enucleated and retinal whole-mounts were prepared as described below.

2.2.4.9 LiCl treatment

Lithium chloride dissolved in PBS was injected according to the table below starting P5 for 5 days. Conditions for the setup of the injection table were from Smith DF, 1978 and Hofman et al., 2010 (Hofmann et al., 2010; Smith1978). Abort criterions were lack of gain in body weight, symptoms of poisoning or death of mice pups.

age [d]	weight of animal [g]	LiCl (4mg/100 µl PBS) [µl]	ul PBS	total volume PBS [ml]	total mass of LiCl [mg]	βi(LiCl) [mg/ml]	c(LiCl) (mmol/l)	mmol/kg	%LD LiCl
5	2.5	11.9	38	0.05	0.48	9.5	225	4.5	23.2
6	3.2	15.3	35	0.05	0.61	12.2	288	4.5	23.2
7	3.8	18.1	32	0.05	0.72	14.5	342	4.5	23.2
8	4.3	20.6	29	0.05	0.82	16.5	388	4.5	23.2
9	4.8	22.7	27	0.05	0.91	18.2	429	4.5	23.2
10	5.2	24.7	25	0.05	0.99	19.8	466	4.5	23.2

Eyes were fixed at P12 and analyzed as described below.

2.2.4.10 Preparation of retinal whole-mounts

Eyes were dissected in PBS and fixed in 4% paraformaldehyde (PFA) for two hours on ice or over night at 4°C. After fixation, retinas were incubated in PBST with 1 to 10% serum together with primary antibodies over night at 4°C. Retinas were washed five times using PBST and subsequently

incubated with secondary antibodies dissolved in PBST. Retinas were washed again five times with PBS and mounted using Fluoro Mount (Sigma-Aldrich, Steinheim, DE). Mounted retinas were analyzed with Zeiss AxioVison microscope in combination with ApoTome and AxioVs40 V4.6.3.0 or a CLSM Leica SP2 inverse microscope (Leica, Wetzlar, DE).

2.2.5 Quantification of retinal parameters

Only one eye per mouse was used for retinal quantification. The results of four single measurements per retina were arithmetically averaged. At least four retinas from four different male mice were used per measurement. Data collection was performed in Excel (Microsoft, Redmont, USA) and subsequent statistic analysis was performed in SPSS 18 or 19 (IBM, New York, USA).

2.2.5.1 Quantification of filopodia per 100 µm vascular front

Eyes were fixed in 4% PFA at 4°C over night and dissected in PBS. Blood vessels were stained with isolectinB4. For quantification, non-overlapping 400x magnified ApoTome™ microscopy pictures were taken from the vascular front (Figure 17). The distance of the vascular front was measured using ImageJ (NIH, Maryland, USA) and the number of filopodia were counted using the "counting tool" from Photoshop (Adobe, Mountain View, USA). Number of filopodia per 100 µm were calculated and compared.

2.2.5.2 Quantification of branchpoints per field

Eyes were fixed in 4% PFA at 4°C over night and dissected in PBS. Blood vessels were stained with isolectinB4 (IB4). Non-overlapping 200x fluorescence microscopy pictures were used for quantification. The "rectangular marquee tool" from Photoshop (Adobe, Mountain View, USA) was used to select a 573x573 pixel square and all branchpoints within that square were counted (Figure 17).

2.2.5.3 Quantification of the vascular density

Eyes were fixed in 4% PFA at 4°C over night and dissected in PBS. Blood vessels were stained with IB4. Non-overlapping 200x fluorescence microscopy pictures were used for quantification. The "rectangular marquee tool" from Photoshop (Adobe, Mountain View, USA) was used to select a 573x573 pixel square. The vasculature within the square was selected using the Photoshop's "color range tool". Unspecific stained objects were manually omitted from the selection using the "magic wand tool". The number of selected pixels was read of the "histogram panel". The vascular density was calculated as the ratio of selected pixels divided by 573^2 (Figure 17).

2.2.5.4 Measurements of the vascular length and thickened vascular regions

To evaluate outcomes of DAPT injections, the vascular radial outgrowth (vascular length) and the area of DAPT induced vascular thickening were quantified (Figure 17). For that, four to six overlapping fluorescence microscopy pictures (5x magnification) of a single retinal whole-mount, stained with isolectinB4, were stitched together using Photoshop's "Photomerge" function. Distances between the retinal outline or the vascular front or boarder of the thickened vascular plexus to the optical disc were measured with the "ruler tool" applying the custom scale 468 px = 1000 µm. The vascular length was calculated by dividing the distance between the optical disc and the vascular front by the distance between the optical disc to the retinal border. The thickened area was calculated by dividing the distance between the optical disc and the border of the thickened vascular region by the distance between the optical disc and the vascular front and subsequently subtracting this ratio from 1.

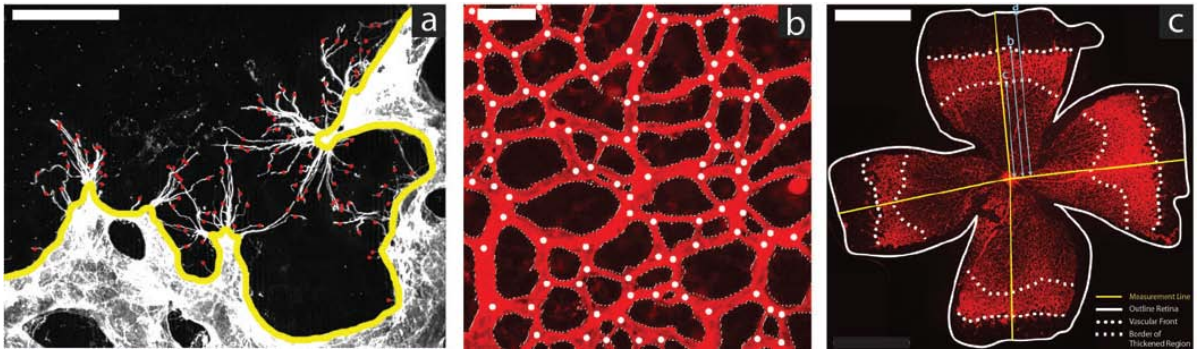

Figure 17: Quantification of retinal parameters. (a) confocal picture of the vascular front stained with isolectin B4 to visualize blood vessels (grey) and filopodia (red dots). The yellow line indicates the measured distance of the vascular front. Scale bar equals 25 µm. (b) Blood vessels of the central retina are stained using isolectin B4 (red). The number of branchpoints (white dots) was counted or the ratio between the red and the total number of pixels of the square calculated (= vascular density). Scale bar equals 50 µm. (c) Blood vessels of the retina are stained with isolectin B4 (red). Blue lines represent the radial distance from the retinal border (=a), vascular front (=b) or the border of the thickened vascular area (=c) to the optical disc (center of yellow cross). All measurements were performed on one measurement line (yellow) for each leave. Scale bars equal 1000 µm. (Pictures are adapted from the Master Thesis of Martin Fritzsche).

2.2.5.5 Statistics

Statistical analysis was performed in SPSS 18 or 19 (IBM, New York, USA) using two-tailed unpaired Student's *t*-test. Quantitative data from DAPT-injection experiments were processed with univariate analysis of variance with two independent variables. Avoiding bias due to unequal sample sizes, the estimated marginal means where calculated instead of arithmetically means. *P*-values below α=0.05 were considered as statistically significant.

3. Results

During my thesis I became first author of the publication "Alterations of the 5' Untranslated Region of SLC16A12 Lead to Age-Related Cataract". This publication is thematically not connected to my thesis and therefore no additional results are shown or discussed here. The paper is available in appendix 5.

Zuercher J, Neidhardt J, Magyar I, Labs S, Moore AT, Tanner FC, Waseem N, Schorderet DF, Munier FL, Bhattacharya S, Berger W, Kloeckener-Gruissem B (2010). Alterations of the 5'untranslated leader region of *SLC16A12* lead to age-related cataract. *Invest Ophthalmol Vis Sci* 51:3354-3361

Own contributions: I cloned the constructs used in the luciferase reporter assay, conducted the luciferase reporter assay, did the RNA in silico analysis, designed the figures and wrote and reviewed the paper.

3.1 Norrin stimulates cell proliferation in the superficial retinal vascular plexus and is pivotal for the recruitment of mural cells

The following publication covers the main results from my thesis project.

Zuercher J, Fritzsche M, Feil S, Mohn L, Berger W (2012) Norrin stimulates cell proliferation in the superficial retinal vascular plexus and is pivotal for the recruitment of mural cells. *Hum Mol Genet* (Epub ahead of print)

Own contributions: I was responsible for animal husbandry, coordinated animal experimentation, designed and performed experiments, analyzed and interpreted data, designed the figures, wrote, reviewed and submitted the manuscript.

HMG Advance Access published March 21, 2012

Human Molecular Genetics, 2012 **1–12**
doi:10.1093/hmg/dds087

Norrin stimulates cell proliferation in the superficial retinal vascular plexus and is pivotal for the recruitment of mural cells

Jurian Zuercher[1,2,†], Martin Fritzsche[1,†], Silke Feil[1], Lucas Mohn[1,2] and Wolfgang Berger[1,2,3,*]

[1]Institute of Medical Molecular Genetics, [2]Neuroscience Center Zurich (ZNZ) and [3]Center for Integrative Human Physiology (ZIHP), University of Zurich, Zurich, Switzerland

Received January 20, 2012; Revised and Accepted February 28, 2012

Mutations in Norrin, the ligand of a receptor complex consisting of FZD4, LRP5 and TSPAN12, cause severe developmental blood vessel defects in the retina and progressive loss of the vascular system in the inner ear, which lead to congenital blindness and progressive hearing loss, respectively. We now examined molecular pathways involved in developmental retinal angiogenesis in a mouse model for Norrie disease. Comparison of morphometric parameters of the superficial retinal vascular plexus (SRVP), including the number of filopodia, vascular density and number of branch points together with inhibition of Notch signaling by using DAPT, suggest no direct link between Norrin and Notch signaling during formation of the SRVP. We noticed extensive vessel crossing within the SRVP, which might be a loss of Wnt- and MAP kinase-characteristic feature. In addition, endomucin was identified as a marker for central filopodia, which were aligned in a thorn-like fashion at P9 in Norrin knockout ($Ndp^{y/-}$) mice. We also observed elevated mural cell coverage in the SRVP of $Ndp^{y/-}$ mice and explain it by an altered expression of *PDGFβ* and its receptor (*PDGFRβ*). *In vivo* cell proliferation assays revealed a reduced proliferation rate of isolectin B4-positive cells in the SRVP from $Ndp^{y/-}$ mice at postnatal day 6 and a decreased mitogenic activity of mutant compared with the wild-type Norrin. Our results suggest that the delayed outgrowth of the SRVP and decreased angiogenic sprouting in $Ndp^{y/-}$ mice are direct effects of the reduced proliferation of endothelial cells from the SRVP.

INTRODUCTION

Mutations in the human *NDP* (*Norrie disease pseudoglioma*) gene, encoding Norrin, cause congenital blindness, progressive deafness and mental retardation, a triad of symptoms characteristic for Norrie disease (ND) (1–5). Alternatively, mutations in *NDP* can exclusively lead to ocular symptoms in X-linked exudative vireoretinopathy (EVR) (6), Coats' disease and retinopathy of prematurity (7,8). EVR is also caused by mutations in Frizzled-4 (*FZD4*, FZD4), low-density lipoprotein receptor-related protein 5 (*LRP5*, LRP5) or tetraspanin-12 (*TSPAN12*, TSPAN12) (9–11). Recessive mutations in *LRP5* may also cause osteoporosis pseudoglioma syndrome (OPPG), which manifests with low bone mass in addition to the ocular phenotype in patients (OMIM: #259770). It has been shown *in vitro* that Norrin is a ligand for the canonical Wnt signaling receptor complex consisting of FZD4, LRP5 and TSPAN12 (12,13). Furthermore, the outgrowth of the superficial retinal vascular plexus (SRVP) from $Ndp^{y/-}$, $Fzd4^{-/-}$, $Lrp5^{-/-}$ and $Tspan12^{-/-}$ is delayed and incomplete and all of these knockout mice lack the deep and intermediate retinal vascular plexuses (12–16). We generated and examined a Norrin knockout mouse model ($Ndp^{y/-}$) that resembles the human Norrie disease phenotype with respect to blindness and hearing loss (4,14,17). Hyaloid vessels do not completely regress in $Ndp^{y/-}$, $Fzd4^{-/-}$, $Lrp5^{-/-}$ and $Tspan12^{-/-}$ knockout mice (12–14,16). Retinal vascular hemorrhage and exudation from retinal blood vessels in *Ndp* knockout mice ($Ndp^{y/-}$) are characteristic features. We previously demonstrated that expression of the plasmalemma vesicle-associated protein (PLVAP), which mediates vascular fenestration and promotes vascular leakiness, is highly

*To whom correspondence should be addressed at: Schorenstrasse 16, CH-8603 Schwerzenbach. Tel: +41 446557031; Fax: +41 446557213; Email: berger@medmolgen.uzh.ch
†These two authors contributed equally.

upregulated in $Ndp^{y/-}$ retinas (18). Upregulation of PLVAP/MECA32 in retinal endothelial cells (ECs) has also been shown for $Lrp5^{-/-}$ and $Tspan12^{-/-}$ mice (13). Furthermore, it was shown that upregulation of PLVAP indicates the loss of canonical Wnt signaling (19). The delayed outgrowth of the SRVP and the absence of deep sprouting could be caused either by defects in sprouting angiogenesis or by reduced proliferation of the SRVP. Sprouting angiogenesis is mediated by endothelial tip cells that guide the growing SRVP from the optic nerve head towards the retinal periphery along a vascular endothelial growth factor (VEGF) gradient (20). Stalk cells following tip cells divide ensuring proliferation and growth. Thus, an imbalance of tip and stalk cells could lead to both observed effects. The proper differentiation of tip and stalk cells is mediated by a balanced expression and interaction of Notch1 with its ligands Dll4 and Jagged1 (21–23). Dll4 is expressed in tip cells and induces Notch signaling in adjacent stalk cells. In contrast, Jagged1 is expressed in stalk cells impeding Notch signaling in adjacent tip cells. Disruption of Notch signaling has been shown to alter morphometric parameters, such as the number of peripheral tip cell filopodia, vascular density and the number of vascular branch points. The outgrowth of the SRVP along the VEGF gradient involves MAPK signaling. VEGF, provided by astrocytes or retinal ganglion cells, binds a receptor complex consisting of VEGF receptor 2 (VEGFR2) and neuropilin 1 (Nrp1) activating downstream MAPK signaling. Loss of the cytoplasmatic Nrp1 domain ($Nrp1^{cyto\Delta/\Delta}$) or nestin-specific knockout of VEGF ($VEGF_{NES\text{-}CRE}$) in mice causes artery/vein crossing (A/V crossing) in the SRVP of these mice. $VEGF_{NES\text{-}CRE}$ mice additionally show aberrant deep sprouting (24,25).

Here, we focused on defects during development of the SRVP in $Ndp^{y/-}$ mice. We quantified several vascular and angiogenic parameters and observed extensive vessel crossing within the SRVP which might be a MAPK-characteristic feature. We found reduced cell proliferation in the SRVP at the vascular front at P6 in $Ndp^{y/-}$ mice which may explain the delayed outgrowth of the SRVP. We also detected elevated mural cell (MC) coverage of the SRVP starting at P9, which is consistent with previously found upregulation of *Tie1*, *Pdgfβ* and *Pdgfrβ*. Finally, we report for the first time endomucin-positive supernumerary central filopodia of the SRVP in $Ndp^{y/-}$ retinas culminating at P9, the time point when the deep retinal vascular plexus (DRVP) normally would develop.

RESULTS

Vascular development in Norrin knockout mice

The wild-type mouse retina is avascular at birth and outgrowth of the SRVP progresses from the center towards the periphery from P1 until P8. Because the outgrowth of the SRVP is incomplete and delayed in $Ndp^{y/-}$ mice (14), we hypothesized that there might be an imbalance between tip cell filopodia and/or adjacent stalk cell proliferation. We quantified the number of filopodia as well as the vascular density and number of branch points in the central plexus at the vascular front at P5 and P7 (Fig. 1) (Supplementary Material, Table S1). The number of filopodia was significantly increased but the vascular density (Fig. 1A, C, E, G, I, K) and the number of branch points (Fig. 1A, C, E, G, J, L) were significantly decreased at P5 and P7 in $Ndp^{y/-}$ mice. Moreover, filopodial protrusions in $Ndp^{y/-}$ mice are straighter and expand with a narrower angle than filopodia of wild-type littermates (Fig. 1O) (Supplementary Material, Table S2). In contrast to the increased number of filopodia, the vascular front in general appears to be less ramified with a reduced amount of long tip cell protrusions (Fig. 1B and F).

Comparison of vascular development in different mouse models

Available morphometric data from three Norrin-Wnt signaling knockout mice ($Fzd4^{-/-}$, $Lrp5^{-/-}$ and $Tspan12^{-/-}$), three Notch signaling knockout mice ($Dll4^{+/-}$, $Jag1^{i\Delta EC}$, $Nrarp^{-/-}$), $Ang2^{LZ/LZ}$ and Pax6 dependent hypoxia inducible factor 1 α ($HIF1\alpha^{\Delta Pax6}$) knockout mice were compared (Table 1). The morphometric comparison of $Jag1^{i\Delta EC}$ with $Ndp^{y/-}$ mice was of special interest since Jag1 has been shown to be a canonical Wnt target gene in hair follicle cells comprising two LEF/TCF-binding sites within its promoter region (26,27). We compared our morphometric data from Norrin KO mice with published morphometric data from $Jag1^{i\Delta EC}$ mice and recognized delayed and incomplete outgrowth of the SRVP, together with a reduced vascular density and a decreased number of branch points in $Jag1^{i\Delta EC}$ and $Ndp^{y/-}$ mice. In contrast to $Ndp^{y/-}$ mice, the number of tip cell filopodia was reduced in $Jag1^{i\Delta EC}$ mice. $Dll4^{+/-}$ mice have an increased number of filopodia, increased number of branchpoints and a denser vascular SRVP. Hence, the $Ndp^{y/-}$ phenotype of the SRVP displays as an intermingled picture, with a peripheral *Jag1* gain of function but central *Jag1* loss of function features. We asked the question whether or not Norrin is a negative regulator of Notch signaling. To answer this question, we examined the effect of Notch inhibition in $Ndp^{y/-}$ mice in order to see if this may rescue the abnormal vascular development. We quantified and compared morphometric parameters in Norrin knockout and wild-type mice after inhibition of Notch signaling by injection of the γ-secretase inhibitor DAPT (Fig. 2). Administration of DAPT increased vascular density in wild-type and $Ndp^{y/-}$ mice (Fig. 2A–E), while the number of filopodia only increased in wild-type but not in $Ndp^{y/-}$ retinas (Fig. 2F–J) (Supplementary Material, Table S3).

Retinal EC proliferation in Norrin-deficient mice

To test the hypothesis if Norrin acts as a mitogen for cells in the SRVP, which would explain the reduced vascular density as well as the delayed and incomplete radial vascular outgrowth in $Ndp^{y/-}$ mice, we quantified central EC proliferation after systemic bromodeoxyuridine (BrdU) injection and found significantly reduced proliferation rates of isolectin B4 (IB4)-positive ECs from the SRVP in $Ndp^{y/-}$ mice at P6 (WT: ME ± SD 101.71 ± 16.54; KO: ME ± SD 52.17 ± 9.62; *P*-value: 1.8E−5) (Fig. 3A and C). The only exceptions from this observation are local hotspots of proliferation within bulky unorganized regions at the vascular front (Fig. 3D). Additionally, we monitored the effect of Norrin on cell cycle progression in cell culture experiments by using an

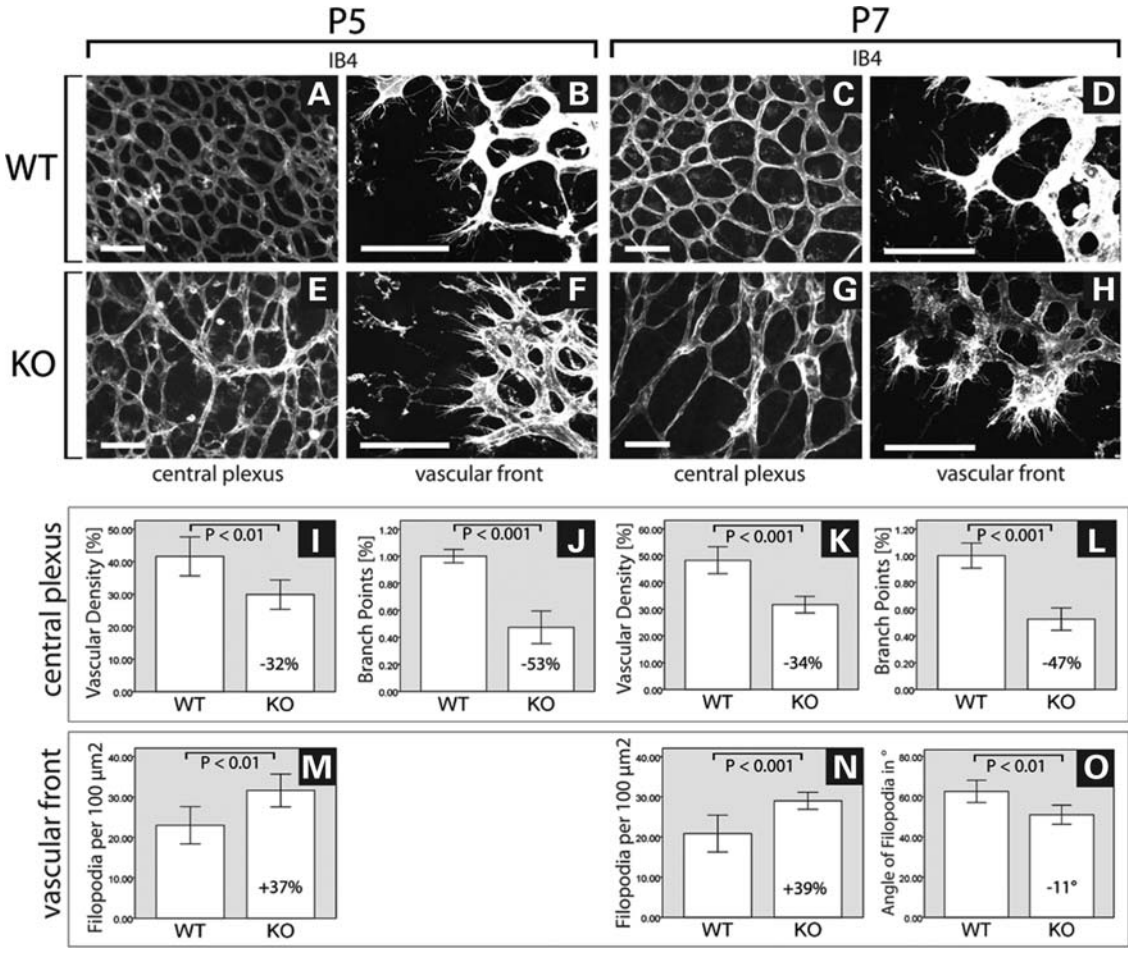

Figure 1. Morphometric parameters in Norrin knockout versus wild-type mice. $Ndp^{y/-}$ mice show decreased vascular density, a decreased number of branch points but supernumerary filopodia, which are aligned in a more narrow angle compared with wild-type mice at P5 and P7. (**A**, **E**, **C**, **G**) Representative central retinal whole-mounts from wild-type (WT) and $Ndp^{y/-}$ (KO) retinas stained with IB4. (**B**, **D**, **F**, **H**) Representative peripheral retinal whole-mounts from WT and $Ndp^{y/-}$ retinas stained with IB4. Emerging filopodia are visible. Quantification of vascular density (**I** and **K**), number of branch points (**J** and **L**), number of filopodia (**M** and **N**) and angle of filopodia (**O**). Average and confidence intervals are shown. *P*-values below $\alpha = 0.05$ were considered statistically significant. Scale bars = 100 μm.

E2F transcription factor-mediated reporter assay (cell proliferation controlling transcription factor-dependent luciferase reporter construct, reviewed in 28). For this, we transiently transfected pE2F luciferase reporter constructs into HEK293T cells which ectopically express the same amount of either human wild-type or a pathogenic variant of Norrin containing the p.C95R mutation (Supplementary Material, Fig. S1), which has been associated with the classic picture of Norrie disease (29). HEK293T cells do not endogenously express Norrin, but were positive in RT–PCR for transcripts from *FZD4*, *LRP5* and *TSPAN12* (Supplementary Material, Fig. S1). Similarly to our BrdU data in $Ndp^{y/-}$ mice, we found almost 6-fold increased cell cycle progression in cells that stably express human wild-type Norrin compared with cells that express the mutant Norrin isoform (Fig. 3F, Supplementary Material, Table S4).

Vascular remodeling in Norrin-deficient mice

Despite the reduced vascular outgrowth of the SRVP, we occasionally noticed bulky vascular areas at the front of $Ndp^{y/-}$ mice, comprising three-dimensional accumulations of ECs (Fig. 4D). To monitor vascular remodeling across the plexus, retinal whole-mounts were double stained for IB4 and collagen IV (ColIV). ColIV-positive tubes lacking IB4 staining represent empty basement membrane sleeves at positions where blood vessels have regressed (30,31). We noticed that vascular remodeling was elevated in $Ndp^{y/-}$ mice at peripheral bulky vascular areas of the SRVP, but not in central areas (Fig. 4C, white dots). Furthermore, we noticed vessel-crossing in $Ndp^{y/-}$ retinas. Vessels that morphologically resemble veins [venous character (VC)] cross and grow below vessels that resemble arteries [arterial character (AC)] between P7 and P21 (A/V crossing) (Fig. 5, Supplementary Material, Fig. S3). ACs in Norrin knockout mice also interconnect less to the central plexus compared with the wild-type and instead grow further into the periphery (Fig. 6D). At P21, disorganized twisted and tangled blood vessels form above the superficial plexus resembling fibrosis (Supplementary Material, Fig. S3t and w). We hypothesized that A/V crossing could be caused by altered astrocyte–EC interaction and therefore co-stained astrocytes against PDGFRα and blood

Table 1. Morphometric data among mutant mice with comparable retinal vascular phenotype

	Ndp$^{y/-}$	*Fzd4*$^{-/-}$	*Lrp5*$^{-/-}$	*Tspan12*$^{-/-}$	*Dll4*$^{+/-}$	*Jag1*$^{i\Delta EC}$	*Nrarp*$^{-/-}$	*Ang2*$^{LZ/LZ}$	*HIF1α*$^{\Delta PAX6}$
Pathway affected	Canonical Wnt-signaling	Canonical Wnt-signaling	Canonical Wnt-signaling	Canonical Wnt-signaling	Notch signaling	Notch signaling; tamoxifen-induced EC-specific deletion	Notch, β-catenin/ Lef1-dependent Wnt signaling	Tie2 signaling; LZ = lacZ	Hypoxia
Vascular outgrowth of SRVP	Delayed and incomplete	Delayed and incomplete	Delayed and incomplete	Delayed and incomplete	Delayed	Delayed (−44%)	Delayed but complete	Periphery remains avascular	Not delayed nor reduced
Vascular density of SRVP	Reduced (−34%, P7)	Not available	Not available	Reduced	Increased (+58%[a])	Reduced (−32%, P6)	Reduced at P5 but not different in adult	Not available	Not available
Number of branch points of SRVP	Reduced (−47%, P7)	Not available	Not available	Not available	Increased (+96%[a])	Reduced (−65%, P6)	Reduced at P5 but not different in adult	Not available	Not available
Number of filopodia of SRVP	Increased (+39%, P7)	Not available	Not available	Not available	Increased (sprouts increased +63%[a])	Reduced (−27%, P6)	Not different at P5	Not available	Not available
A/V crossing in SRVP till P7	Present	Present	Present	Present	Absent	Absent	Present	Not deducible due to picture quality	Absent
DRVP	Absent	Absent	Absent	Absent	Present	Present	Present	Absent	Present
Intermediate retinal vascular plexi	Absent	Absent	Absent	Absent	Present	Present	Present	Absent	Absent
References	Luhmann *et al.* (14), this work	Xu *et al.* (12)	Xia *et al.* (16,41) and Chen *et al.* (42)	Junge *et al.* (13)	Lobov *et al.* (21)	Benedito *et al.* (22)	Phng *et al.* (43)	Gale *et al.* (44)	Caprara *et al.* (45)

[a]% estimated from graph.

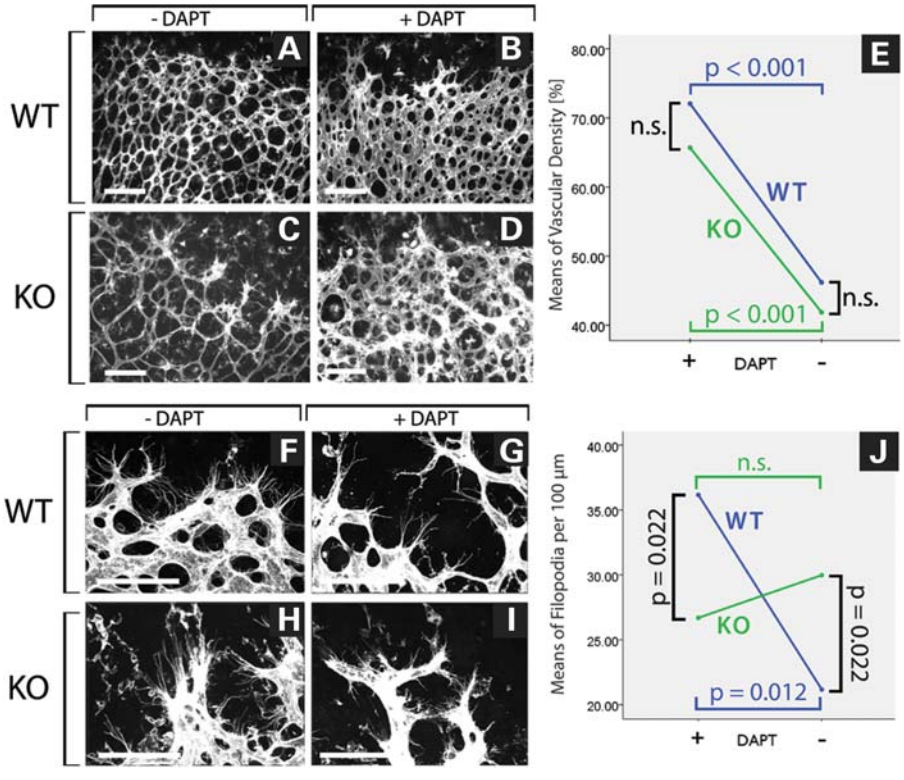

Figure 2. Effects of Notch signaling inhibition in wild-type and Norrin knockout mice. Pharmacological administration of DAPT increases vascular density at the vascular front in wild-type and *Ndp*$^{y/-}$ mice. The number of filopodia only increases in wild-type but not in *Ndp*$^{y/-}$ mice upon DAPT treatment. (**A**–**D**) Representative retinal whole-mounts stained with IB4 48 h after DAPT injection in P7 wild-type (WT) and *Ndp*$^{y/-}$ (KO) animals. (**E**) Statistical analysis shows that peripheral vascular density increases in both genotypes upon DAPT treatment. (**F**–**I**) Representative retinal whole-mounts of IB4 staining 48 h after DAPT treatment of P7 wild-type (WT) and *Ndp*$^{y/-}$ (KO) animals. Filopodia at the vascular front are visible. (**J**) Statistical analysis shows that number of filopodia increases only after DAPT treatment in the WT but not in *Ndp*$^{y/-}$ mice. *P*-values below $\alpha = 0.05$ were considered statistically significant. Scale bars = 100 μm.

vessels with IB4 (Supplementary Material, Fig. S2). We did not observe an altered astrocytic network in *Ndp*$^{y/-}$ retinas compared with wild-type and alignment between astrocytes and ECs was normal.

Mice lacking the Nrp1 cytoplasmatic domain or $VEGF_{NES\text{-}CRE}$ mice also show A/V crossing in the SRVP (24,25). This suggests that the loss of MAPK signaling might cause this phenotype. Therefore, we made use of our stably wild-type or p.C95R Norrin expressing HEK293T cell lines (Supplementary Material, Fig. S1) to monitor MAPK activity. We found a 1.9-fold increase in MAPK signaling in cells that express wild-type Norrin compared with those that expressed the mutant, disease-associated variant (Fig. 5I, Supplementary Material, Table S5).

Because of the above-described, strong SRVP phenotype in *Ndp*$^{y/-}$ mice, it was crucial to examine whether the VCs and ACs exhibit characteristic molecular features of the respective vessel types. Retinal flatmounts were stained either for endomucin or for smooth muscle actin (SMA) at P7, P9, P12 and P21. In both, wild-type and *Ndp*$^{y/-}$ mice, endomucin stained veins and venous portions while staining of arteries and arterioles was less intense (Fig. 6, Supplementary Material, Fig. S4) (32,33). Interestingly, the endomucin staining revealed supernumerary thorn-like assembled central filopodia around veins and capillaries of *Ndp*$^{y/-}$ retinas (Fig. 6D and E). In contrast, capillary sprouts were much less abundant and, if present, much shorter in wild-type mice. Staining for the arterial and MC marker α-SMA in wild-type mice specifically labeled arteries at P7, P9 and P12 as well as arteries and large veins at P21. In *Ndp*$^{y/-}$ retinas, arteries, veins and capillaries were covered with SMA-positive cells at P9, P12 and P21 (Fig. 7, Supplementary Material, Fig. S5). Thus, MC recruitment to the SRVP is abnormally increased in *Ndp*$^{y/-}$ retinas.

DISCUSSION

Deficiency of Norrin is known to cause Norrie disease, a severe X-linked recessive human disease characterized by congenital blindness, progressive hearing loss and, in some patients, mental retardation. We made use of a mouse model which mimics the human disease in eye and ear and applied morphometric analyses, Notch-inhibition by DAPT administration, as well as cell proliferation assays to characterize the angiogenic processes in the retina. We provide evidence that Norrin is a mitogenic stimulus for cells in the SRVP. Consistently, wild-type Norrin promotes E2F transcription factor-mediated cell cycle progression in a cell culture assay. Further, we identified endomucin as a marker for central filopodia, which were aligned in a thorn-like fashion at P9 in *Ndp*$^{y/-}$ mice. Finally, we found aberrant vascular SMA-positive MC coverage of veins and capillaries in the SRVP

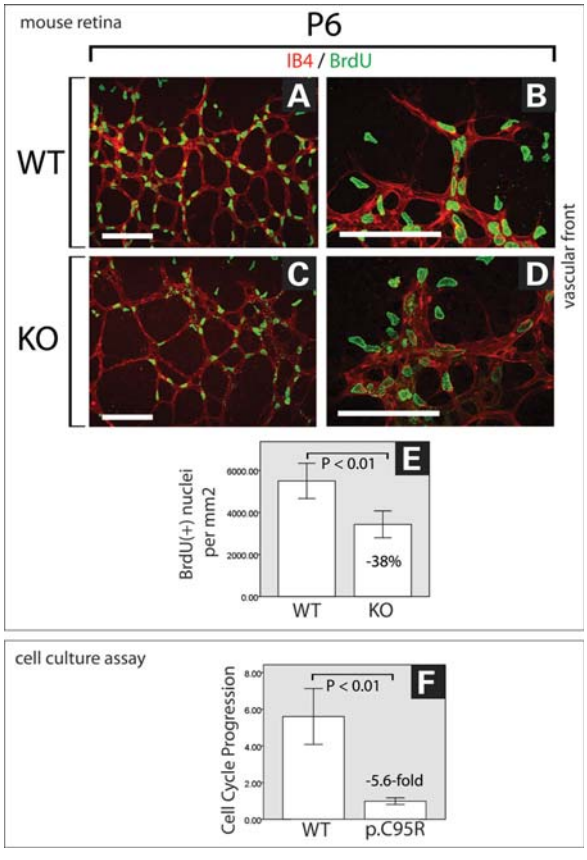

Figure 3. Decreased proliferation rate of ECs in Norrin knockout mice and reduced cell cycle progression due to a mutation (p.C95R) in human Norrin. Overall proliferation is reduced in $Ndp^{y/-}$ mice at P6. Representative retinal whole-mounts of wild-type (WT) (**A** and **B**) and $Ndp^{y/-}$ mice (KO) (**C** and **D**) were stained for blood vessels with IB4 (red) and for proliferating cells after BrdU incorporation (green). (D) Local hotspots of proliferation within thickened areas of the vascular front are occasionally seen in $Ndp^{y/-}$ mice and were excluded from quantification of proliferation. (**E**) Quantification of proliferating vascular ECs after BrdU-incorporation revealed a reduced proliferation rate (−38%) in $Ndp^{y/-}$ mice. (**F**) Expression of wild-type Norrin (WT) leads to 5.6-fold increase in the proliferation rate in HEK293T cells compared with cells expressing a mutant (p.C95R) human Norrin. Average and confidence intervals are shown. *P*-values below $\alpha = 0.05$ were considered statistically significant. Scale bars = 100 μm.

in $Ndp^{y/-}$ mice which indicates abnormally increased MC recruitment of the SRVP from Norrin KO mice.

Norrin and Notch signaling are not directly linked

We examined features of the SRVP in $Ndp^{y/-}$ mice by quantifying and comparing morphometric parameters (Figs 1 and 2, Supplementary Material, Tables S1–S3) with published data from different mouse models with retinal vascular phenotypes (Table 1). We did not quantify later stages than P7 since the outgrowth of the superficial plexus in wild-type mice ends soon after this stage of development.

We noticed that the outgrowth of the SRVP is delayed in all mouse models (Table 1), but incomplete vascular outgrowth was only observed in mutants with disrupted canonical Wnt signaling ($Ndp^{y/-}$, $Fzd4^{-/-}$ and $Lrp5^{-/-}$). Both the deep

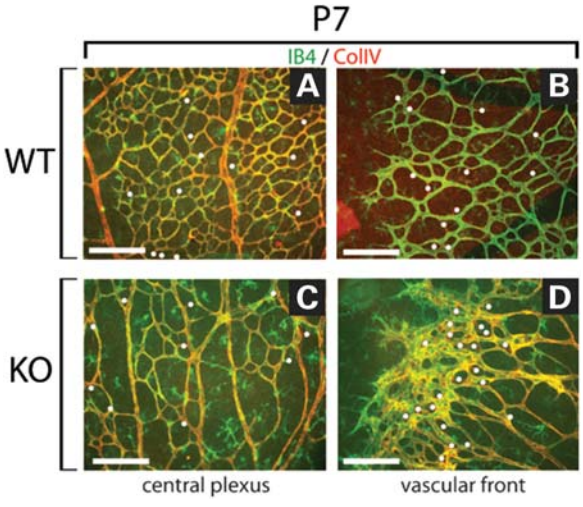

Figure 4. Massive vessel regression at the bulky vascular front in $Ndp^{y/-}$ mice at P7. IB4 (green) and ColIV (red) co-stained retinal whole-mounts from wild-type (WT) (**A** and **B**) and $Ndp^{y/-}$ mice (KO) (**C** and **D**). ColIV+, IB4-stainings represent empty membrane sleeves, where blood vessels have regressed (white dots). Regression was increased at the bulky vascular front in $Ndp^{y/-}$ retinas (D). Scale bars = 100 μm.

and intermediate retinal vascular plexuses (DRVP, IRVP) are absent in mice with deficient Wnt signaling components ($Ndp^{y/-}$, $Fzd4^{-/-}$, $Lrp5^{-/-}$ and $Tspan12^{-/-}$) and in $Ang2^{LZ/LZ}$ mice, but not in Notch signaling deficient mice ($Dll4^{+/-}$ or $Jag1^{i\Delta EC}$). The intermediate plexus is absent in $HIF1\alpha^{\Delta Pax6}$ mice, while the deep plexus is present (Table 1). We hypothesized that the canonical Wnt target gene *Jag1* might link Norrin-Wnt and Notch signaling during development of the SRVP, since knocking out *Ndp* or *Jag1* leads to aberrant SRVP development. However, we found significant differences in morphometric parameters between $Ndp^{y/-}$ and $Jag1^{i\Delta EC}$ retinas, which are in conflict with this hypothesis. The number of filopodia was increased in $Ndp^{y/-}$ and reduced $Jag1^{i\Delta EC}$ mice. $Jag1^{i\Delta EC}$ retinas also do not display defects in deep vascular development (22) which is a characteristic feature in $Ndp^{y/-}$ retinas. All these phenotypic differences suggest that there is no direct link between Norrin-Wnt and Notch signaling via Jag1.

Inhibiting Notch signaling through systemic DAPT administration led to an increased vascular density in $Ndp^{y/-}$ mice, but it did not reduce the supernumerary filopodia. Furthermore, vascular density increased similarly in wild-type and $Ndp^{y/-}$ retinas after DAPT treatment, excluding a synergistic effect (Fig. 2E). Accordingly, interaction effects were rejected by univariate analysis of variance (data not shown). Although the peripheral vascular network at the front is denser in DAPT-treated $Ndp^{y/-}$ mice (Fig. 2D), it still seems disorganized, three-dimensional and not planar. This implies that Notch inhibition can induce a peripheral hyper angiogenic response in $Ndp^{y/-}$ mice but not re-establish normal vascular development. The diameter of the peripheral blood vessels increased, which might be due to involvement of Dll4-Notch signaling in A/V differentiation, leading to a more pronounced venous phenotype after DAPT injection and to an increase in vessel diameter (Fig. 2A–D). The number of filopodia significantly

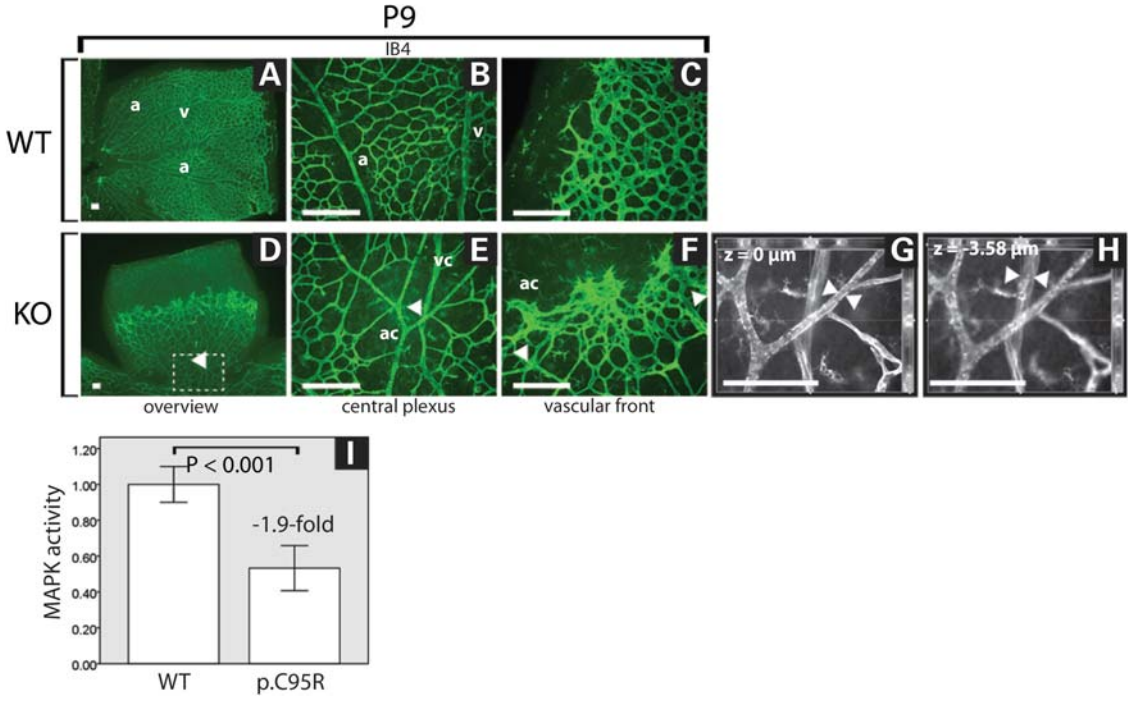

Figure 5. Blood vessel crossing in Norrin knockout mice. Arteries and veins often cross each other in *Ndp*$^{y/-}$ retinas. Retinal whole-mounts of wild-type (WT) (**A**–**C**) and *Ndp*$^{y/-}$ mice (KO) (**D**–**H**) were stained with IB4 to label blood vessels (green A–F, or grey G + H). We noticed abundant A/V crossings at the center (E, arrowheads) and periphery (F, arrowheads) of the SRVP from *Ndp*$^{y/-}$ retinas. Note, that (E) represents the box indicated in (D). (G) and (H) are confocal images from the blood vessels marked in (E), focused on the upper artery (G), and on the lower vein (H). The distance between both vessels is 3.58 μm. (I) Ectopic expression of wild-type Norrin (WT) leads to 1.9-fold increase in MAPK signaling in HEK293T cells compared with cells expressing a mutant (p.C95R), disease-associated human Norrin. a, artery; ac, arterial character; v, vein; vc, venous character. Scale bars = 100 μm.

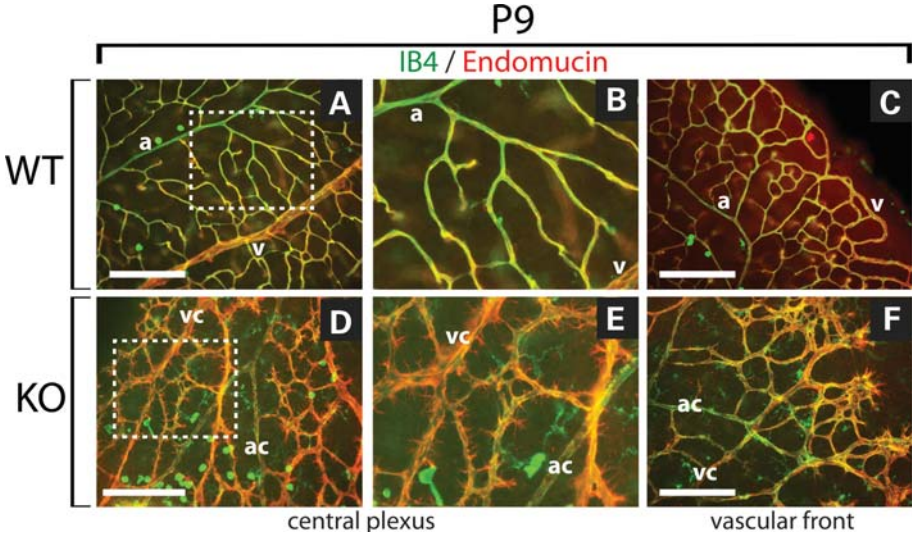

Figure 6. Large central filopodia in *Ndp*$^{y/-}$ mice at P9. Retinal whole-mounts from wild-type (WT) (**A**–**C**) and *Ndp*$^{y/-}$ mice (KO) (**D**–**F**) were co-stained with IB4 (green) to label blood vessels and with endomucin (red) which preferentially stains veins, venous vessels and central filopodia. (B) represents box in (A) and (E) represents box in (D). Endomucin staining revealed that vessels with a venous character (vc) but not with an arterial character (ac) are laced with supernumerary central filopodia. a, artery; v, vein. Scale bars = 100 μm.

increased in wild-type mice, but was unaltered in *Ndp*$^{y/-}$ retinas upon DAPT administration (Fig. 2G, I, J).

Vascular remodeling in Norrin-deficient mice

We found enhanced vascular proliferation (Fig. 3) and also enhanced vascular regression/remodeling (Fig. 4) at the vascular bulky front in *Ndp*$^{y/-}$ mice after BrdU injection and by co-staining of ColIV and IB4. We interpret the vessel regression of *Ndp*$^{y/-}$ retinas as secondary effect which ensures a planar vascular plexus at positions where bulky vascular fronts were present before moving towards the periphery. Disorganized vascular fronts are also present in *Fzd4*$^{-/-}$, *Lrp5*$^{-/-}$ and *Tspan12*$^{-/-}$ retinas (12,13,34).

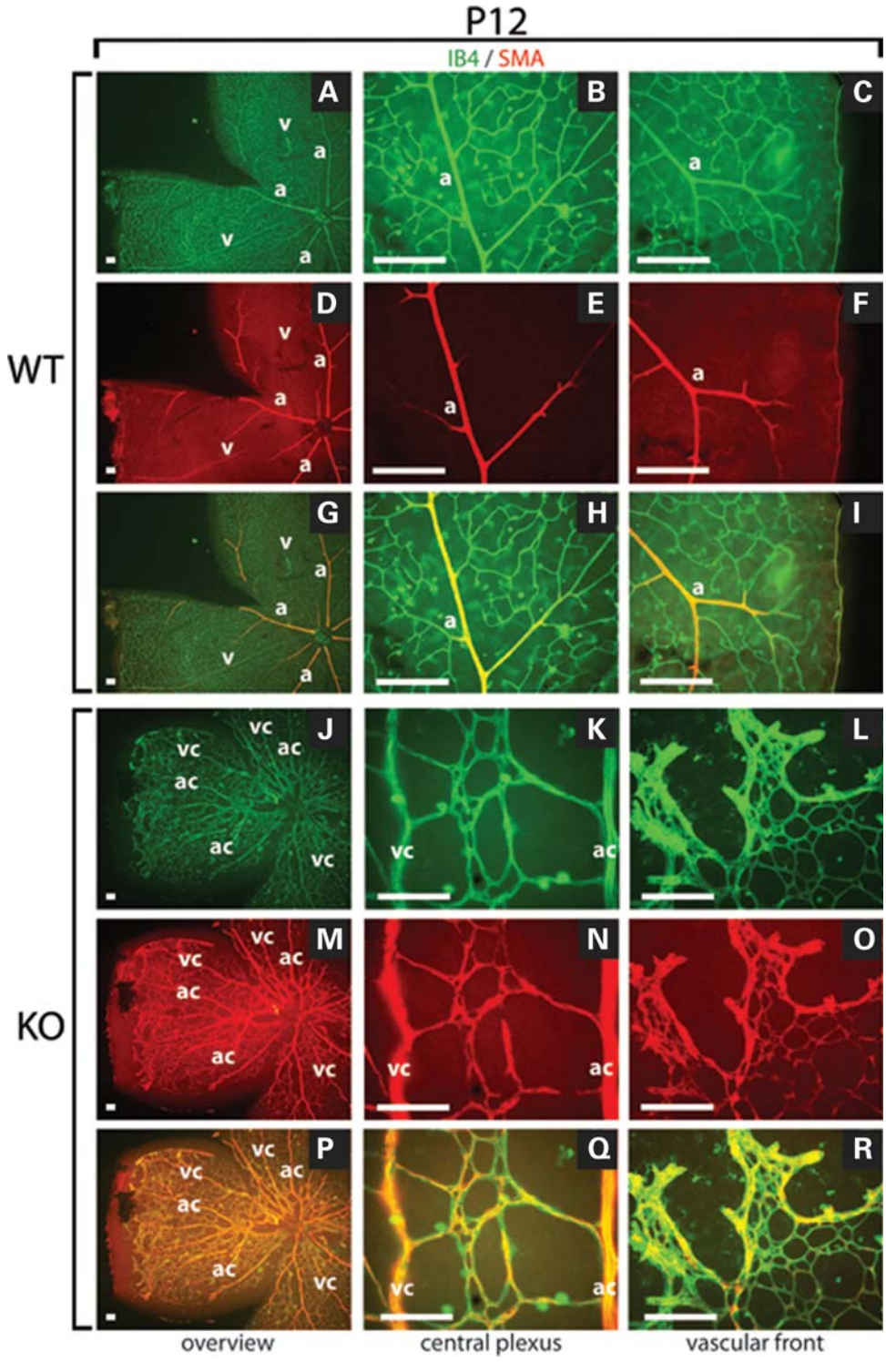

Figure 7. Retinal veins and capillaries are abundantly covered by mural cells (MCs) in $Ndp^{y/-}$ mice at P12. Retinal whole-mounts were co-stained with IB4 to label blood vessels (green) and against SMA to label arteries covered by MCs (red). Only arteries were covered by MCs in wild-type (WT) retinas. In contrast, arteries, veins and capillaries were covered by MCs in $Ndp^{y/-}$ retinas (KO). a, artery; ac, arterial character; v, vein; vc, venous character. Scale bars = 100 μm.

Further, we observed extensive crossing of arteries and veins (A/V) in $Ndp^{y/-}$ retinas and we excluded an altered astrocytic scaffold to be the reason for these observations (Supplementary Material, Fig. S2).

Loss of Norrin signaling might alter MAPK signaling

A/V crossing is a feature of all Norrin-Wnt signaling deficient mice and also (12,13,16,24,25) the lack of the cytoplasmatic

domain of Nrp1 (*Nrp1*$^{cyto\Delta/\Delta}$) or dosage-dependent reduction in neuronal VEGF-A paracrine signaling (VEGF-A$_{NES\text{-}CRE}$) lead to A/V crossing (24,25). The receptor pair consisting of VEGFR2 and Nrp1 triggers VEGF-mediated downstream MAPK signaling. Thus, the existence of A/V crossing in *Ndp*$^{y/-}$ retinas and in retinas from VEGF-A$_{NES\text{-}CRE}$ and *Nrp1*$^{cyto\Delta/\Delta}$ mice suggests that both pathways influence each other. Supporting this, Norrin-stimulated cells have elevated MAPK signaling activity compared with cells stimulated with mutant Norrin (Fig. 5I). Similarly, we previously reported MAPK signaling to be the major pathway influenced by Norrin signaling according to transcriptome analyses using microarray data from *Ndp*$^{y/-}$ retinas (18). Therefore, it will be intriguing to investigate the putative link between Norrin-Wnt and VEGF/Nrp1/MAPK signaling.

Norrin stimulates mitogenic activity in retinal ECs

Since the loss of Norrin leads to delayed and incomplete outgrowth of the SRVP, we analyzed the mitogenic activity of Norrin in mouse retinas and in cell culture using systemic BrdU injection and reporter assays, respectively. The reduced proliferation of IB4-positive ECs from the SRVP in *Ndp*$^{y/-}$ retinas, as revealed after BrdU injection, indicates that Norrin might act as a mitogenic stimulus (Fig. 3). Additionally, we monitored cell cycle progression by using the pE2F luciferase reporter construct. As expected, HEK293T cells, which endogenously express FZD4, LRP5 and TSPAN12 but not Norrin, and ectopically express human wild-type Norrin had an increased cell cycle progression compared with ectopically p.C95R mutant Norrin expressing cells (Fig. 3F). Consistently, Ohlmann *et al*. (35) observed, by using a BrdU ELISA, that Norrin efficiently stimulates proliferation of human retinal microvascular ECs *in vitro* in a Wnt-dependent manner. Our findings together with the BrdU ELISA suggest that Norrin might act as a mitogenic stimulus on microvascular/capillary ECs of the SRVP (Fig. 3C). This also can explain the delayed outgrowth of the SRVP. A key to understand the complexity of the retinal vascular phenotype in *Ndp*$^{y/-}$ mice could be the differentiated view of events at the angiogenic front and within the central plexus. Transient peripheral phenomena like local hotspots of proliferation and remodeling, thickening of the vasculature and supernumerary filopodia could be interpreted as inability of vascular sprouts to escape the existing plexus. Hence, filopodia-projecting tip cells could be overrun by stalk cells, cluster and form the observed bulky areas. The supposed explanation for the *Ndp*$^{y/-}$ superficial plexus phenotype is also supported by *in silico* models of vascular network formation. Travasso *et al*. (36) recently found, utilizing a mathematical model of sprouting angiogenesis, that low tip cell motility leads to a sparsely ramified plexus and increased stalk cell proliferation. Due to the lack of long tip cell protrusions projecting into the avascular space ahead of the vascular front, also characteristic for *Ndp*$^{y/-}$ mice, stalk cells spend more angiogenic factors which decrease its concentrations and inhibits branching. The same study highlights that low overall EC proliferation also leads to reduced vessel ramification, corroborating our observations.

Veins and capillaries of *Ndp*$^{y/-}$ retinas possess supernumerary central filopodia

To investigate the properties of ACs and VCs, we stained retinal whole-mounts against endomucin and SMA.

The surface of veins and capillaries in *Ndp*$^{y/-}$ retinas was laced with endomucin-positive filopodia instead of being smooth and covered with none or very few filopodia as in control mice. The abundance of central filopodia peaks around P9, exactly when deep vascular sprouting in wild-type mice occurs. Interestingly, deep sprouting exclusively originates from venous vessels and capillaries but not from arteries. Therefore, it seems that veins and capillaries of the SRVP from *Ndp*$^{y/-}$ retinas are able to create misaligned central filopodia. However, these filopodia might not be functional, since *Ndp*$^{y/-}$ mice lack deep sprouting. It is also unclear which molecular mechanisms lead to those central supernumerary filopodia since published data focuses exclusively on the regulation of tip cell filopodia.

Veins and capillaries of *Ndp*$^{y/-}$ retinas are excessively covered by MCs

Staining of retinal blood vessels for SMA revealed extensive MC coverage of veins and capillaries from P9 onwards. This coverage persists at least till P21. We previously reported upregulation of *PDGFβ* and *PDGFRβ* within the same timeframe (14). Interaction of all these genes regulates MC recruitment. Here, overexpression of *PDGFβ* and its receptor (*PDGFRβ*) could stimulate MC recruitment and the missing upregulation of *Ang1* on MCs might prevent restriction of MC recruitment. Considering this as the likely mechanism of the excessive MC recruitment, we believe that this might be a response to vessel leakiness caused by upregulation of *VEGF-A* and *PLVAP* (14,18) due to hypoxia. Currently, it is unclear if this extensive MC recruitment goes along with a gain of AC in the affected veins and venules. If so, the gain in arterial or loss of VC could explain the disability to form the DRVP out of the SRVP from *Ndp*$^{y/-}$ retinas, since deep sprouts emerge exclusively from venous vessels and capillaries of the SRVP (37). The fact that we still can morphologically distinguish ACs and VCs and that we detected supernumerary endomucin-positive central filopodia on veins, venules and capillaries, but not on arteries, argues against a complete loss of the VC. However, the formation of uncoordinated central endomucin-positive filopodia at P9 and the excessive MC recruitment of venous vessels may indicate at least a partial loss of venous identity of the respective ECs with the consequence that central tip cells might develop, but being unable to induce proper deep sprouting.

The morphometric analysis together with results from the DAPT injections does not suggest a direct link between Norrin-Wnt and Notch signaling via Jag1. Our results suggest that Norrin is a mitogenic stimulus for IB4-positive ECs of the SRVP which explains its delayed outgrowth in *Ndp*$^{y/-}$ mice. The A/V crossing occurs unlikely due to a disturbed astrocyte–EC interaction and it is unclear if the altered basal membrane of the SRVP contributes to this effect. We found that Norrin is able to stimulate MAPK signaling and also previously reported that MAPK signaling

might be the primarily altered pathway in Norrin KO retinas. All this together with the A/V crossing phenotype suggests that MAPK signaling might be significantly altered in Norrin KO retinas. We also found excessive MC coverage of veins, venules and capillaries in $Ndp^{y/-}$ retinas which might indicate a partial loss of venous identity but also contribute to the appearance of the altered basal lamina and possibly to the appearance of the thorn-like supernumerary central filopodia. Postnatal stages after P7 in mice mimic developmental stages from patients when hypoxia increases and leads to pathologic alterations of various retinal angiogenic maturation processes. These data are crucial for the investigation of related diseases, like familial exudative vitreoretinopathy or Coats' disease, with a less severe phenotype than Norrie disease, which have a realistic chance for the development of treatment regimens.

MATERIALS AND METHODS

Animals

Generation of the $Ndp^{y/-}$ mouse line has been described elsewhere (4). The research was performed in accordance with the ARVO Statement for the Use of Animals in Ophthalmic and Vision Research and was approved by the Veterinary Office of the State of Zurich (Switzerland).

Immunohistochemical staining

Retinas for whole-mount immunohistochemistry were fixed in 4% paraformaldehyde for 2 h or overnight at 4°C. After fixation, retinas were blocked using 1–10% normal goat or rabbit serum (VectorLabs) in PBST and subsequently incubated overnight with biotinylated IB4 (1:200; VectorLabs). The following primary antibodies were diluted in 1–5% serum in PBST and incubated over night: αSMA-CY3 (1:500; Sigma), ColIV (AbD serotec, 1:200), PDGFRα (R&D Systems, 1:500) and Endomucin (R&D Systems, 1:100). For secondary detection, Alexa Fluor streptavidin conjugates (Molecular Probes, 1:100) or anti-goat/rabbit Alexa Fluor-coupled secondary antibodies (Invitrogen, 1:500) were used. Retinas were washed five times with PBS, flat mounted and analyzed under bright-light illumination with a microscope (Axioplan 2, AxioCam HRc; Carl Zeiss) equipped with ApoTome (Carl Zeiss) or by confocal imaging using the CLSM Leica SP2 inverse microscope (Leica). The protocol from Pitulescu *et al*. (46) was used to stain for proliferating ECs (BrdU staining).

Image processing

Image J 1.44p (NIH) and Photoshop CS5 (Adobe) software were used for image processing. Overall image brightness was adjusted in a linear fashion on whole images if it was necessary to improve picture quality for prints. These adjustments did not influence interpretation and are in concert with suggestions for image processing in reference (38). Results shown were obtained by performing at least two different independent experiments including at least four mutant or control animals per stage.

Morphometric analysis of retinal flatmounts

Each morphometric parameter was determined by averaging over four non-overlapping images per retina (one retina used per animal) with a minimum of four animals per group. Vascular density was determined by measuring the endothelial coverage per 300 × 300 μm field at the vascular front. The number of branch points was determined by counting vessel branch points within 300 × 300 μm fields. The number of filopodia at the vascular front within 68 × 51 μm fields was counted and normalized to 100 μm length of vasculature. BrdU-positive endothelial nuclei were counted in 424 × 317 μm fields at the vascular front and normalized to endothelial coverage within the same field (21).

In vivo Notch inhibition

Notch signaling was inhibited by subcutaneous injection of 0.3 mg/g body weight N-[N-(3,5-Difluorophenacetyl-L-alanyl)]-S-phenylglycine t-butylester (DAPT, Merck) dissolved in 10% ethanol and 90% peanut oil. DAPT solution was injected twice at P5 and P6. Retinas were collected at P7. Control litters were injected with vehicle only. Seven litters were DAPT injected. Quantification of vascular density and number of filopodia in DAPT-treated versus untreated KO and WT mice were performed as described above (23).

Quantification of Norrin-dependent proliferation and MAPK signaling *in vitro*

Stably wild-type or mutant p.C95R Norrin expressing HEK293T cells were used in these assays. Equal expression levels of wild-type and mutant Norrin were determined by western blot analysis (data not shown). To examine the proliferation rate or MAPK signaling activity, 8×10^4 cells/well of a 24-well plate were seeded and incubated at 37°C/5% CO_2 overnight. Cells were transiently co-transfected with pE2F or pSRF firefly luciferase reporter and pRenilla constructs (SABiosciences) using the calcium precipitation method (39,40). Luciferase activity was measured using DualGlo-LuciferaseReporterAssaySystem (Promega). Firefly luciferase activity was normalized to co-transfected *Renilla* luciferase.

Statistical analysis

Statistical analysis was performed in SPSS 18.0 (IBM) using two-tailed unpaired Student's *t*-test.

Quantitative data from DAPT-injection experiments were processed with univariate analysis of variance with two independent variables. Avoiding bias due to unequal sample sizes, the estimated marginal means were calculated instead of arithmetically means. *P*-values below $\alpha = 0.05$ were considered significant.

SUPPLEMENTARY MATERIAL

Supplementary Material is available at *HMG* online.

ACKNOWLEDGEMENTS

We thank Britta Seebauer for contributing the immunostainings against α-SMA at P7. We also would like to thank Rui Benedito, Ralf Adams and Hiroyuki Yamamoto for giving practical advice and discussing this work as well as Wei Chi for donating the pFZD4 construct and He Xi and Bryan McDonalds for providing the pLRP5 construct.

Conflict of Interest statement. None declared.

FUNDING

This work was supported by the Velux Foundation, Zurich, Switzerland and by the Swiss National Science Foundation (Grant number 31003A_122359), Bern, Switzerland.

REFERENCES

1. Berger, W., Meindl, A., van de Pol, T.J., Cremers, F.P., Ropers, H.H., Doerner, C., Monaco, A., Bergen, A.A., Lebo, R. and Warburg, M. (1992) Isolation of a candidate gene for Norrie disease by positional cloning. *Nat. Genet.*, **1**, 199–203.
2. Berger, W., van de Pol, D., Warburg, M., Gal, A., Bleeker-Wagemakers, L., de Silva, H., Meindl, A., Meitinger, T., Cremers, F. and Ropers, H.H. (1992) Mutations in the candidate gene for Norrie disease. *Hum. Mol. Genet.*, **1**, 461–465.
3. Warburg, M. (1966) Norrie's disease. A congenital progressive oculo-acoustico-cerebral degeneration. *Acta Ophthalmol. (Copenh.)*, **85 (suppl.)**, 5–147.
4. Berger, W., van de Pol, D., Bachner, D., Oerlemans, F., Winkens, H., Hameister, H., Wieringa, B., Hendriks, W. and Ropers, H.H. (1996) An animal model for Norrie disease (ND): gene targeting of the mouse ND gene. *Hum. Mol. Genet.*, **5**, 51–59.
5. Chen, Z.Y., Battinelli, E.M., Fielder, A., Bundey, S., Sims, K., Breakefield, X.O. and Craig, I.W. (1993) A mutation in the Norrie disease gene (NDP) associated with X-linked familial exudative vitreoretinopathy. *Nat. Genet.*, **5**, 180–183.
6. Shastry, B.S., Hejtmancik, J.F. and Trese, M.T. (1997) Identification of novel missense mutations in the Norrie disease gene associated with one X-linked and four sporadic cases of familial exudative vitreoretinopathy. *Hum. Mutat.*, **9**, 396–401.
7. Black, G.C., Perveen, R., Bonshek, R., Cahill, M., Clayton-Smith, J., Lloyd, I.C. and McLeod, D. (1999) Coats' disease of the retina (unilateral retinal telangiectasis) caused by somatic mutation in the NDP gene: a role for norrin in retinal angiogenesis. *Hum. Mol. Genet.*, **8**, 2031–2035.
8. Shastry, B.S., Pendergast, S.D., Hartzer, M.K., Liu, X. and Trese, M.T. (1997) Identification of missense mutations in the Norrie disease gene associated with advanced retinopathy of prematurity. *Arch. Ophthalmol.*, **115**, 651–655.
9. Ye, X., Wang, Y. and Nathans, J. (2010) The Norrin/Frizzled4 signaling pathway in retinal vascular development and disease. *Trends Mol. Med.*, **16**, 417–425.
10. Nikopoulos, K., Gilissen, C., Hoischen, A., van Nouhuys, C.E., Boonstra, F.N., Blokland, E.A., Arts, P., Wieskamp, N., Strom, T.M., Ayuso, C. *et al.* (2010) Next-generation sequencing of a 40 Mb linkage interval reveals TSPAN12 mutations in patients with familial exudative vitreoretinopathy. *Am. J. Hum. Genet.*, **86**, 240–247.
11. Poulter, J.A., Ali, M., Gilmour, D.F., Rice, A., Kondo, H., Hayashi, K., Mackey, D.A., Kearns, L.S., Ruddle, J.B., Craig, J.E. *et al.* (2010) Mutations in TSPAN12 cause autosomal-dominant familial exudative vitreoretinopathy. *Am. J. Hum. Genet.*, **86**, 248–253.
12. Xu, Q., Wang, Y., Dabdoub, A., Smallwood, P.M., Williams, J., Woods, C., Kelley, M.W., Jiang, L., Tasman, W., Zhang, K. and Nathans, J. (2004) Vascular development in the retina and inner ear: control by Norrin and Frizzled-4, a high-affinity ligand-receptor pair. *Cell*, **116**, 883–895.
13. Junge, H.J., Yang, S., Burton, J.B., Paes, K., Shu, X., French, D.M., Costa, M., Rice, D.S. and Ye, W. (2009) TSPAN12 regulates retinal vascular development by promoting Norrin- but not Wnt-induced FZD4/beta-catenin signaling. *Cell*, **139**, 299–311.
14. Luhmann, U.F., Lin, J., Acar, N., Lammel, S., Feil, S., Grimm, C., Seeliger, M.W., Hammes, H.P. and Berger, W. (2005) Role of the Norrie disease pseudoglioma gene in sprouting angiogenesis during development of the retinal vasculature. *Invest. Ophthalmol. Vis. Sci.*, **46**, 3372–3382.
15. Richter, M., Gottanka, J., May, C.A., Welge-Lussen, U., Berger, W. and Lutjen-Drecoll, E. (1998) Retinal vasculature changes in Norrie disease mice. *Invest. Ophthalmol. Vis. Sci.*, **39**, 2450–2457.
16. Xia, C.H., Yablonka-Reuveni, Z. and Gong, X. (2010) LRP5 is required for vascular development in deeper layers of the retina. *PLoS ONE*, **5**, e11676.
17. Rehm, H.L., Zhang, D.S., Brown, M.C., Burgess, B., Halpin, C., Berger, W., Morton, C.C., Corey, D.P. and Chen, Z.Y. (2002) Vascular defects and sensorineural deafness in a mouse model of Norrie disease. *J. Neurosci.*, **22**, 4286–4292.
18. Schafer, N.F., Luhmann, U.F., Feil, S. and Berger, W. (2009) Differential gene expression in Ndph-knockout mice in retinal development. *Invest. Ophthalmol. Vis. Sci.*, **50**, 906–916.
19. Liebner, S., Corada, M., Bangsow, T., Babbage, J., Taddei, A., Czupalla, C.J., Reis, M., Felici, A., Wolburg, H., Fruttiger, M. *et al.* (2008) Wnt/beta-catenin signaling controls development of the blood-brain barrier. *J. Cell Biol.*, **183**, 409–417.
20. Gerhardt, H., Golding, M., Fruttiger, M., Ruhrberg, C., Lundkvist, A., Abramsson, A., Jeltsch, M., Mitchell, C., Alitalo, K., Shima, D. and Betsholtz, C. (2003) VEGF guides angiogenic sprouting utilizing endothelial tip cell filopodia. *J. Cell Biol.*, **161**, 1163–1177.
21. Lobov, I.B., Renard, R.A., Papadopoulos, N., Gale, N.W., Thurston, G., Yancopoulos, G.D. and Wiegand, S.J. (2007) Delta-like ligand 4 (Dll4) is induced by VEGF as a negative regulator of angiogenic sprouting. *Proc. Natl Acad. Sci. USA*, **104**, 3219–3224.
22. Benedito, R., Roca, C., Sorensen, I., Adams, S., Gossler, A., Fruttiger, M. and Adams, R.H. (2009) The notch ligands Dll4 and Jagged1 have opposing effects on angiogenesis. *Cell*, **137**, 1124–1135.
23. Hellstrom, M., Phng, L.K., Hofmann, J.J., Wallgard, E., Coultas, L., Lindblom, P., Alva, J., Nilsson, A.K., Karlsson, L., Gaiano, N. *et al.* (2007) Dll4 signalling through Notch1 regulates formation of tip cells during angiogenesis. *Nature*, **445**, 776–780.
24. Fantin, A., Schwarz, Q., Davidson, K., Normando, E.M., Denti, L. and Ruhrberg, C. (2011) The cytoplasmic domain of neuropilin 1 is dispensable for angiogenesis, but promotes the spatial separation of retinal arteries and veins. *Development*, **138**, 4185–4191.
25. Haigh, J.J., Morelli, P.I., Gerhardt, H., Haigh, K., Tsien, J., Damert, A., Miquerol, L., Muhlner, U., Klein, R., Ferrara, N. *et al.* (2003) Cortical and retinal defects caused by dosage-dependent reductions in VEGF-A paracrine signaling. *Dev. Biol.*, **262**, 225–241.
26. Katoh, M. and Katoh, M. (2006) Notch ligand, JAG1, is evolutionarily conserved target of canonical WNT signaling pathway in progenitor cells. *Int. J. Mol. Med.*, **17**, 681–685.
27. Estrach, S., Ambler, C.A., Lo, C.C., Hozumi, K. and Watt, F.M. (2006) Jagged 1 is a beta-catenin target gene required for ectopic hair follicle formation in adult epidermis. *Development*, **133**, 4427–4438.
28. Singh, S., Johnson, J. and Chellappan, S. (2010) Small molecule regulators of Rb-E2F pathway as modulators of transcription. *Biochim. Biophys. Acta*, **1799**, 788–794.
29. Isashiki, Y., Ohba, N., Yanagita, T., Hokita, N., Doi, N., Nakagawa, M., Ozawa, M. and Kuroda, N. (1995) Novel mutation at the initiation codon in the Norrie disease gene in two Japanese families. *Hum. Genet.*, **95**, 105–108.
30. Baluk, P., Morikawa, S., Haskell, A., Mancuso, M. and McDonald, D.M. (2003) Abnormalities of basement membrane on blood vessels and endothelial sprouts in tumors. *Am. J. Pathol.*, **163**, 1801–1815.
31. Baffert, F., Le, T., Sennino, B., Thurston, G., Kuo, C.J., Hu-Lowe, D. and McDonald, D.M. (2006) Cellular changes in normal blood capillaries undergoing regression after inhibition of VEGF signaling. *Am. J. Physiol. Heart Circ. Physiol.*, **290**, H547–H559.
32. Liu, C., Shao, Z.M., Zhang, L., Beatty, P., Sartippour, M., Lane, T., Livingston, E. and Nguyen, M. (2001) Human endomucin is an endothelial marker. *Biochem. Biophys. Res. Commun.*, **288**, 129–136.
33. Samulowitz, U., Kuhn, A., Brachtendorf, G., Nawroth, R., Braun, A., Bankfalvi, A., Bocker, W. and Vestweber, D. (2002) Human endomucin: distribution pattern, expression on high endothelial venules, and decoration with the MECA-79 epitope. *Am. J. Pathol.*, **160**, 1669–1681.

34. Chen, J., Stahl, A., Krah, N.M., Seaward, M.R., Dennison, R.J., Sapieha, P., Hua, J., Hatton, C.J., Juan, A.M., Aderman, C.M. *et al.* (2011) Wnt signaling mediates pathological vascular growth in proliferative retinopathy. *Circulation*, **124**, 1871–1881.
35. Ohlmann, A., Seitz, R., Braunger, B., Seitz, D., Bosl, M.R. and Tamm, E.R. (2010) Norrin promotes vascular regrowth after oxygen-induced retinal vessel loss and suppresses retinopathy in mice. *J. Neurosci.*, **30**, 183–193.
36. Travasso, R.D., Poire, E.C., Castro, M., Rodrguez-Manzaneque, J.C. and Hernandez-Machado, A. (2011) Tumor angiogenesis and vascular patterning: a mathematical model. *PLoS ONE*, **6**, e19989.
37. Fruttiger, M. (2007) Development of the retinal vasculature. *Angiogenesis*, **10**, 77–88.
38. Rossner, M. and Yamada, K.M. (2004) What's in a picture? The temptation of image manipulation. *J. Cell Biol.*, **166**, 11–15.
39. Jordan, M., Schallhorn, A. and Wurm, F.M. (1996) Transfecting mammalian cells: optimization of critical parameters affecting calcium-phosphate precipitate formation. *Nucleic Acids Res.*, **24**, 596–601.
40. Jordan, M. and Wurm, F. (2004) Transfection of adherent and suspended cells by calcium phosphate. *Methods*, **33**, 136–143.
41. Xia, C.H., Liu, H., Cheung, D., Wang, M., Cheng, C., Du, X., Chang, B., Beutler, B. and Gong, X. (2008) A model for familial exudative vitreoretinopathy caused by LPR5 mutations. *Hum. Mol. Genet.*, **17**, 1605–1612.
42. Chen, J., Stahl, A., Krah, N.M., Seaward, M.R., Joyal, J.S., Juan, A.M., Hatton, C.J., Aderman, C.M., Dennison, R.J., Willett, K.L. *et al.* (2012) Retinal expression of wnt-pathway mediated genes in low-density lipoprotein receptor-related protein 5 (lrp5) knockout mice. *PLoS ONE*, **7**, e30203.
43. Phng, L.K., Potente, M., Leslie, J.D., Babbage, J., Nyqvist, D., Lobov, I., Ondr, J.K., Rao, S., Lang, R.A., Thurston, G. and Gerhardt, H. (2009) Nrarp coordinates endothelial Notch and Wnt signaling to control vessel density in angiogenesis. *Dev. Cell*, **16**, 70–82.
44. Gale, N.W., Thurston, G., Hackett, S.F., Renard, R., Wang, Q., McClain, J., Martin, C., Witte, C., Witte, M.H., Jackson, D. *et al.* (2002) Angiopoietin-2 is required for postnatal angiogenesis and lymphatic patterning, and only the latter role is rescued by Angiopoietin-1. *Dev. Cell*, **3**, 411–423.
45. Caprara, C., Thiersch, M., Lange, C., Joly, S., Samardzija, M. and Grimm, C. (2011) HIF1A is essential for the development of the intermediate plexus of the retinal vasculature. *Invest. Ophthalmol. Vis. Sci*, **52**, 2109–2117.
46. Pitulescu, M.E., Schmidt, I., Benedito, R. and Adams, R.H. (2010) Inducible gene targeting in the neonatal vasculature and analysis of retinal angiogenesis in mice. *Nat. Protoc.*, **5**, 1518–1534.

Supplementary data

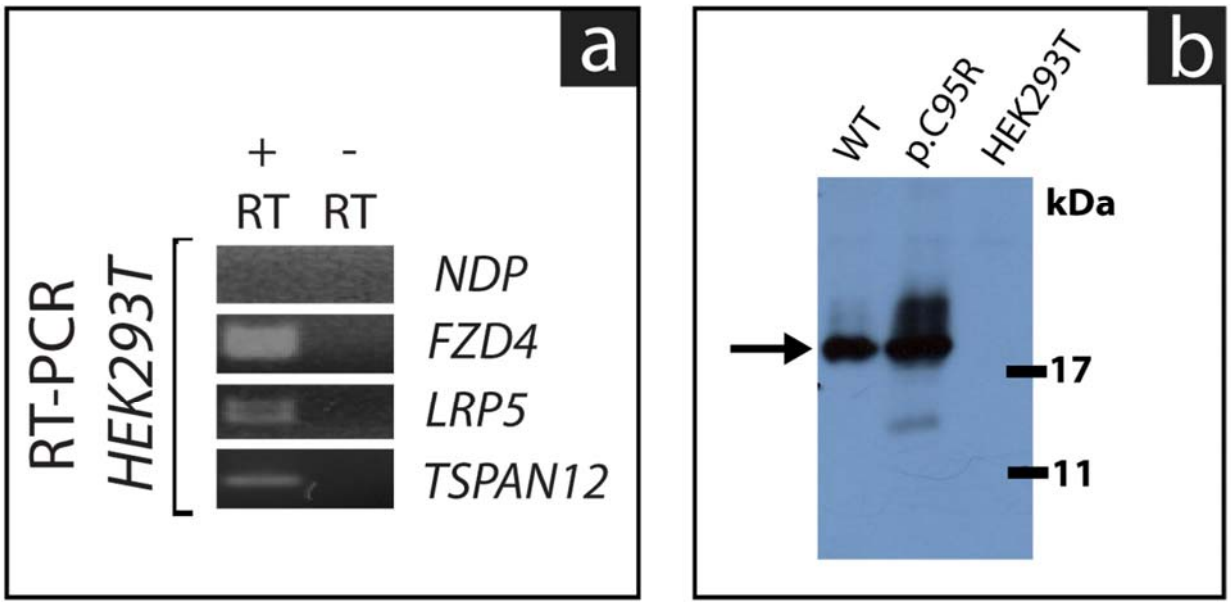

Supplementary Fig 1 HEK293T cells endogenously express Norrin receptors but no Norrin and the quantity of ectopic expression of wildtype and p.C95R Norrin in HEK293T cells is the same in both cell lines. (a) HEK293T cells used for this assay endogenously express *FZD4*, *LRP5*, *TSPAN12* but no *NDP*. (b) Western blot analysis from protein extracts of HEK293T cells that express either wildtype (WT) or p.C95R (p.C95R) mutant Norrin or Mock (HEK293T). The arrow indicates the respective Norrin which appear slightly above 17 kDa.

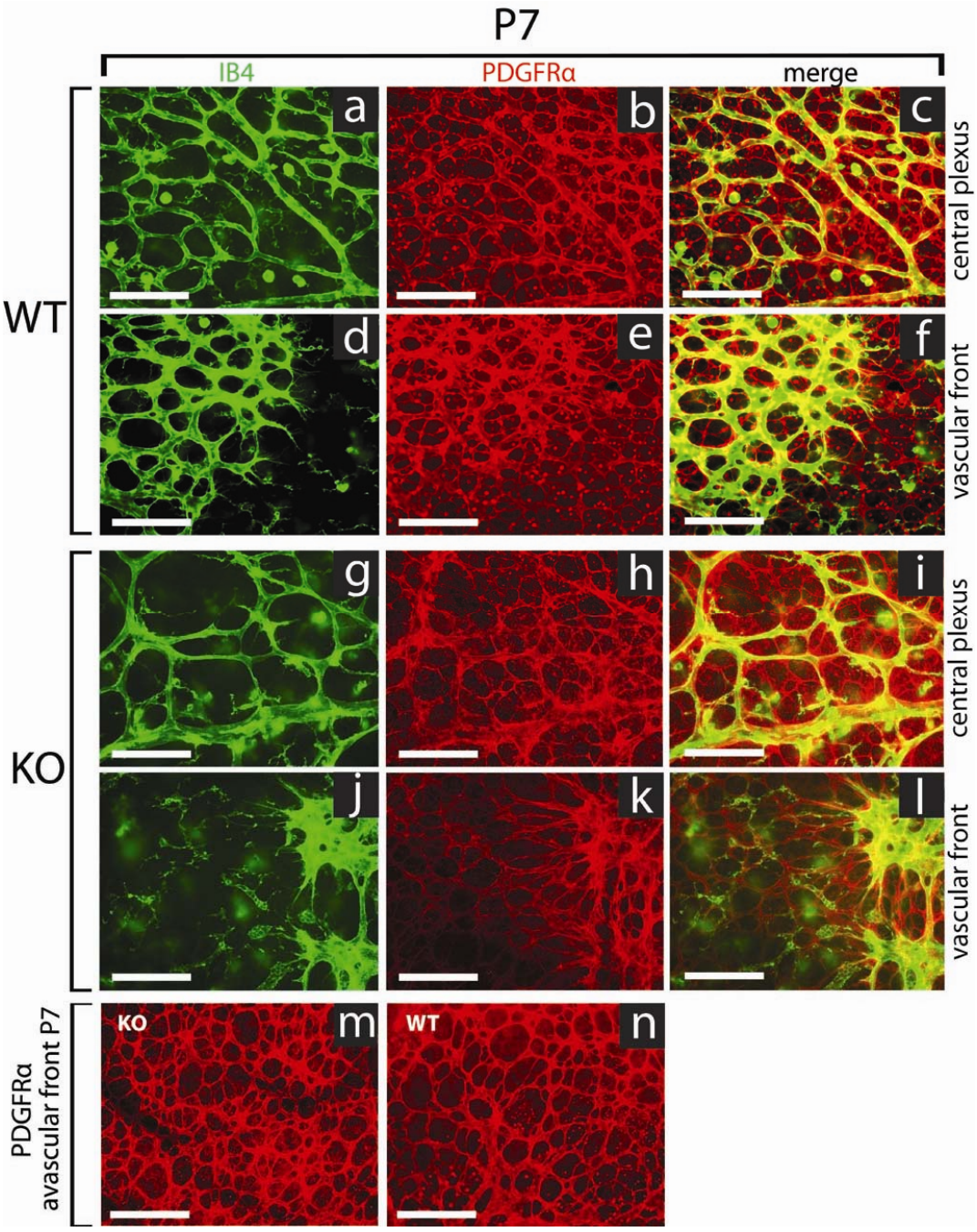

Supplementary Fig 2 Alignment of endothelial cells and astrocytes. Astrocyte/endothelial cell alignment is not altered in *Ndph*$^{y/-}$ mice at P7. Blood vessels of wildtype (WT) (a-f) and *Ndph*$^{y/-}$ retinas (KO) (g-l) were stained with isolectin B4 (IB4) to label blood vessels (green) and against PDGFRα to label astrocytes (red). Astrocytes align around the covering blood vessels in WT and KO mice. The density of the retinal astrocytic network at the avascular front is similar in *Ndph*$^{y/-}$ and wildtype retinas (m,n). Scale bar = 100 µm.

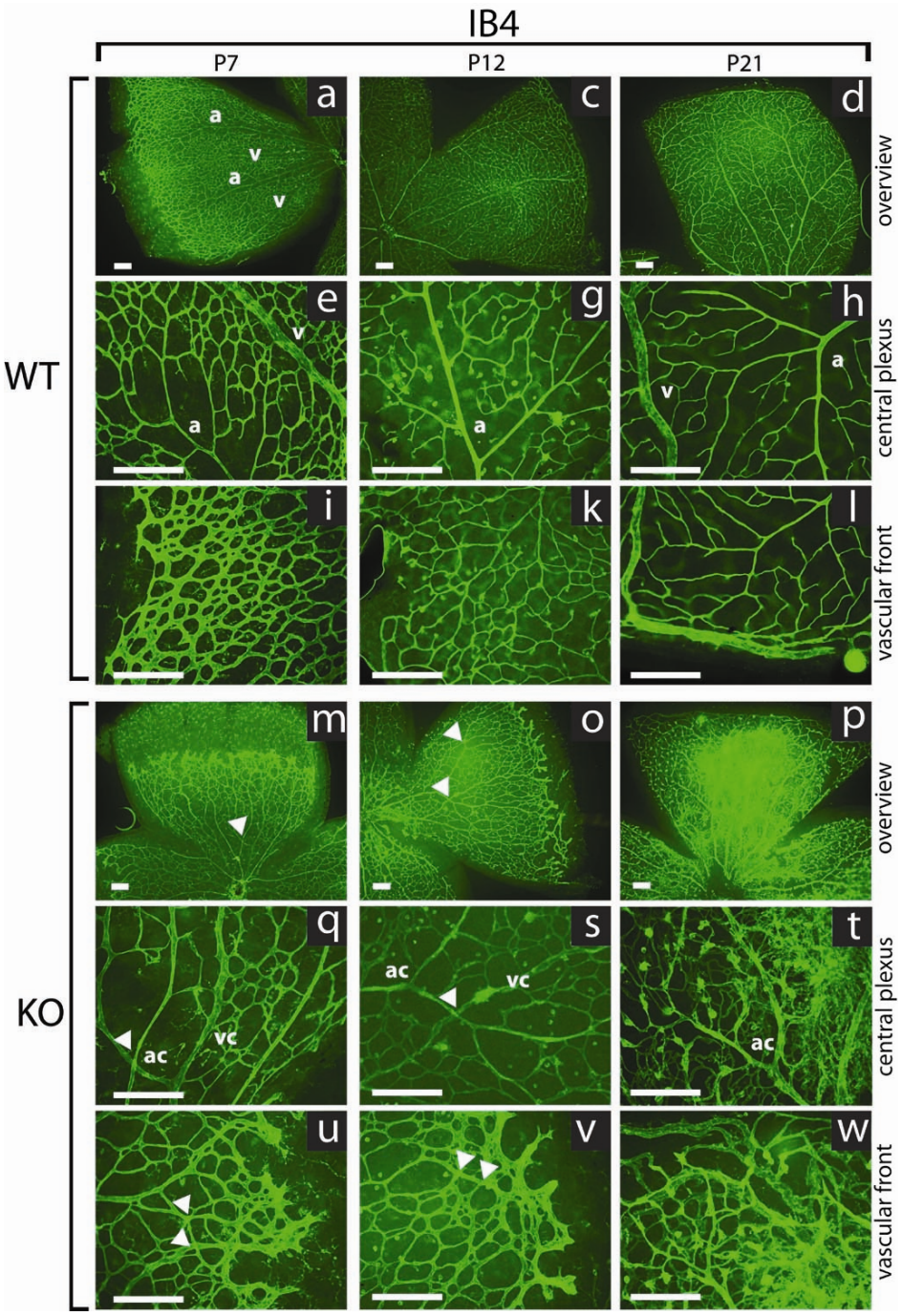

Supplementary Fig 3 Vessel crossing in norrin knockout mice. Arteries and veins often cross each other in *Ndph*$^{y/-}$ retinas between P7 and P21. Retinal wholemounts of wildtype (WT) (a-l) and *Ndph*$^{y/-}$ mice (KO) (m-w) were stained with isolectin B4 (IB4) to label blood vessels (green). We noticed abundant artery/vein crossing at the center (q, s, t) and in the periphery (u, v, w) of the superficial retinal vascular plexus from *Ndph*$^{y/-}$ retinas. a = artery, ac = arterial character, v = vein, vc = venous character. Scale bars = 100 μm

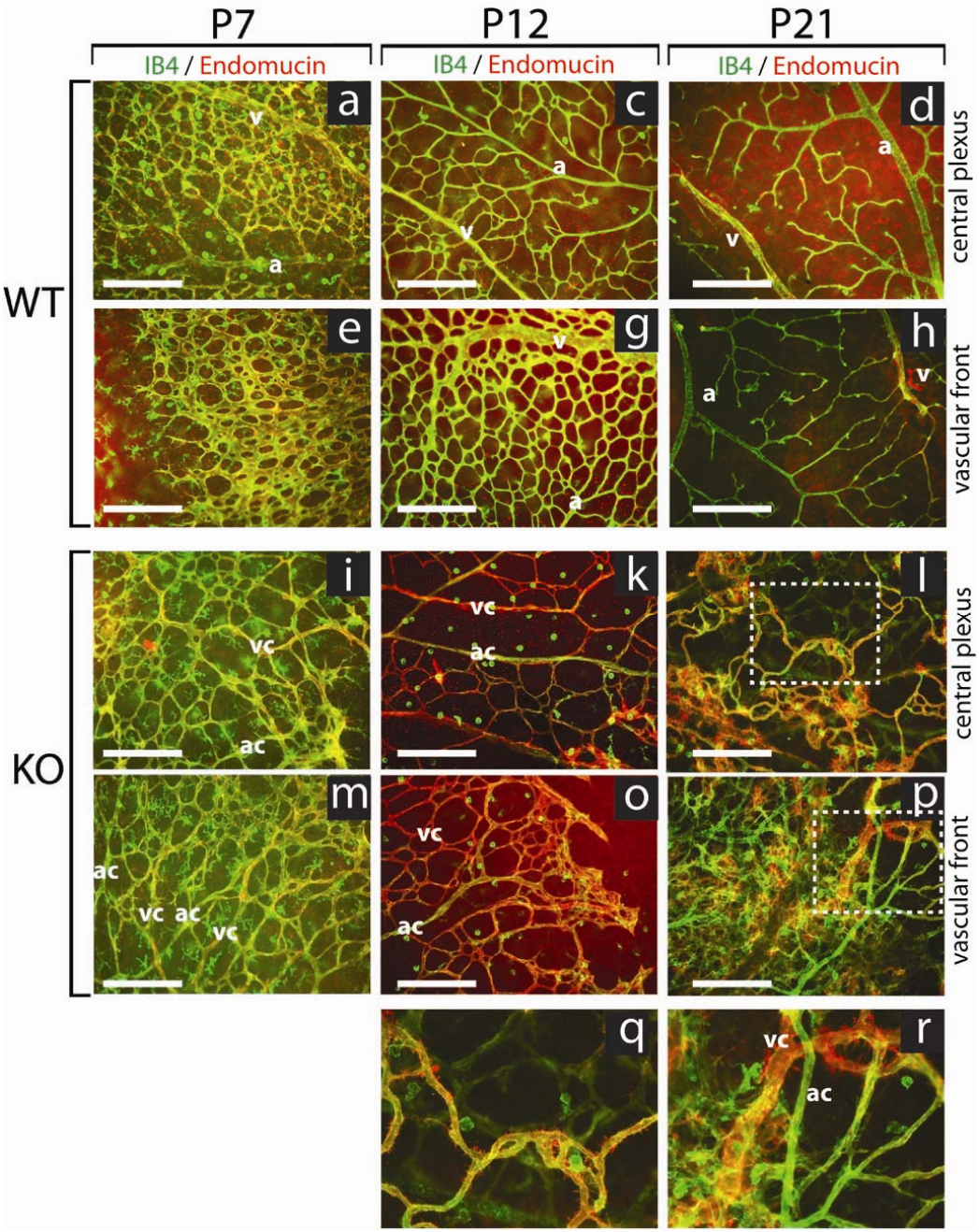

Supplementary Fig 4 *Ndph*$^{y/-}$ mice display small central filopodia at P12 and P21. Retinal flatmounts from wildtype (WT) (a-h) and *Ndph*$^{y/-}$ mice (KO) (i-r) were co-stained with isolectin B4 (IB4, green) to label blood vessels and with endomucin (red), which preferentially stained veins, venous vessels and central filopodia. (q) represents box in (l), (r) represents the box in (p). Endomucin staining revealed that vessels with venous character (vc) but no vessels with an arterial character (ac) are laced with small supernumerary central filopodia at P12 and P21 but not at P7. At P21, vessels grew above the superficial retinal vascular plexus resembling fibrosis. Fibrous vessels with vc but not ac were also laced with small filopodia (l, p, q, r). a = artery, v = vein. Scale bars = 100 μm.

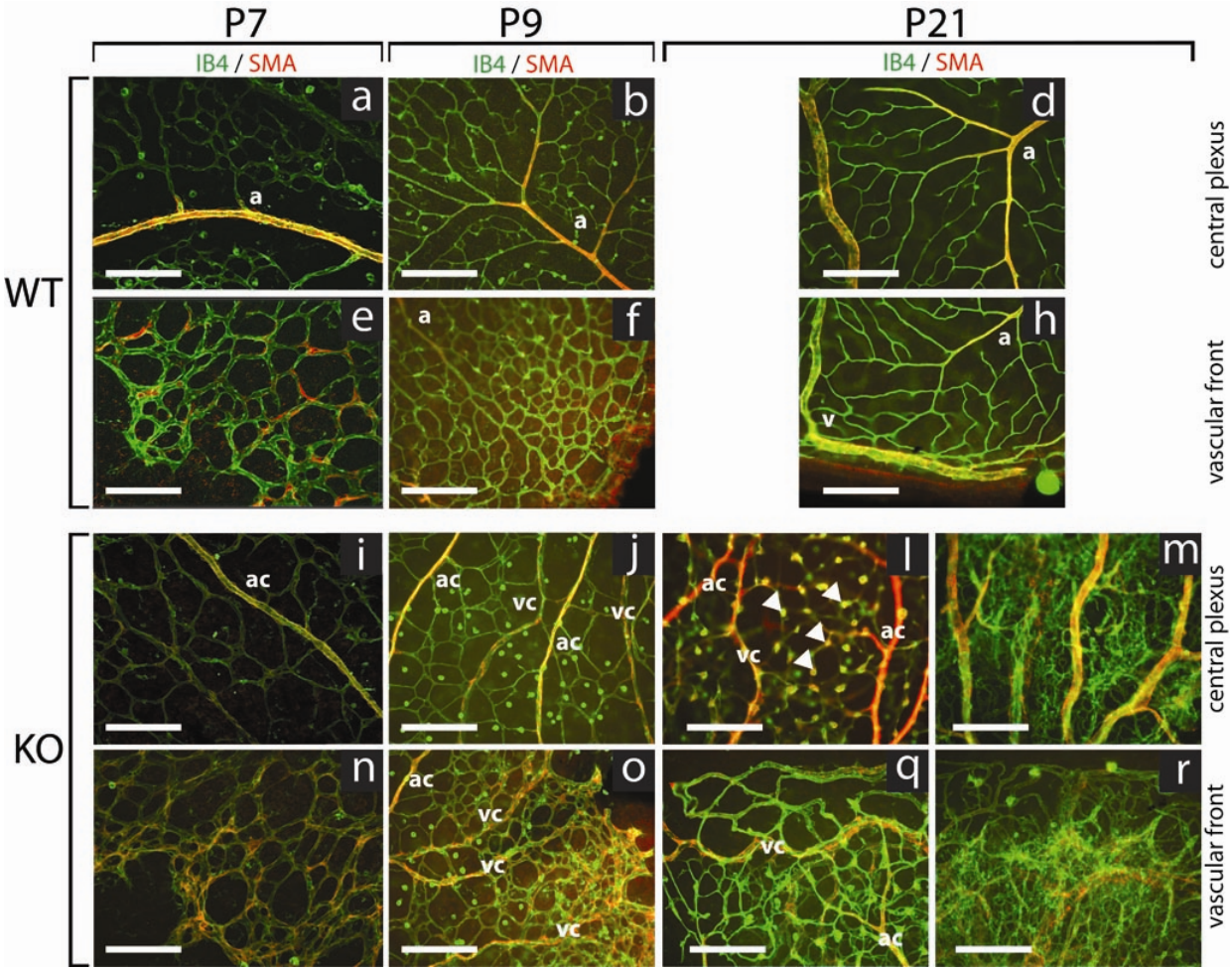

Supplementary Fig 5 Increased smooth muscle cell coverage of retinal veins and capillaries in norrin knockout mice. Retinal veins and capillaries are abundantly covered by vascular smooth muscle cells (vSMCs) in *Ndph*$^{y/-}$ mice at P9 and P21. Retinal flatmounts were co-stained with isolectin B4 (IB4) to label blood vessels (green) and against smooth muscle actin (SMA) to label arteries covered by vSMCs (red). Arteries were covered by vSMCs in wildtype (WT) retinas at P7 and P9 and arteries and veins at P21. In contrast, arteries, veins and capillaries were covered by vSMCs in *Ndph*$^{y/-}$ retinas (KO) between P9 and P21. At P21, some areas of the superficial retinal vascular plexus (SRVP) are abundantly overgrown with blood vessels resembling fibrosis (m, r). Overgrowth with blood vessels is prevented in other areas of the SRVP (l, q). These areas display drum stick like elongations that are entirely covered by vSMCs (arrowhead). a = artery, ac = arterial character, v = vein, vc = venous character. Scale bars = 100 µm.

Supplementary Table 1 Morphometric data from wildtype and *NDPh*$^{y/-}$ retinas

		wildtype retinas	NDPhy/- retinas
P5	Number of filopodia	23 ± 2 (n=5)	32 ± 5 (n=6; p-value = 0.001)
	Vascular density	42 ± 5 (n=5)	30 ± 4 (n=5; p-value = 0.002)
	Number of branchpoints	30 ± 1 (n=5)	14 ± 3 (n=5; p-value <0.0001)
P7	Number of filopodia	21 ± 3 (n=4)	29 ± 2 (n=7, p-value <0.0001)
	Vascular density	48 ± 4 (n=5)	32 ± 3 (n=7; p-value = 0.0006)
	Number of branchpoints	89 ± 7 (n=5)	47 ± 8 (n=7; p-value <0.0001)

average ± standard deviation are reported; n= number of retinas;

Supplementary Table 2 Filopodia angle

	wildtype retinas	*NDPh*$^{y/-}$ retinas
Filopodia angle in °	62.6 ± 29.0 (n=109)	51.0 ± 24.7 (n=109; p-value=0.002)

average ± standard deviation are reported; n= number of filopodia;

Supplementary Table 3 Quantification of morphometric parameters from wildtype and *NDPh*$^{y/-}$ mice after DAPT injection

Mean filopodia per 100 µm		WT +DAPT	WT -DAPT	KO +DAPT	KO -DAPT
	WT +DAPT	36 ± 7 (n=6)	p-value = 0.012	p-value =0.022	
	WT -DAPT		21 ± 3 (n=4)		p-value = 0.025
	KO +DAPT			27 ± 5 (n=6)	p-value = 0.279 (N.S.)
	KO -DAPT				30 ± 4 (n=4)
Mean vascular density		WT +DAPT	WT -DAPT	KO +DAPT	KO -DAPT
	WT +DAPT	72 ± 6 (n=6)	p-value = 0.00005	p-value = 0.149 (N.S.)	
	WT -DAPT		46 ± 5 (n=4)		p-value = 0.323 (N.S.)
	KO +DAPT			66 ± 8 (n=6)	p-value = 0.00067
	KO -DAPT				42 ± 5 (n=4)
Mean vascular length		WT +DAPT	WT -DAPT	KO +DAPT	KO -DAPT
	WT +DAPT	87 ± 3 (n=6)	p-value = 0.075 (N.S.)	p-value = 0.00002	
	WT -DAPT		83 ± 1 (n=4)		p-value = 0.00003
	KO +DAPT			70 ± 5 (n=6)	p-value = 0.022
	KO -DAPT				62 ± 2 (n=4)

average ± standard deviation are reported; n= number of retinas;

Supplementary Table 4 Cell cycle progression

	WT norrin	p.C95R norrin
Cell cycle progression	5.60 ± 0.61 (n=3)	0.99 ± 0.07 (n=3; p-value=0.00021)

average ± standard deviation are reported; n= number of technical replicas;

Supplementary Table 5 MAPK activity

	WT norrin	p.C95R norrin
MAPK activity	1.00 ± 0.040 (n=3)	0.53 ± 0.052 (n=3; p-value=0.00023)

average ± standard deviation are reported; n= number of technical replicas;

3.2 Establishing calcium phosphate precipitation transfection method

Before starting animal experiments, we investigated the interaction between Norrin-Wnt and Norrin-Notch signaling in HEK293T cells. The HEK293T cells used did not endogenously express *NDP* but *FZD4, LRP5* and *TSPAN12* (Master Thesis of Jurian Zuercher, 2007). The following section describes results obtained while establishing the pathway reporter assays and obtained from Norrin interaction assays. First, transfection parameters for the calcium phosphate precipitation method were established.

A prerequisite to perform luciferase assays is an efficient transfection. A widely used transfection method for HEK293T cells is the calcium phosphate precipitation (Jordan et al., 1996; Jordan et al., 2004). To establish a protocol for 24-well plates, a constitutive enhanced green fluorescent protein (GFP) expressing vector was applied in amounts ranging from 300 to 1500 ng/well according to conditions described under Methods (Figure 18). The achieved transfection efficiency was visually estimated to be 90% to 95% if 1500 ng eGFP vector were transfected per well (Figure 18).

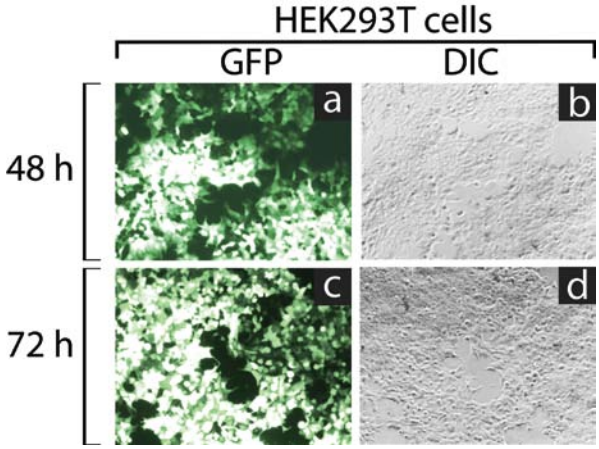

Figure 1: High transfection efficiency in HEK293T cells is achieved using the calcium phosphate precipitation method. a - d) 5*10^4 cells were incubated at 37°C/ 5%CO2 for 24 h and transfected with 1500 ng pGFP construct. Pictures of the same well were taken 48h (a, b) and 72h (c, d) post transfection. Transfection efficiency was visually estimated to be 90% to 95%. GFP = green fluorescent protein; DIC = differential interference contrast.

3.3 Establishing Wnt reporter assay

We used the pTopflash reporter construct to analyze Norrin-Wnt activity. The pTopflash harbors six TCF/LEF binding sites in front of a firefly luciferase gene. Therefore expression of firefly luciferase is Wnt activity dependent in pTopflash. Renilla luciferase was constitutively expressed and served as internal standard. Wnt activity was expressed as ratio of firefly/renilla luciferase activity. Additionally we co-expressed *FZD4* and *LRP5* during assay (Smallwood et al., 2007; Xu et al., 2004). Wnt reporter assays were optimized for transiently and stably Norrin expressing HEK293T cells. Mouse Wnt3A and lithium chloride (LiCl) served as positive controls, sodium chloride (NaCl) was used as negative control.

3.3.1 Wnt-reporter assay for transiently Norrin expressing HEK293T cells

Lithium chloride (LiCl) is an inhibitor of the canonical Wnt signaling inhibitor GSK3 and therefore activates Wnt signaling by disinhibition. First, 5, 10, 15 and 25 mM LiCl per well were applied to

HEK293T cells transfected with pTopflash and pRenilla to monitor LiCl dependend activation of the pTopflash. Natrium chloride (NaCl) served as a negative control and was applied at the highest concentration tested. Readout was performed after 24 h of incubation (Figure 19a). LiCl activated pTopflash concentration dependent, but NaCl did not trigger Wnt activity.

Next we wanted to monitor the Wnt activity of wildtype and mutant Norrin constructs from our lab. Therefore, Norrin constructs, pTopflash, pRenilla, pFZD4 and pLRP5 were co-transfected and analyzed 72 hours later. Wildtype Norrin activity was arbitrary set to 1 (Figure 19b). We found that only wildtype Norrin (Norrin) but none of the mutant Norrin variants (p.C95R, p.C96W, p.R121W, p.R121L) was able to trigger canonical Wnt signaling.

Heparin might enhance binding of Norrin to its receptor FZD4 (Smallwood et al., 2007). We tested if addition of heparin to the assay would ameliorate Wnt reporter assay performance (Figure 19c). Wnt3A expression served as positive control. We compared Wnt signaling activity between wildtype and p.C95R mutant Norrin and detected significant differences with or without addition of heparin. Nonetheless, addition of heparin led to enlarged confidence intervals, rendering the assay less robust. Therefore we relinquished to add heparin for future assays.

Tspan-12 was identified as a novel co-receptor for Norrin (Junge et al., 2009) and therefore we wanted to investigate if co-expression of TSPAN12 would ameliorate the readout of our Wnt reporter assay. For that, we co-expressed the indicated receptors together with pTopflash and pRenilla in wildtype or p.C95R Norrin expressing HEK293T cells (Figure 19d). We saw that FZD4 and LRP5 expression are crucial for the Wnt reporter assay, but additional expression of TSPAN12 has no influence on its performance.

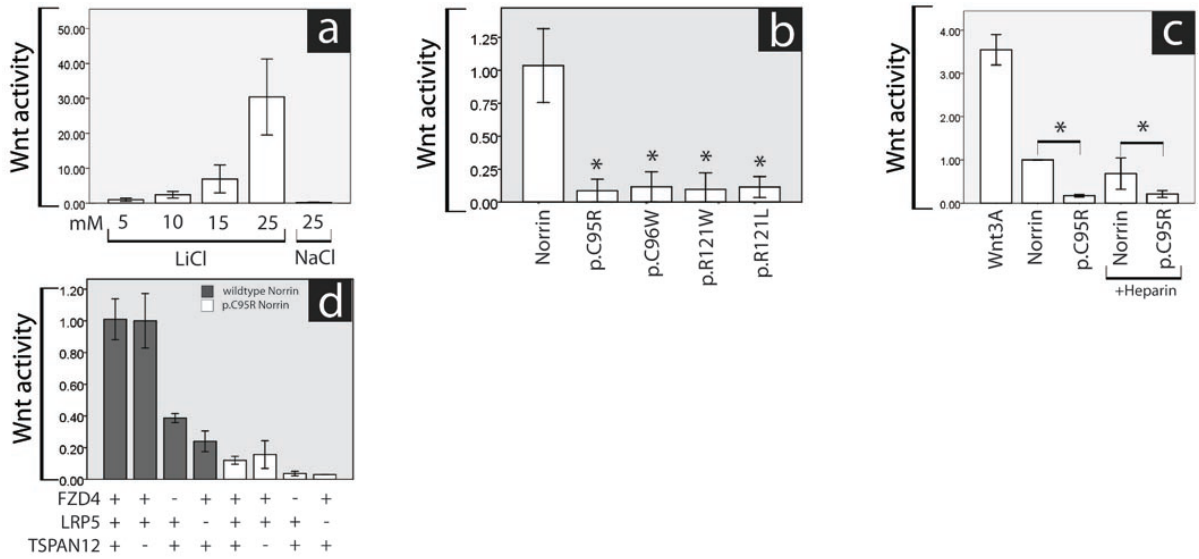

Figure 2: Establishing Wnt reporter assay for transiently Norrin expressing HEK293T cells. a) LiCl is able to activate the Wnt reporter in a dose dependent manner. NaCl did not activate Wnt reporter. b) Only transient expression of wildtype Norrin (Norrin) but none of the mutant Norrin variants (p.C95R, p.C96W, p.R121W, p.R121L) was able to activate the Wnt reporter. c) Wildtype Norrin without or with 5µl heparin/well was able to significantly trigger Wnt signaling compared to mutated Norrin (p.C95R). But robustness of the assay decreased upon addition of heparin visible by enlarged confidence intervals. Wnt3A was used as a positive control. d) Co-expression of *TSPAN12* does not ameliorate the readout of the Wnt reporter assay. Average and confidence intervals are displayed. P-values below α=0.05 were considered statistically significant (*).

3.3.2 Wnt-Reporter assay for stably Norrin expressing HEK293T cells

HEK293T cells with stable expression of wildtype Norrin and a mutant variant (p.C95R)(Master Thesis, Lucas Mohn, 2007), which is associated wit Norrie disease as well as non-Norrin expressing HEK293T cells (MOCK, generated by Stephan Labs by stable transfection of empty pBUD CE4.1 vector) were co-transfected with pTopflash, pRenilla, pFZD4 and pLRP5 and analyzed 48 hours later. LiCl and NaCl served as positive and negative controls, respectively (data not shown)(Figure 20). Wnt activity of MOCK cells was arbitrary set to 1. Wnt signaling activity was induced in wildtype but reduced in p.C95R Norrin expressing HEK293T cells.

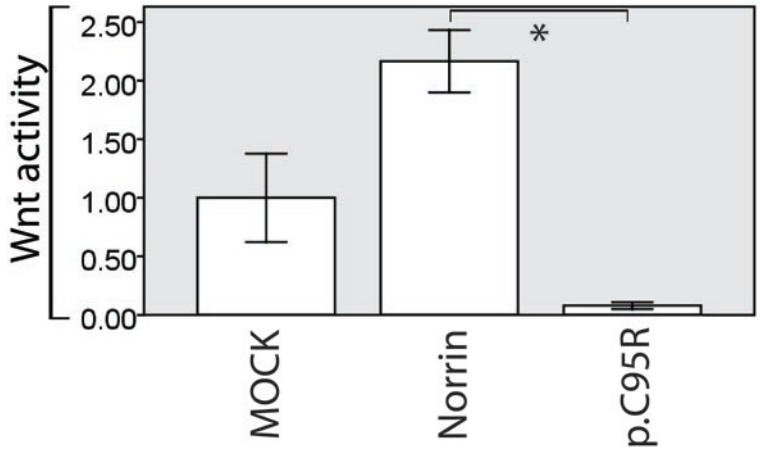

Figure 3: Activation of canonical Wnt signaling in HEK293T cells with stable expression of wildtype or mutant Norrin. Values were normalized on MOCK samples. Wildtype Norrin expressing cells (Norrin) showed an increased, mutant Norrin (p.C95R) expressing cells showed a decreased Wnt signaling activity compared to MOCK cells. Average and confidence intervals are displayed. P-values below α=0.05 were considered statistically significant (p-value < 10^{-5}).

HEK293T cells stably expressing Norrin isoforms showed an improved performance of the Wnt reporter assay compared to those with transient expression, as reflected by reduced incubation time and higher firefly/renilla ratios in the raw data (data not shown). Therefore we only used stable Norrin isoform expressing HEK293T cells for further experiments.

3.4 Analysis of Norrin-Wnt and Norrin-Notch signaling interactions in HEK293T cells

We wanted to monitor the effect of Norrin on Notch1 mediated signaling and additionally elucidate the effect of the interaction between disheveled 1, 2 and 3 and notch1 intracellular domain (N1ICD) on Notch and Wnt signaling (Figure 21). Overexpression of N1ICD did not trigger Notch signaling in stable wildtype Norrin (Norrin) expressing HEK293T cells, in contrast, Notch signaling was triggered in p.C95R Norrin (p.C95R) expressing and MOCK cells (Figure 21a). Activation of Notch activity was impeded if Dvl1, Dvl2 or Dvl3 were co-expressed with N1ICD (Figure 21b). N1ICD was able to downregulate Dvl1, Dvl2 or Dvl3 mediated Wnt signaling (Figure 21c, d, e).

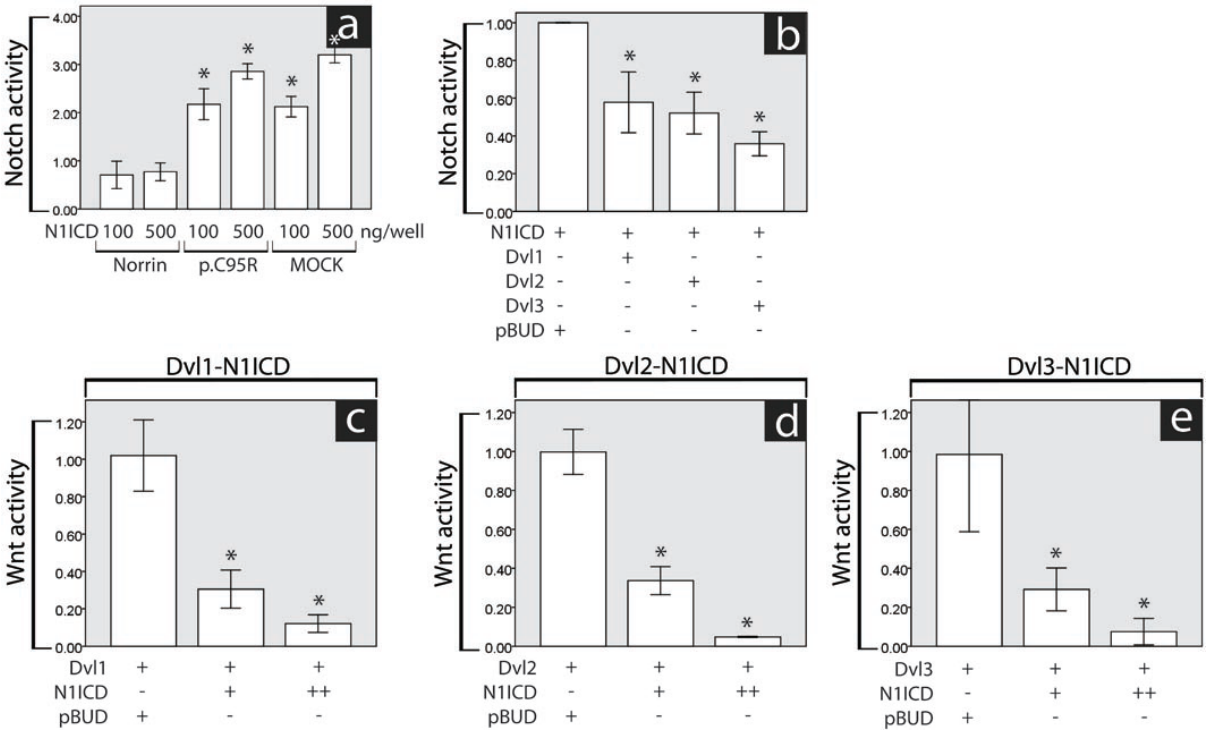

Figure 4: Wildtype Norrin is able to downregulate Notch1 mediated signaling in HEK293T cells. (a) Overexpression of N1ICD did not trigger Notch activity in wildtype Norrin expressing HEK293T cells. In contrast, Notch activity was triggered by N1ICD overexpression in p.C95R or non-Norrin (MOCK) expressing HEK293T cells. (b) Dvl1, Dvl2 and Dvl3 were able to downregulate N1ICD mediated Notch signaling in HEK293T cells. (c, d, e) N1ICD is able to downregulate Dvl1, Dvl2 or Dvl3 mediated Wnt signaling. Average and confidence intervals are displayed. P-values below α=0.05 were considered statistically significant.

3.5 Analysis of Norrin-Notch signaling interaction in mouse retina

Ndph$^{y/-}$ mice were crossed with Notch reporter mice (*Tg(Cp-EGFP)25Gaia/J*, TNR1 mice, (Hellstrom et al., 2007a; Hellstrom et al., 2007b) to monitor Notch activity in *Ndph*$^{y/-}$ retinas. The Notch activity pattern in wildtype males looked random (Figure 22). Therefore no comparison between wildtype and *Ndph*$^{y/-}$ retinas was done and the breeding of mice was stopped.

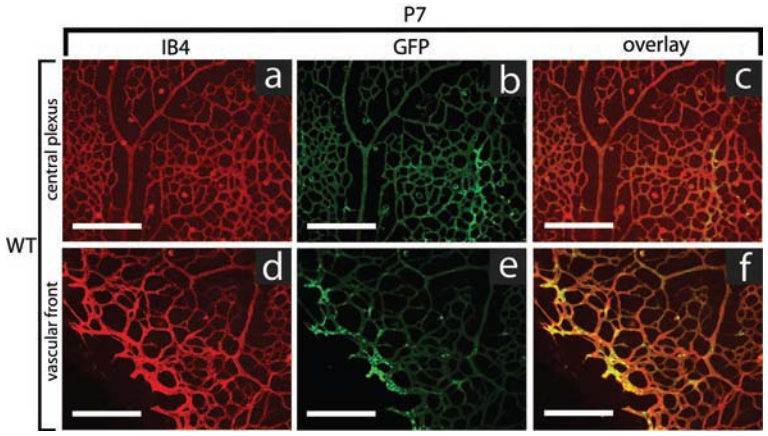

Figure 5 : Notch pathway analysis *of Ndph*$^{+/+}$ x TNR1 wildtype (WT) mice at P7. Blood vessels were stained using isolectin B4 (IB4, red) and Notch activity was detected using an anti green fluorescent (GFP) antibody (green). Central (a-c) and peripheral (d-f) sections of a retinal wholemount from a wildtype male mouse are shown. The activation pattern looks random and unspecific. Scale bar = 100 µm.

3.6 Influence of Norrin on TGFβ signaling, ER stress and Estrogen response

We replaced the pTopflash by different reporter constructs to investigate influence of Norrin on other pathways (Figure 23). We used pSMAD to monitor TGFβ signaling and found reduced TGFβ activity in cells expressing wildtype Norrin. ER stress was elevated in cells expressing the mutated p.C95R Norrin isoform, as monitored by using the pERSE reporter construct. Estrogen response was reduced in cells expressing the mutated p.C95R Norrin isoform, monitored by pERE reporter construct.

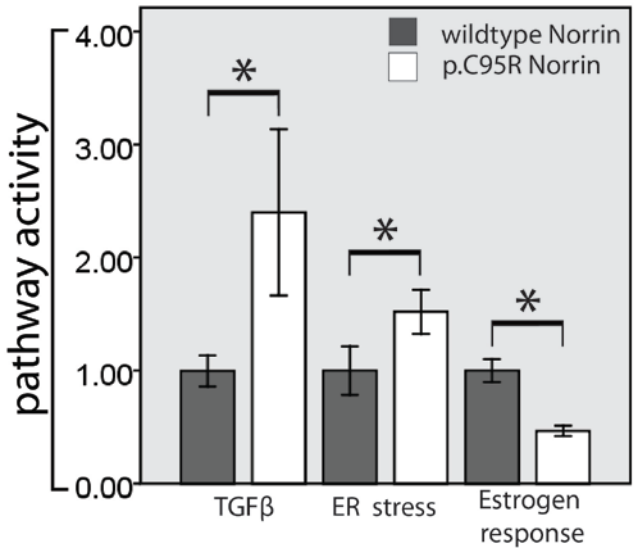

Figure 6: Wildtype Norrin reduces TGFβ and enhances estrogen response, while mutated p.C95R Norrin enhances ER stress. An independent samples T-test was used to analyze the data. Average and confidence intervals are shown. P-values below α=0.05 were considered statistically significant. P-values are: TGFβ = 0.001, ER stress = 0.002 and estrogen response = 0.00003.

3.7 Quantification of Notch target genes after Norrin expression in HEK293T cells

We checked if Norrin expression would alter expression of Notch target genes Hes1, Hes2, Hes5, Hey1 or Hey2 in HEK293T cells. Therefore we transiently expressed wildtype Norrin during 72 hours in HEK293T cells (Norrin). Empty vector transfected cells served as control (MOCK) (Figure 24). Only Hey1 expression was significantly increased upon Norrin expression.

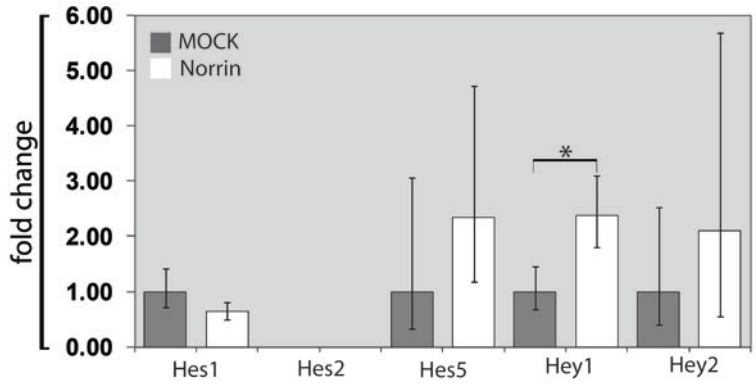

Figure 7: Expression of Norrin leads to an increase of Hey1 expression in HEK293T cells. Hes1, Hes5 and Hey2 expression was not altered and Hes2 was not expressed nor induced after Norrin expression in HEK293T cells. Hey1 expression was doubled upon Norrin expression. Average and confidence intervals are shown. P-values lower than α=0.05 were considered statistically significant (*). P-value of Hey1 is 0.0023.

The focus of the next section is on experiments using the *Ndph*$^{y/-}$ mouse. Some of the results were discussed in the publication (see 3.1). Only results that were not included in the manuscript are reported below.

3.8 Analysis of the retinal vascular phenotype in *Ndph*$^{y/-}$ mice

3.8.1 Establishing weight control table for *Ndph*$^{y/-}$ and wildtype littermates

Vascular defects affect normal development in mice. Consequences can be dwarfish appearance and reduced body weight of mice pups. Therefore, we quantified body weight of all mice pups and subsequently analyzed data using SPSS (IBM, New York, USA). For that, eight mice litters per stages at P5, P7, P9, P12 and P21 were weighted and statistically analyzed. Mice weights were plotted in following groups (Figure 25):

- Weight differences depending on sex and postnatal age (Figure 25a)
- Weight difference depending on genotype and postnatal age (Figure 25b)
- Weight differences between different mice litters of a certain postnatal age (Figure 25c)
- Average body weight of mice dependent on postnatal age (Figure 25d)

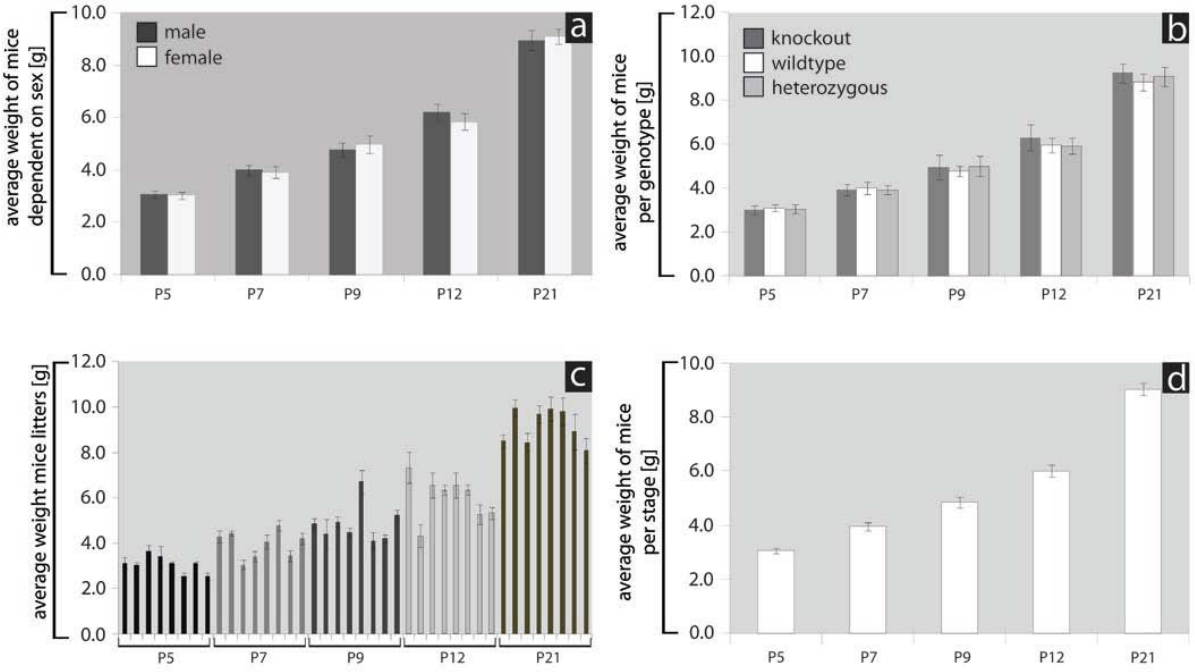

Figure 8: Sex or genotype of mice have no influence on their weight between P5 and P21, but litter affiliation matters. (a) Sex of mice has no influence on their weight during development from P5 to P21. (b) The genotype of mice has no influence on their weight during development from P5 to P21. (c) Eight litters per stage were analyzed. The average weight between mouse litters of the same postnatal age can differ significantly from each other. (d) The average weight of mice per postnatal age was calculated averaging

eight randomly selected mice litters (see c). Average and confidence intervals are displayed. P-values (not shown) lower than α=0.05 were considered statistically significant.

Sex or genotype at the *Ndph* locus of the C57BL/6J mice did not influence body weight during postnatal development between day 5 to 21 (Figure 25a, b). In contrast, the average weight of mice significantly differed between litters of the same stage (Figure 25c). Nevertheless, we calculated the average weight of mice depending on the stage pooling weights from all males, females and genotypes (Figure 25d). Exact statistical values are given in Appendix 3.

3.8.2 Inhibition of Notch signaling partially rescues delayed outgrowth of the SRVP

Comparison of vascular length between DAPT and non treated wildtype and *Ndph*$^{y/-}$ littermates revealed a significant increase in vascular length in *Ndph*$^{y/-}$ but not in wildtype mice at postnatal day 6 (Figure 26).

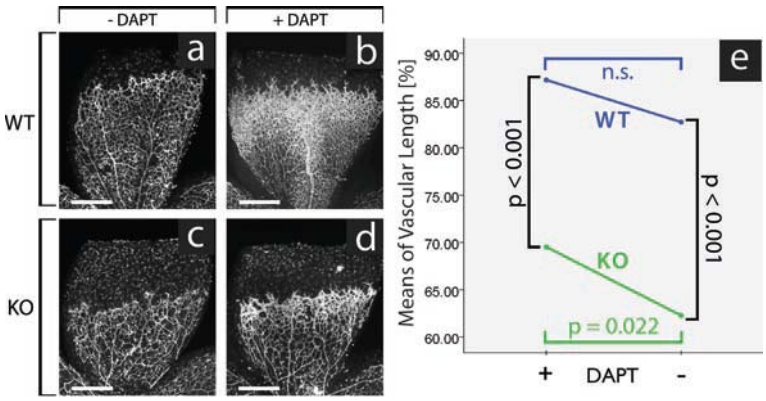

Figure 9: Inhibition of Notch signaling by administration of DAPT at P6increases vascular length in *Ndph*$^{y/-}$ (KO) but not in wildtype (WT) retinas. (a-d) Retinal whole-mounts stained with isolectin B4 to visualize blood vessels. Vascular length between untreated (a) and DAPT treated (b) wildtype animals did not increase significantly (e). In contrast, vascular length between untreated (c) and DAPT treated (d) *Ndph*$^{y/-}$ animals increased significantly (e). P-values below α=0.05 were considered to be statistically significant. Scale bar = 100 µm.

3.8.3 The bulky front of the SRVP from *Ndph*$^{y/-}$ mice shows enhanced Dll4 expression

We continued staining of SRVP from *Ndph*$^{y/-}$ and wildtype littermates against the Notch1 ligand Dll4 (Figure 27) and found elevated Dll4 expression levels at bulky vascular fronts in the SRVP of *Ndph*$^{y/-}$ retinas.

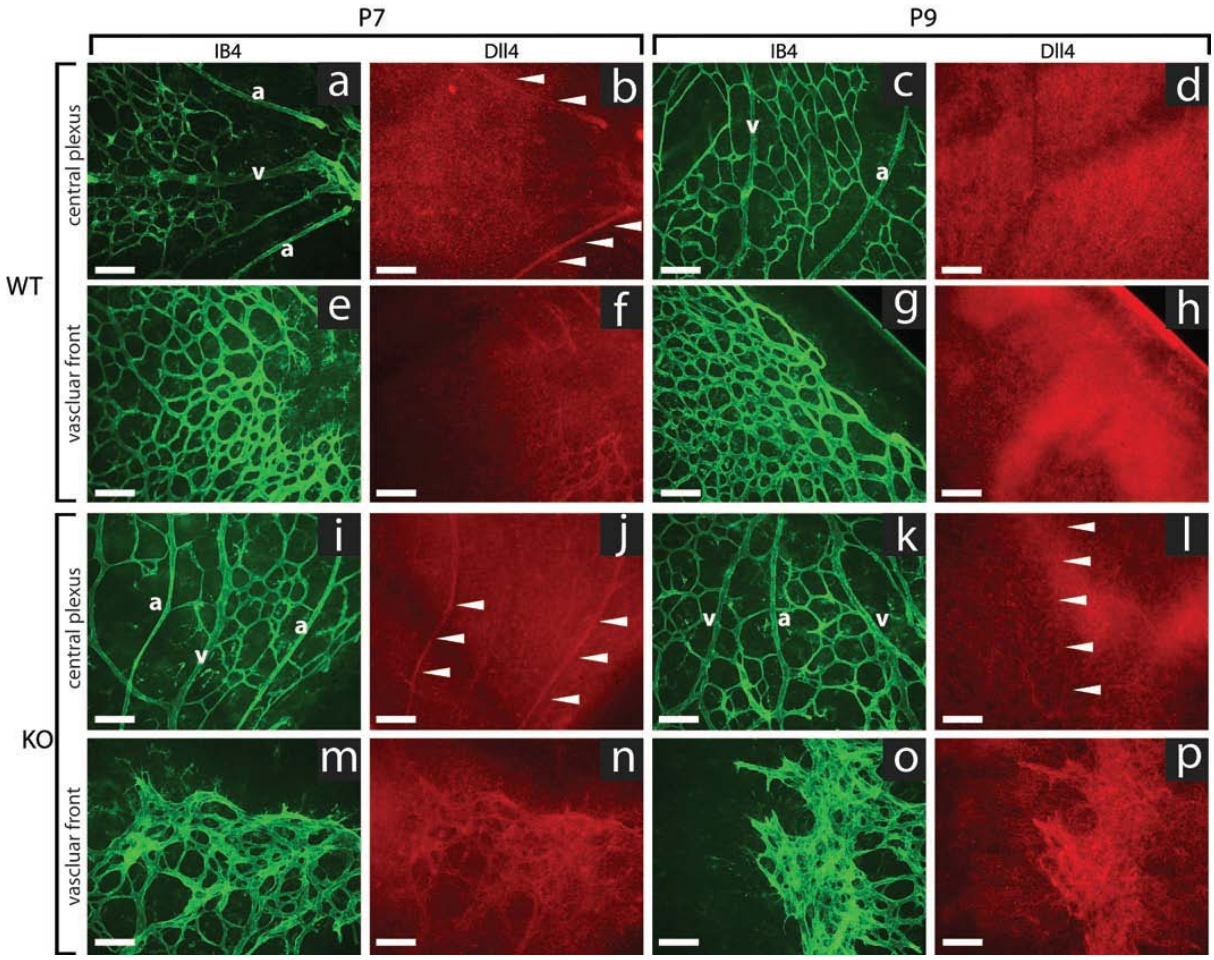

Figure 10: The vascular plexus and the bulky front of *Ndph*$^{y/-}$ mice show enhanced Dll4 protein expression. Wildtype (WT) and *Ndph*$^{y/-}$ (KO) retinas were co-stained at P7 (a, b, e, f, i, j, m, n) and P9 (c, d, g, h, k, l, o, p) with isolectin B4 (IB4, green) and an anti-Dll4 antibody (Dll4, red). Arteries (b, j; arrowheads) and the vascular front were Dll4 positive in wildtype and *Ndph*$^{y/-}$ retinas at P7. At P9, no Dll4 staining was detectable on arteries or on the vascular plexus from wildtype retinas (d, h), but in contrast, Dll4 was still expressed on arteries (k, l; arrowheads) and at the vascular front on *Ndph*$^{y/-}$ mice. Scale bars = 50 µm.

3.8.4 The number of hyaloid vessel-associated macrophages persists between P7 and P12 in *Ndph*$^{y/-}$ retinas

Next we wanted to quantify the number of macrophages which are associated with hyaloid vessels. Therefore retinal whole-mounts were prepared without removing the hyaloid vessels. The whole-mounts were co-stained against induction of brown adipocytes 1 (Iba1) and IB4 to visualize macrophages and blood vessels, respectively (Figure 28). We saw that hyaloid vessels regressed in both phenotypes, but that regression was dramatically delayed in *Ndph*$^{y/-}$ mice (Figure 28 a, b, c, j, k, l). The number of macrophages decreased with progressing regression in wildtype retinas (Figure 28 d-i, s) but was not reduced in *Ndph*$^{y/-}$ mice between P7 and P12 (Figure 28 g-i vs. m-r, s).

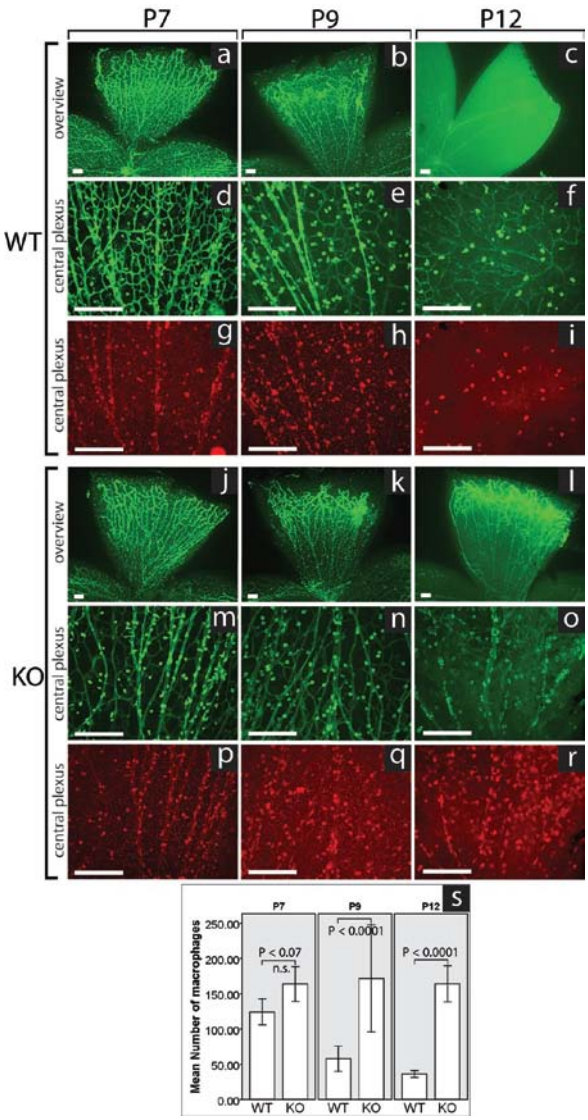

Figure 11: Hyaloid regression is delayed in *Ndph*$^{y/-}$ mice and the number of hyaloid vasculature associated macrophages persists between P7 and P12. Retinal whole-mounts of wildtype (WT, a-i) and *Ndph*$^{y/-}$ (KO) mice (j-r) were double-stained with an antibody against IBA1 (red) and with IB4 (green) to label macrophages and blood vessels at P7, P9 and P12. The number of macrophages decreased in wildtype retinas from P7 to P12 but not in knockout retinas (s). Average and confidence intervals are shown. P-values below α=0.05 were considered statistically significant. Scale bar = 100 µm.

3.8.5 LiCl administration does not rescue deep vascular sprouting in *Ndph*$^{y/-}$ mice

We wanted to see if injection of LiCl, an activator of canonical Wnt signaling, might restore proper DRVP formation and deep sprouting in *Ndph*$^{y/-}$ mice. For that, LiCl was injected into mouse litters subcutaneously from P5 for five subsequent days with increasing doses of LiCl dissolved in PBS (see methods). Doses were weight adjusted and always 25% of lethal doses for adult C57BL/6J mice (Smith1978). Two litters were injected (Table 2). Litter 1 pups were above average weight at P5. Therefore higher doses of LiCl were injected at P6 and P7. Litter 2 pups were at average weight, therefore standard doses were injected each stage. One mouse in litter 1 lost weight at P7 and died at P8. A second mouse of the same litter died at P10. Because of that, injections were stopped at P8. Mice of litter 2 only moderately gained weight and many started to die at P8.

Table 1: Monitoring of gain in body weight of LiCl injected pups

	Weight of animals [g]					
	P5	P6	P7	P8	P9	P10
Litter 1	4	4.4	5.1	5.6	5.7	n.a.
	4.1	5.4	5.2	5.7	5.3	n.a.
	3.7	4.4	5.2	5.3	5.5	n.a.
	3.7	4.7	5.1	5.7	4.1	dead
	3.8	4.1	3.8	dead	dead	dead
Average weight [g]	3.86	4.6	4.9	5.7	5.2	n.a.
Dose injected	P5	P8	P8	-	-	-

	Weight of animals [g]					
	P5	P6	P7	P8	P9	P10
Litter 2	2.3	2.5	3.7	dead	dead	dead
	2.3	3.0	2.8	dead	dead	dead
	2.3	2.6	3.6	dead	dead	dead
	2.4	2.7	3	dead	dead	dead
	2.4	3.0	3.1	dead	dead	dead
	2.1	2.3	3.1	n.a.	dead	dead
	2.5	2.9	3.1	n.a.	dead	dead
	2.4	3.0	3.2	n.a.	dead	dead
	2.3	2.4	3.2	n.a.	dead	dead
	2.3	2.7	2.2	n.a.	n.a.	dead
	2.1	2.8	2.1	n.a.	n.a.	dead
	2.4	3.1	1.9	n.a.	n.a.	n.a.
Average weight [g]	2.3	2.8	2.9	n.a.	n.a.	n.a.
Dose injected	P5	P6	P7	-	-	-

n.a.= not available

We took the eyes of the mice that survived and prepared retinal whole-mounts (Figure 29). Two were knockout males, three were wildtype females and one was a heterozygous female.

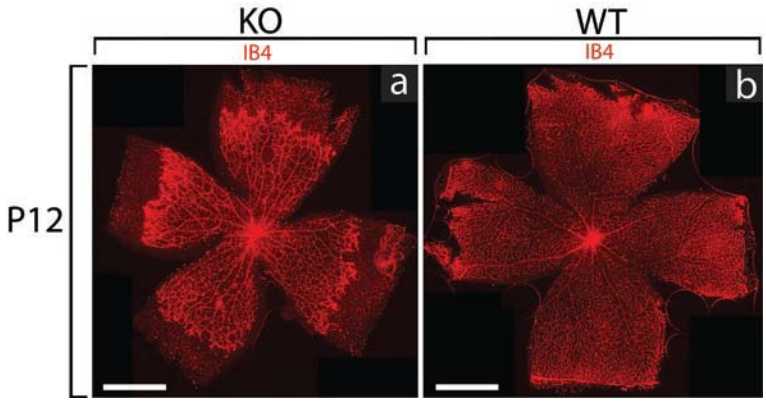

Figure 12: Retinal whole-mounts at P12 from wildtype (WT) and *Ndph*$^{y/-}$ (KO) mice injected with LiCl form P5 to P8. Retinal whole-mount of an *Ndph*$^{y/-}$ male (a), and of a wildtype female (b) mouse retina. Blood vessels were stained with isloectin B4 (IB4, red). The heterozygous female plexus was identical to the ones from wildtype males (not shown). Scale bar = 1000 µm.

We did not see any gross difference of blood vessels of the SRVP in LiCl injected retinas from knockout males (Figure 29a) or wildtype females (Figure 29b) compared to uninjected animals (data not shown). No initiation of deep vascular sprouting was visible in LiCl treated *Ndph*$^{y/-}$ retinas.

4. Discussion

This thesis primarily aimed in investigating a putative role of Norrin as a Notch signaling inhibitor.
For that we measured Dvl-N1ICD interaction and quantified the differential expression of Notch target genes *Hes1, Hes2, Hes5, Hey1* and *Hey2 in vitro*. In mice, we conducted IHC of Dll4, Jag1 and a-SMA on retinas and systemically inhibited Notch signaling by DAPT injection. Finally we compared morphometric data from *Ndph*$^{y/-}$ with *Jag1*$^{i\Delta EC}$ and *Dll4*$^{-/-}$ mice. Considering all the results, we concluded that Norrin signaling does not interact with Notch signaling during the formation of the SRVP in mice.
We found artery/vein crossing, which, together with results from a Norrin-MAPK luciferase reporter assay suggests that MAPK signaling might be significantely altered during the development of the SRVP in *Ndph*$^{y/-}$ mice. We could show that the lack of Norrin leads to decreased proliferation of ECs from the SRVP which could explain the delayed outgrowth of the SRVP observed in *Ndph*$^{y/-}$ mice.
We also found excessive mural cell coverage of veins, venules and capillaries in *Ndph*$^{y/-}$ retinas which might indicate a partial loss of venous identity. Further, we identified endomucin as a marker for thorn-like aligned central filopodia in *Ndph*$^{y/-}$ mice.
In contrast to wildtype retinas, we found a constant number of hyaloid associated macrophages between P7 and P12 in *Ndph*$^{y/-}$ mice. This may suggests that the hyaloid vessel might fail to regress despite a sufficient number of macrophages present.

4.1 Establishing the luciferase assay

The Calcium phosphate precipitation transfection method in HEK293T cells has proven to be efficient to perform luciferase based reporter assays. This method was also found to be very efficient for the transfection of COS7 cells (data not shown).

LiCl has been shown to be a reliable and cheap positive control for Wnt luciferase assays (Figure 19a). It should be applied at concentrations of 15 or 25 mM 24 hours before measurement. The negative control, NaCl, is applied in similar concentrations for the same period of time. p*Wnt3A* is a second, also very reliable positive control and can be co-transfected between 24 and 72 hours during the assay (Figure 19c). Commercially available Wnt3A protein (R&D Systems, Minneapolis, USA) is also suitable as positive control and can be applied with 300 ng/well 24 hours prior to measurement (data not shown).

The plasmids which were used by Lucas Mohn to generate stably Norrin or mutant Norrin isoform expressing HEK293T cells were tested for their ability to activate canonical Wnt signaling in the Wnt reporter assay by transiently expressing them for 72 hours in HEK293T cells (Figure 19b). As expected, only wildtype Norrin was able to trigger canonical Wnt signaling but none of the mutant Norrin isoforms. Addition of heparin rendered the assay less robust, indicated by enlarged confidence intervals (Figure 19c). Therefore addition of heparin during Norrin-Wnt reporter assays is not recommended.

It was known from literature (Smallwood et al., 2007; Xu et al., 2004) that FZD4 and LRP5 essentially need to be co-expressed with pTopflash and pRenilla while conducting the Norrin-Wnt reporter assay. We tested if expression of the recently discovered co-receptor Tspan-12 would ameliorate the assays, but it did not (Figure 19d). Therefore it is sufficient but essential to co-express *FZD4* and *LRP5* while performing Norrin-Wnt reporter assay. Tspan-12 might be essential to specify the Norrin-Wnt signal but not necessary to convey the canonical Wnt signal.

We tested if the use of stable Norrin isoforms expressing HEK293T cells would ameliorate the readout and lead to stronger signal intensity (Figure 20). We used stably wildtype and mutant (p.C95R) Norrin expressing HEK293T cells since they have been shown to express similar amounts of the respective proteins (Zuercher et al., 2012). Indeed, using stably Norrin isoforms expressing HEK293T cells led to stronger signal intensity without amplification of background noise (Figure 20 and data not shown). Therefore we decided to use this cell lines for Norrin-Notch interaction studies.

4.2 Establishing quality control for mice litters

We established body weight based quality control for mice litters, since vascular defects affect normal development in vertebrates. For that we measured body weight of all mice used in our experiments and plotted data to enlighten the following correlations:

- Weight differences depending on sex and postnatal age (Figure 25a)
- Weight difference depending on genotype and postnatal age (Figure 25b)
- Weight differences between different mice litters of a certain postnatal age (Figure 25c)
- Average body weight of mice dependent on postnatal age (Figure 25d)

Only mouse litter affiliation influenced body weight, but not sex and genotype at the *Ndph* locus (Figure 25a - c). The average body weights from different litters of the same age often differ significantly. We noticed that mice of small litters were often heavier than mice of the same age belonging to a bigger litter (data not shown). We also noticed significant differences in body weight of mice from equal membered litters of different breeding pairs (data not shown). We cannot deduce if the cause is genetic or if parent animals influence the frequency of food intake of their pups. Based on this data, we excluded from experiments mice that differed two or more standard deviations from the average weight of their litter. The average body weights of mice per stage (Figure 25d) served only as landmarks for body weight of the respective postnatal age.

4.3 Molecular mechanisms of sprouting angiogenesis in the retina: crosstalk between Notch and Norrin signaling.

One goal was to investigate a possible crosstalk between Norrin-Wnt and Notch signaling. For this purpose, we established Wnt and Notch reporter assays in cell culture using luciferase constructs, crossed *Ndph*$^{y/-}$ with Notch reporter mice (*Ndph*$^{y/-}$ x TNR1), quantified morphometric parameters of the retina (number of filopodia, number of branch points and vascular density), monitored proliferation by BrdU staining and reporter assays, applied immunohistochemistry for Jag1, Dll4, endomucin, SMA and IBA1 on retinal whole-mounts, inhibited Notch signaling in *Ndph*$^{y/-}$ mice by injecting DAPT and tried to rescue deep vascular sprouting from the SRVP by injection of LiCl.

4.3.1 Norrin-Wnt signaling is unlikely to interact with Notch signaling in stalk cells

Our initial hypothesis suggested that Norrin-Wnt signaling might impede Notch1 signaling in stalk cells. We suggested disheveled or GSK3 mediated inhibition of N1ICD or Jagged1 mediated lateral inhibition of tip cell sprouting (Figure 15) as possible modes of interaction. We tested the ability of Norrin to downregulate N1ICD mediated Notch signaling in HEK293T cells. For that we expressed the Notch reporter construct pJH23a either in wildtype, mutant (p.C95R) and none-Norrin expressing HEK293T cells (Figure 21a). We found that wildtype Norrin was able to downregulate N1ICD mediated Notch signaling during the first 24 hours. This effect was lost if the reporter assay was

incubated for more than 24 hours (data not shown), possibly because luciferase expression reached saturation levels. GSK3 unlikely inhibits Notch1 signaling in tip cells. GSK3 exists in two isoforms (GSK3α and GSK3β), both of which are repressors of Wnt-signaling and thus are expected to be inactive during canonical Wnt-signaling. Inactivation of GSK3α/β enhances Notch1 activity *in vitro*, ruling out GSK3 to be part of the Norrin-mediated Notch1 inhibition (Jin et al., 2009). Therefore we focused on Dvl-N1ICD interactions (Figure 21b, c, d, e). We found that Dvl1, 2 and 3 are capable of impeding N1ICD mediated Notch signaling, but the presence of N1ICD also downregulated Dvl1, 2 or 3 mediated Wnt signaling. It is noteworthy that N1ICD was transfected in moderate concentrations of 20 ng/well but any of the Dvls at 500 ng/well. This implies that N1ICD has a stronger influence on Dvls and Wnt signaling than vice versa. This might indicate that Dvl-N1ICD interactions unlikely link Norrin-Wnt and Notch signaling within stalk cells. This does not explain our previous findings, where Norrin was able to decrease N1ICD mediated Notch signaling (Figure 21). A disadvantage of the reporter assay might be that it was performed in HEK293T cells instead of primary human ECs (e.g. HUVECs). It is not clear to what extent HEK293T cells mimic interactions between pathways in human ECs. However, it is unlikely that Dvl-N1ICD interaction mainly links Norrin-Wnt and Notch signaling in endothelial cells.

Additionally, we found supernumerary filopodia in *Ndph*$^{y/-}$ retinas which suggests enhanced Dll4 mediated Notch1 signaling in stalk cells. Indeed, we found enhanced Dll4 expression in bulky vascular fronts of *Ndph*$^{y/-}$ retinas (Figure 27). Notch inhibition, by DAPT administration, did not diminish the number of filopodia at the vascular front, but it rescued vascular outgrowth in *Ndph*$^{y/-}$ retinas (Figure 26). Thus, Notch signaling might be slightly out of balance in *Ndph*$^{y/-}$ mice, but it might not be the main cause for the severe vascular phenotype. Additionally, we tried to monitor Notch signaling in *Ndph*$^{y/-}$ retinas by crossing *Ndph*$^{y/-}$ with Notch reporter mice (TNR1) (Figure 22). Unfortunately, we found random activation of the Notch reporter in wildtype retinas and therefore could not assess if Notch signaling was elevated in stalk cells from *Ndph*$^{y/-}$ retinas using the Notch reporter mice. All together, the data suggested that Notch signaling might be slightly altered in *Ndph*$^{y/-}$ mice, but the observed effects were too small and inconsistent to suggest a direct interaction of both pathways.

4.3.2 TaqMan analysis of Notch target genes in vitro

TaqMan analysis was performed in wildtype and none-Norrin expressing HEK293T cells to measure Notch target gene expression of *Hes1*, *Hes2*, *Hes5*, *Hey1* and *Hey2*. Hey1 was higher expressed after Norrin expression (Figure 24). Hey1 encodes a bHLH transcription factor which is an important modulator of A/V specification (De et al., 2009; Fischer et al., 2004; Roca et al., 2007). Hey1$^{-/-}$ mice are fertile, viable and do not develop defects in all organs of prominent Hey1 expression such as somites, kidney, heart atria and nervous tissue. An explanation might be the redundancy with *Hey2*. Fischer et al., 2004 therefore analyzed *Hey1/2* double knockout mice (DKO). DKO mice died between E9.5 and E11.5 due to a global lack of vascular remodeling and massive hemorrhage. Initial vasculogenesis was unaffected but subsequent development of major vessels in the yolk sac and embryo was perturbed (Fischer et al., 2004). Similarly, the same authors found reduced *Hey1* and *Hey2* expression in *Notch1* knockout mice together with failure of arterial marker expression (CD44, neuropilin1 and ephrinB2). Expression of Norrin enhanced Hey1 expression in our assay and thus we would expect that Hey1 would be downregulated in *Ndph*$^{y/-}$ mice. We were not able to assess the *Hey1* expression profile in the SRVP from *Ndph*$^{y/-}$ retinas since *Hey1* is abundantly expressed in neural tissue which would interfere with qPCR measurements in whole retinas. But we found

elevated SMC coverage of veins and capillaries from *Ndph*$^{y/-}$ retinas which might indicate a gain in arterial character. This suggests that *Hey1* expression might be elevated in retinal *Ndph*$^{y/-}$ ECs. This is in contradiction with results from our cell culture assay. It might be worth to repeat the TaqMan experiment in Norrin-stimulated primary endothelial cells (e.g. HUVECs, HMEC-1 or HMECS) since HEK293T cells are derived from human kidney and are not of endothelial nature.

4.3.3 Extended pathway analysis of Norrin in vitro

We extended our pathway analysis on other signaling cascades than Notch, starting with MAPK signaling (Zuercher et al., 2012). We previously performed a pathway interaction analysis based on 730 differentially expressed genes in *Ndph*$^{y/-}$ compared to wildtype retinas. MAPK signaling ranked at the top position, Wnt signaling was ranked at position five (Schafer et al., 2009). Expression of Norrin in HEK293T cells indeed triggered MAPK signaling by downstream activation of the SRF transcription factor (Figure 23). Furtermore mice that lack the intracellular Nrp1 domain or $VEGF_{NES\text{-}CRE}$ knockout mice, representing mice with altered MAPK signaling, display artery/vein crossing of the SRVP, similarly as *Ndph*$^{y/-}$ mice do (Fantin et al., 2011; Haigh et al., 2003). A recent paper describes artery/vein crossing in apelin receptor deficient mice (McKenzie et al., 2012) and apelin has been shown to be a MAPK target gene in cells different than ECs. Apelin could therefore also be a MAPK target gene in ECs and its expression pattern might also be altered in the SRVP from *Ndph*$^{y/-}$ retinas. A striking difference between *Ndph*$^{y/-}$ and *Apln*$^{-/-}$ retinas is that the DRVP and IRVP do both develop in *Apln*$^{-/-}$ mice. However, the findings of Schaefer et al., 2008 and my data indicate a possible link between Norrin-Wnt and MAPK signaling via SRF activation. Interestingly, SRF has a well known history of mediating sprouting angiogenesis. In sprouting angiogenesis, SRF mediates VEGF-A signaling via VEGFR2-MAPK-RhoA signaling (Franco et al., 2009). VEGF-A induces SRF expression and SRF is mandatory for VEGF-A-mediated angiogenesis (Chai et al., 2004). SRF is also involved in the recruitment of SMCs (Franco et al., 2009; Miano et al., 2004). Inactivation of SRF in mice leads to a decrease in the number of branch points, altered tip cell morphology and disruption of EC junctions with vessel leakiness, hemorrhage and aneurisms leading to death at E14.5 (Franco et al., 2008). These experiments highlight the importance of MAPK signaling and SRF during angiogenesis in mice. It should therefore be assessed if MAPK signaling is altered in *Ndph*$^{y/-}$ mice and if SRF plays a role in Norrie disease or related disorders.

Next, we assessed estrogen response. We previously published that *Ndph*$^{-/-}$ mice are viable but mostly infertile due defective vascular differentiation during decidualisation together with reduced decidualisation itself (Luhmann et al., 2005b). In rat, Norrin regulates decidual reaction and the placental angiogenesis along with the survival and differentiation of luminal and glandular epithelial and decidual cells. It also plays indirect roles controlling trophoblastic invasion and programmed cell death (Kaloglu et al., 2011). During pregnancy, estrogen promotes blood perfusion of the endometrium, initiates opening of the cervix and renders the cervical secret permeable for sperm. Estrogen was found to be 3.5-fold downregulated in placenta of *Ndp*$^{-/-}$ mice (U.F. Luhmann, personal communication). Here, we monitored estrogen response in wildtype and p.C95R mutant Norrin expressing HEK293T cells using a pERE (estrogen response element) luciferase reporter construct (Figure 23) and found an elevated estrogen response in wildtype Norrin expressing cells, which is in concert with previous observations. It is not clear whether the reduced estrogen response is the cause for the effects or whether if it is the consequence of failed decidualisation. It is also not clear if this effect of Norrin also occurrs in human females since no reports exist. Therefore I suggest not to focus on that. It is also not clear how transferable data from mouse to humans are. The hemichorial

placenta in mice consists of three trophoblastic layers including the giant cells, glycogen trophoblast cells and spongiotrophoblast. In humans, first trimester placenta is hemodichorial consisting of an outer layer of syncitiotrophoblast and an inner layer of cytotrophoblast. At term, the human placenta is hemomonochorial with only the syncitiotrophoblast present (Herr et al., 2010; Rossant et al., 2001). Our lab has currently no expertise in analysis of the placenta, therefore it makes sense to keep the focus on eye research. Furtermore *FZD4*$^{-/-}$ females were reported to be infertile due to defective corpora lutea formation causing the failure of implantation in contrast to decidualisation defects of *Ndp*$^{-/-}$ mice (Hsieh et al., 2005).

TGFβ signaling is known to be involved in SMC differentiation (Bertolino et al., 2005) and we found elevated smooth muscle cell (SMC) coverage in *Ndph*$^{y/-}$ retinas (Zuercher et al., 2012). Therefore we assessed the influence of Norrin on TGFβ signaling. Norrin expression reduced TGFβ signaling in HEK293T cells (Figure 23) which is in contradiction with the observed elevated SMC coverage found in *Ndph*$^{y/-}$ retinas. Thus, Norrin deficiency might indirectly cause smooth muscle cell recruitment to the SRVP, which is in concert with the relatively late apperance of this effect. First, it might be worth to repeat this measurement in primary endothelial cells. The design of the assay is crucial since it is known that TGFβ exerts bifunctional effects on endothelial cells *in vitro*. The choice of the primary cell line for the assay is also crucial (Bertolino et al., 2005; Goumans et al., 2003). Goals of these investigations should be to determine if the downstream TGFβ signaling of Alk1-Smad1/5 or Alk5-Smad2/3 is altered. Blood vessels of *Smad5* knockout mouse embryos are less covered by SMCs (Goumans et al., 2003) but Alk5-Smad2/3 pathway activity promotes binding of δEF1, Smad3 and SRF to the SMA promoter enhancing SMA expression (Nishimura et al., 2006). Additionally, TGFβ induced under the involvement of Smad2 and Smad3 general smooth muscle markers in Monc-1 cells while epithelial markers were downregulated (Chen et al., 2004). *In vitro* stimulation of primary endothelial cells with recombinant Norrin and subsequent analysis of the phosphorylation pattern of the respective proteins could reveal alterations in the affected pathway. It might also be that Norrin indirectly activates ALK1-Smad1/5 signaling leading to the upregulation of endoglin, an accessory receptor for TGFβ (Ota et al., 2002). Endoglin was found to counteract the inhibitory effect of TGFβ/Alk5 signaling on cellular proliferation in HUVECS (Li et al., 2000) and we found reduced proliferation of vascular endothelial cells is in *Ndph*$^{y/-}$ retinas. It might be important to investigate a dose dependent effect of Norrin, since effects of TGFβ on angiogenesis are essentially dose dependent (Bertolino et al., 2005; Goumans et al., 2003). Furthermore it is possible to assess influence of Norrin on SMC differentiation. For that, SM precursor cells (VEGFR2+, PDGFRβ+) (Bergers et al., 2005) can be isolated from *Ndph*$^{y/-}$ retinas and stimulated with recombinant TGFβ to differentiate into SMCs. Analysis of epithelial/endothelial markers of these SMCs and their contractile behavior after carbachol (a muscarinic agonist that can induce contraction of cultured SMCs) administration can be used for monitoring the state of SMC differentiation (Chen et al., 2004). Interestingly, a recent publication has shown that maternal derived Norrin is a TGFβ antagonist and that it controls early neuroectoderm specification in *Xenopus laevis*. The authors suggested a model of specification in *Xenopus* where dorsal active Norrin counteracts the BMP4 signal from the ventral side and the Nodal-related signal from the vegetal half of the blastula. They could also show that p.R40K xNorrin lost its ability to trigger Wnt signaling but not its ability to inhibit TGFβ signaling. In contrast, p.K57N xNorrin had moderately increased Wnt signaling activity but it lost its ability to inhibit TGFβ signaling (Xu et al., 2012). This study is interesting in two regards, first it is in concert with the findings from our TGFβ luciferase reporter assay, showing reduced TGFβ signaling activity

upon Norrin expression. Second, this study shows for the first time a differential analysis of mutant Norrin isoforms with different effects on different pathways. Xu et al., 2004, Smallwood et al., 2005 and we (data not shown) analyzed already human pathogenic mutant Norrin isoforms that did not display a loss of canonical Wnt signaling activity in luciferase reporter assays. It will now be important to test those Norrin mutations using our TGFβ and possibly also using our MAPK luciferase reporter assays – even though it is currently not clear if Norrin influences TGFβ signaling in ECs. It is likely that some mutations that do not show altered Wnt signaling have lost their ability either to inhibit TGFβ signaling or that they have lost their ability to stimulate MAPK signaling or both. It will also be intriguing to correlate the gained data from these reporter assays with the reported human phenotypes of the respective Norrin mutations. This may yield in a genotype-phenotype correlation for EVR spectrum diseases for the first time.

Finally, we found slightly elevated endoplasmatic reticulum (ER) stress in HEK293T cells that express mutant Norrin (p.C95R) compared to wildtype Norrin expressing cells (Figure 23). ER stress is a term that describes disturbance of cellular homeostasis due to accumulation of unfolded protein in the ER lumen. ER stress is transduced by three different mechanisms which are summarized as unfolded protein response (UPR). Details of the UPR pathways are nicely reviewed in the literature (Bernales et al., 2006; Ron et al., 2007; Schroder2006). Heavy ER stress can lead to cell death, but no increased numbers of dead cells were observed while performing the assay (data not shown). Therefore it might be possible that the p.C95R mutation leads to accumulation of an un- or misfolded Norrin protein within the lumen of the ER which is sensed by ATF6. The cystein at position 95, which is suspected to be involved in Norrin dimerisation, is exchanged by an arginine in p.C95R Norrin and this may putatively lead to misfolding of Norrin or to failure in Norrin dimerisation. Thus, monitoring ER stress may provide a first-impression to evaluate if mutations lead to ER stress, but subsequent analysis of ER stress should be performed to consolidate this result. Possible experiments include monitoring of expression of UPR target genes, including such from the other two cascades (e.g. XBP1s, XBP1u and ATF4 and CHOP target genes). The degree of phosphorylation from UPR cascade proteins and/or proteins involved in apoptosis might also be assessed.

4.3.4 The number of hyaloid vasculature associated macrophages persists between P7 and P12 in *Ndph*$^{y/-}$ retinas

Ndph$^{y/-}$ retinas have a reduced vascular density in the SRVP compared to retinas from wildtype littermates, a reduced angle of the brush of filopodia extending from each retinal tip cell and delayed and incomplete regression of the hyaloid vessels. These features are also seen in PU.1 null mice which lack monocyte derived retinal microglia cells, *csf-1*$^{op/op}$ mice that lack retinal microglial cells (Kubota et al., 2009b; McKercher et al., 1996) as well as in *FZD4*$^{+/-}$, *LRP5*$^{-/-}$ and *TSPAN12*$^{-/-}$ mice (Junge et al., 2009; Luhmann et al., 2005a; Xia et al., 2008; Xia et al., 2010; Xu et al., 2004). Altered macrophage function can contribute to the narrower angle of filopodia, reduced vascular density and delayed hyaloid regression (Kubota et al., 2009b; Lobov et al., 2005; Rymo et al., 2011). Hyaloid regression is strongest between P7 and P12 and therefore we decided to quantify hyaloid regression during that period (Figure 28). Hyaloid regression progressed fast in wildtype mice but was dramatically delayed in *Ndph*$^{y/-}$ retinas. Quantification of IBA1 positive hyaloids vasculature associated macrophages revealed a persistent number of macrophages between P7 and P12 in *Ndph*$^{y/-}$ retinas but a decreasing number of macrophages in wildtype retinas (Figure 28s). The similar number of macrophages at P7 indicates that similar numbers of macrophages had migrated towards the hyaloid vessels. In wildtype mice, the number of macrophages decreased with hyaloid

regression. In mice, pericytes express Ang2 which induces Wnt7b expression in macrophages (Rao et al., 2007). This Wnt7b is a paracrine ligand that binds Fz-4 and LRP-5 on hyaloid vessels and triggers canonical Wnt-signaling mediating hyaloid regression (Lobov et al., 2005). Why hyaloid regression in *Ndph*$^{y/-}$ retinas fails, despite a sufficient number of macrophages, remains an open question. It might be necessary that Wnt7b/Norrin heterodimers are needed to activate canonical Wnt signaling in hyaloid vessel associated macrophages. This combination could be a feedback loop signalizing the ability for deep sprouting of the SRVP through the presence of Norrin and macrophages. If this holds true, hyaloid vessels would start to regress at P7, when deep sprouting starts but hyaloid regression would fail if any compound required for deep sprouting like Norrin, Fz-4, LRP-5, Tspan-12 or macrophages are missing. In that case, deep sprouting would not occur and instead hyaloid vessels would persist and nourish the retina. This suggests that macrophages are equally important as Norrin, Fz-4, LRP-5 and Tspan-12 for deep sprouting. Supporting this, several recent publications highlight the importance of macrophages in superficial and deep vascular sprouting. Rymo et al., 2011 found that microglia are present at sites of endothelial tip cell anastomosis and that ablation of microglia causes a sparser retinal vascular network together with a reduced number of filopodia bearing sprouts (Rymo et al., 2011). Microglia are attracted by vascular endothelial cells to localize at places of sprouting and anastomosis (Outtz et al., 2011) and in turn, macrophages secrete proangiogenic factors distinct from VEGF-A to stimulate endothelial outgrowth of the SRVP (Rymo et al., 2011). Interestingly, retinal myeloid cells (RMCs), have recently been shown to balance deep vascular sprouting by non-canonical Wnt signaling (Stefater et al., 2011). RMCs that are associated to deep retinal vascular sprouts express Wnt5a and Wnt11, which act in an autocrine fashion via a FZD receptor leading to the expression of sVEGFR1 which in turn reduces deep vascular sprouting. Expression of the canonical Wnt pathway co-receptor LRP-5 in RMCs supresses this non-canonical Wnt response by acting as a sink for Wnt5a/11. Interestingly, RMC-specific deletion of LRP5 leads to a hypovascular deep retinal plexus, but systemic deletion of LRP5 prevents development of the deep vascular plexuses entirely (Xia et al., 2008). The latter effect might be caused by the absence of LRP5 on vascular ECs. There are a few emerging questions about the role of Norrin and macrophages during sprouting angiogenesis: Do Norrin and Wnt7b act as heterodimers via FZD4/LRP5 on macrophages during hyaloid vessel regression? Is the number of macrophages within or at avascular areas of the SRVP altered in *Ndph*$^{y/-}$ compared to wildtype retinas? Are macrophages differentially aligned at the sprouting front of the developing SRVP or at deeper layers within the plexus between *Ndph*$^{y/-}$ and wildtype retinas? Is Norrin also expressed in macrophages? Does Norrin trigger Wnt7b expression in macrophages? Is Norrin involved in the regulation of migration of macrophages e.g. together with VEGF-A? Can Norrin influence non-canonical Wnt signaling in macrophages? These questions can be addressed by several experiments. Heterodimerisation of Norrin and Wnt7b could be investigated by immunoprecipitation or using a BRET^2 assay. The alignment of Iba1 or F4/80 positive macrophages with endothelial tip cells could be quantified on whole-mounts from wildtype and *Ndph*$^{y/-}$ retinas to detect any misalignment or reduced numbers of EC associated macrophages. Superficial (CD11b+, F4/80+, CD240+) and deep (CD11b+, F4/80+, CD240-) macrophages (Stefater et al., 2011) isolated from wildtype and *Ndph*$^{y/-}$ retinas can be used in aortic ring assays to figure out if migration of macrophages or their release of angiogenic cues are altered. By applying sVEGFR1 protein while conducting the assays one can figure out if those macrophages release VEGF-A (Rymo et al., 2011). One might also check if the different macrophages express Norrin and Wnt7b by qPCR (Lobov et al., 2005). One could also check if Norrin is able to alter non-canonical Wnt signaling in deep retinal macrophages by Fura-2 analysis *in vitro* (Stefater et al., 2011).

4.3.5 Lithium chloride is toxic for mice pups

Our goal was to rescue the deep retinal vascular sprouting in *Ndph*$^{y/-}$ mice by reactivation of canonical Wnt-signaling. A rescue of the ocular phenotype in our mice was already achieved by overexpressing Norrin in the lens (Ohlmann et al., 2005), but we wanted to see if stimulation of canonical Wnt signaling with lithium chloride (LiCl) would be sufficient to rescue blood vessel defects. For that we subcutaneously injected low doses of LiCl into mice pups between P5 and P12. Injections were aborted at P8 due to the unexpected high toxicity of low LiCl doses in mice pups (Table 2). Deep vascular sprouting was not rescued in surviving *Ndph*$^{y/-}$ mice despite the almost lethal dose of LiCl in surviving pups (Figure 29). Therefore, systemic administration of LiCl is not recommended to rescue the vascular phenotype of *Ndph*$^{y/-}$ mice. LiCl administration is also not the treatment of choice for human patients. Firstly, we did not find any efficacy. Secondly, we estimated the lethal dose (LD_{50}) to be more than three times lower for mice pups than for adult mice. The LD_{50} might be even lower for developing mouse embryos. This is likely to be similar in humans. The vascular plexuses in humans develops prenatally and hence, pregnant women would have to take LiCl which would put mother and child at risk. A more promising approach to rescue deep vascular sprouting in mice could be intravitreal injection of Norrin or intravitreal or subretinal injection of Norrin encoding adeno-associated viral (AAV) particles. Injection of Norrin protein has the disadvantage that it might be necessary to inject Norrin repeatedly and that the purification of Norrin might be difficult. AAV injection has the disadvantage that virus particles need to be purified prior to injection and that integrated viral DNA might alter function of endogenously encoded genes. Advantages are that many different serotypes recombinant AAVs are available for desired cell tropism (Petrs-Silva et al., 2009) and that the expression specificity can be enhanced by using the endogenous Norrin promoter. Since the viral DNA integrates stably into the host DNA, persistent expression of the gene of interest is achieved. In addition, AAV was proven as a vector for gene therapy in the human retina (RPE65) (Bainbridge et al., 2008). To rescue the ocular phenotype in *Ndph*$^{y/-}$ mice, the AAV serotype 8 Y773F shuttle could be used, since this virus transduces also Müller cells after subretinal injection (Petrs-Silva et al., 2009). The most exciting experiments using AAVs might be to express putative downstream components or target genes of Norrin-Wnt signaling in vascular endothelial cells or macrophages of *Ndph*$^{y/-}$ retinas. Such experiments could give more insight into the mechanism of deep retinal vascular sprouting.

4.3.6 Outlook and future experiments

This section covers suggestions concerning the investigation of the role of Norrin. The suggestions are partially based on data from literature.

Establishing ISH on retinal whole-mounts is mandatory for this lab, since reliable working antibodies are not commercially available for all the proteins of interest. Initially, ISH should be performed for arterial and venous markers (e.g. ephrinB2, EphB4, APJ).

Norrin is expressed in Müller cells and acts on endothelial cells that express Fz-4, LRP-5 and Tspan-12. Therefore it is essential to get a *Fzd4* or *Lrp5* or *Tspan12* knockout mouse as a source for primary endothelial cells for cell culture experiments. A *Fzd4* knockout mouse is available from Jackson Lab (stock number: 012823). These homozygous *Fzd4* knockout mice have a congenital retinal hypovascularization, a progressive inner ear vascular atrophy, a defect in the blood brain barrier in the cerebellum, and a progressive cerebellar degeneration associated with severe ataxia. These mice also show an absence of a skeletal muscle sheath around the lower esophagus associated with

progressive esophageal distension (http://jaxmice.jax.org/strain/012823.html). I suggest to use this mouse as a source for primary endothelial cells. Additionally, different commercially available primary endothelial cells should be purchased and tested (e.g. HUVECs, MAE, HMECs, BCE). I recommend to conduct RT-PCRs from all of the endothelial cell lines to test the following markers: *EphB4*, *ephrinB2*, *Vegf-Axxx*, *Vegf-XXXb*, *Vegfr2*, *Vegfr1*, *Fgf*, *Plgf*, *sVEGFR1*, *Nrp1*, *Pcam1*, *Fzd4*, *Lrp5*, *Tspan12*, *Ndph*. This helps to characterize the endothelial cells and facilitates interpretation of the outcome from the assays. For the same reason, macrophages should be isolated and tested for the expression of *Wnt7b*, *Fzd4*, *Lrp5*, *Tspan12*, *Ndph*, *Iba1*, *F4/80, CD11b, CD240*.

We previously reported upregulation of *Vegf-A* in *Ndph*$^{y/-}$ mice during the hypoxic stage of Norrie disease (Luhmann et al., 2005a). For that, TaqMan probes binding in exon 2 and exon 3 were used. These primers recognize all VEGF-A splice variants including the anti-angiogenic b-variants (Ladomery et al., 2007). However, the detailed expression profile of the respective *Vegf-A-a-* and *–b* variants is crucial, since all splice isoforms exert specific effects on vascular development. Therefore I recommend to perform an extensive analysis monitoring the up- and downregulation of the known *Vegf-A* splice variants in *Ndph*$^{y/-}$ retinas at P5, P7 and P12. This work may help to explain reduction in vascular density and it may also provide a primer for the angiogenesis community of how to proper analyze VEGF-A in mice retinas.

The endothelial cell alignment of *Ndph*$^{y/-}$ and their *Ndph*$^{y/+}$ littermates should be analyzed by electron microscopy with the goal to reveal if the phalanx structure, tight junctions, SMC coverage or vascular fenestrations are altered. An altered phalanx structure of ECs in *Ndph*$^{y/-}$ mice could be caused by altered PHD2 expression (Mazzone et al., 2009). Regarding thight or adherens junctions and vascular fenestrations, we previously reported downregulation of *cldn5 (claudin-5)* in vessels of *Ndph*$^{y/-}$ retinas (Schafer et al., 2009) together with elevated vascular permeability (Luhmann et al., 2005a). This strongly indicates a loss of blood-retinal barrier. Therefore it would be interesting to focus on zonula occludens and zonula adherens forming molecules (e.g. claudin5, ZO-1, ZO-2, VE-cadherin, N-cadherin, cingulin, 7H6, rab13 and occludin) (Barber et al., 2003; Kevil et al., 1998; Wong et al., 1997). Misalignment of these compounds may also cause loss of phalanx structure of retinal endothelial cells and vascular permeability. It has been shown that alterations in the axin cytoskeleton also lead to vascular leakage. Therefore altered axin alignment within the cell or altered localization of any of the axin-associated proteins may also contribute to vascular permeability. MAPK signaling also influences axin-cytoskelleton formation via SRF. Apart from SRF, axin, integrin linked kinase (ILK) and Rho kinase (ROCK) are good candidates (Kogata et al., 2009) to investiagte. Amot might play a controlling permeability of cell-cell junctions or to establish polarity of ECs (Bratt et al., 2005) (see below).

We found extensive smooth muscle cell coverage of the SRVP in *Ndph*$^{y/-}$ mice after P9, which likely involves altered PDGFB/PDGFRβ and Ang1/Tie-2 signaling (Zuercher et al., 2012). Preventing extensive SMC coverage after P9 by injection of antibodies against these proteins would be a strong argument for that (Falcon et al., 2009; Uemura et al., 2002). Additionally, the influence of Norrin on the differentiation of SMCs can be analyzed in cell culture. For that, C3H10T1/2 cells could be stimulated to differentiate into SMCs in presence or absence of Norrin. This work requires NG2 and SMA IHC, application of Wnt inhibitors and constructs to label the cells in co-culture (e.g. GFP/Cherry) (Darland et al., 2001). During this work IHC for the pericyte markers Desmin, NG2 and PDGFRβ should be established. A mouse anti-Desmin antibody is available in this lab, but unspecific

binding of the secondary anti-mouse antibody limited reliability of the histological stainings. Specific blocking of retinal whole-mounts with a mouse on mouse (M.O.M.) kit could help to avoid this problem. PDGFRβ staining is described in Falcon et al., 2009. Finally, the influence of Norrin on SMC recruitment could be monitored. This could involve downstream activity of SRF (Miano et al., 2004).

We noticed extensive central sprouting peaking at P9 in *Ndph*$^{y/-}$ mice (Zuercher et al., 2012). The etiology of this pathogenic central sprouting is not clear, because the current literature exclusively deals with peripheral sprouting. VEGFR3 (Tammela et al., 2008; Tammela et al., 2011) is a known tip cell marker and therefore it might be interesting to co-stain retinas at P9 for VEGFR3 and endomucin or isolectinB4. The polarity of the endothelial cells or their responsiveness to growth factors might be lost. Thus, analyzing *Angiomotin (Amot)* expression profiles might be interesting in this regard. Amot is a receptor for the angiogenesis inhibitor angiostatin and Amot is expressed in ECs during normal physiological angiogenesis of the mouse retina (Bratt et al., 2005). It has been shown in a Boyden chamber assay that EC migration towards sources of VEGF, bFGF is reduced in Amot deficient or knockdown ECs. Amot is not required for tight junction formation, but for the organization of actin and focal adhesions. The interaction partner of Amot is Syx, a synectin-binding guanine exchange factor that is specifically expressed in blood vessels (Aase et al., 2007; Ernkvist et al., 2009; Garnaas et al., 2008). Otherwise, a partial loss the venous character could account for extensive central sprouting. Venous insufficiency has also been reported in a Norrie disease family from Costa Rica (Rehm et al., 1997). To assess that, ephrinB2-lacZ or EphB4-lacZ mice could be crossed with *Ndph*$^{y/-}$ mice and expression of the pan-arterial parker ephrinB2 could be described (Stalmans et al., 2002; Wang et al., 1998). ECs of these mice could be used in cell culture to monitor the effect of Norrin on A/V specification. Another promising work could be to investigate the ratio between Nrp1 and Nrp2 which are arterial and venous markers, respectively. The distribution of these markers on arteries and veins could be addressed by ISH or IHC, depending on the availability of working antibodies. It might be likely that Nrp1 expression is altered, since *Nrp1* knockout mice display also A/V crossing (Fantin et al., 2011), a phenotypic feature I also described in *Ndph*$^{y/-}$ mice.

ColIV stainings in *Ndph*$^{y/-}$ mice show broader and thickened basement membrane sleeves on retinal whole-mounts and on cryosections. Therefore it would be interesting to analyze the basement membrane extensively (Baluk et al., 2003). Several stainings (e.g. fibronectin, laminin, SMA) could be done on cryosections which might help to answer whether the basement membrane is enlarged or just fails to be degraded during deep sprouting. MT1-MMP or similar metalloproteinases could be involved in this process (van Hinsbergh et al., 2008; Yana et al., 2007).

EGFL7 expression or deposition next to vascular sprouts could be monitored (Schmidt et al., 2007). *EGFL7*$^{-/-}$ mice display a delayed outgrowth of the SRVP and an increased number of stalk cells following the tip cell. The retinal vascular front is bulky, similar to *Ndph*$^{y/-}$ mice (Schmidt et al., 2007, supplementary data). A locally altered expression of EGFL7 could explain the occurrence of the bulky vascular front in *Ndph*$^{y/-}$ mice. The defects reported for EGFL7 might alternatively be caused by altered levels of the *EGFL7* intronic aligned miRNA-126 (Nikolic et al., 2010). Therefore it might be worth to investigate the abundance of miRNA-126 or its localization in blood vessels from *Ndph*$^{y/-}$ retinas.

Different pathway inhibitors or activators might be injected into *Ndph*$^{y/-}$ mice and their littermates and their influence on the vasculature might be described. Possible candidate targets of these inhibitors or activating drugs are Rho kinase, MAPK or TGFβ inhibitors and activators.

It is still not clear if or how Angpt2 and Norrin-Wnt signaling are linked. Overexpression of Angpt2 in *Ndph*$^{y/-}$ retinas and overexpression of Norrin in *Angpt2*$^{-/-}$ retinas after transduction might help to determine if one of the mentioned proteins acts ectopic to the other. Angpt2 might also be worth to be investigated regarding its role in hyaloid regression. Angpt2 seems, like Wnt7a, Norrin, Fz-4, LRP-5 and Tspan12, to be mandatory for hyaloid regression. Regarding the screening of patients, it might be worth to consider Angpt2 mutations and Dickkopf1 (Dkk1) gain-of-function mutations as candidate genes for EVR phenotypes. The interpretation of Dkk1 mutations might be difficult, especially if they occur in promoter or silencer regions.

Acknowledgements

Most importantly, I want to thank Prof. Dr. Wolfgang Berger for giving me the opportunity to do my thesis in his lab on this fascinating project. I always appreciated his constant support and trust, his open-minded view and his motivating enthusiasm for my project. The various scientific and personal discussions with him helped me to mature to a critical responsible scientist.

My warmest thanks goes to the members of the Norrie team. I thank Lucas Mohn for his inspiring discussions, for his discussions during ZNZ exam preparations and for being a persisting night life partner when meetings were off. Finally I thank him for providing the Norrin and mutant Norrin isoform expressing stable HEK293T cell lines. I thank Martin Fritzsche for contributing to major parts of this work including retinal whole-mount stainings, DAPT and BrdU experiments and for the scientific discussions and his great support whenever there was a need for it. Nikolaus Schäfer for his support with TaqMan analysis and the many scientific discussions. Britta Seebauer and Lea Sollfrank for their constructive comments on my work and Silke Feil for her constant support, general lab organization, genotyping of the mice and for the organization of the cell culture lab.

Great thanks goes to Dr. Barbara Kloeckener-Gruissem for all the personal and scientific discussions, critical perusal of my work and for the nice and copious teamwork which lead to the publication of my first paper.

Many thanks go to the RP group including Dr. John Neidhardt, Dr. Sandra Brunner and Dr. Fabian Schmid. I thank them for all the inspiring discussions we had and for creating a good atmosphere in the lab and abroad. I also thank Esther Glaus for organizing the lab and for her support. Further thanks goes to Mariana Wittmer and István Magyar for all their support and for creating a nice atmosphere.

I want to pay great credits to Severin Schwendener and Dr. Jean-Charles Paterna, both ETH Zurich Alumni, for their help with establishment of Ca-precipitation transfection method. Further credits go to Dr. Riu Benedito and Prof. Dr. Ralph Adams from the Max Planck Institute in Münster, Germany, for their technical help while establishing retinal whole-mount preparations and for their inspiring discussions during my Münster visit.

I also want to thank all the other members of the Institute for Molecular Medical Genetics for their personal and technical support.

I also thank Josef Maier for his great friendship and the regular lunch work outs, wellness sessions and the many discussions.

Further I thank:

Dr. Diane Hayward from the John Hopkins University, Baltimore, USA, for providing the Notch reporter constructs. Prof. Dr. Konrad Basler and Dr. George Hausman from University of Zurich for providing the Wnt reporter constructs. Dr. Xi He and Bryan Macdonald from Harvard Medical School, Boston , USA, for providing the *LRP5* construct. Dr. Wei Chen from the Duke University, Durham, USA, for providing the *FZD4* construct.

References

Aase, K., Ernkvist, M., Ebarasi, L., Jakobsson, L., Majumdar, A., Yi, C., Birot, O., Ming, Y., Kvanta, A., Edholm, D., Aspenstrom, P., Kissil, J., Claesson-Welsh, L., Shimono, A., and Holmgren, L. (2007). Angiomotin regulates endothelial cell migration during embryonic angiogenesis. Genes Dev. 21:2055-2068

Adams, R. H., Wilkinson, G. A., Weiss, C., Diella, F., Gale, N. W., Deutsch, U., Risau, W., and Klein, R. (1999). Roles of ephrinB ligands and EphB receptors in cardiovascular development: demarcation of arterial/venous domains, vascular morphogenesis, and sprouting angiogenesis. Genes Dev. 13:295-306

Allain, B., Jarray, R., Borriello, L., Leforban, B., Dufour, S., Liu, W. Q., Pamonsinlapatham, P., Bianco, S., Larghero, J., Hadj-Slimane, R., Garbay, C., Raynaud, F., and Lepelletier, Y. (2012). Neuropilin-1 regulates a new VEGF-induced gene, Phactr-1, which controls tubulogenesis and modulates lamellipodial dynamics in human endothelial cells. Cell Signal. 24:214-223

Almodovar, C., Lambrechts, D., Mazzone, M., and Carmeliet, P. (2009). Role and therapeutic potential of VEGF in the nervous system. Physiol Rev. 89:607-648

Anand, S., Majeti, B. K., Acevedo, L. M., Murphy, E. A., Mukthavaram, R., Scheppke, L., Huang, M., Shields, D. J., Lindquist, J. N., Lapinski, P. E., King, P. D., Weis, S. M., and Cheresh, D. A. (2010). MicroRNA-132-mediated loss of p120RasGAP activates the endothelium to facilitate pathological angiogenesis. Nat.Med. 16:909-914

Antonetti, D. A., Barber, A. J., Khin, S., Lieth, E., Tarbell, J. M., and Gardner, T. W. (1998). Vascular permeability in experimental diabetes is associated with reduced endothelial occludin content: vascular endothelial growth factor decreases occludin in retinal endothelial cells. Penn State Retina Research Group. Diabetes 47:1953-1959

Bainbridge, J. W., Smith, A. J., Barker, S. S., Robbie, S., Henderson, R., Balaggan, K., Viswanathan, A., Holder, G. E., Stockman, A., Tyler, N., Petersen-Jones, S., Bhattacharya, S. S., Thrasher, A. J., Fitzke, F. W., Carter, B. J., Rubin, G. S., Moore, A. T., and Ali, R. R. (2008). Effect of gene therapy on visual function in Leber's congenital amaurosis. N.Engl.J.Med. 358:2231-2239

Baluk, P., Morikawa, S., Haskell, A., Mancuso, M., and McDonald, D. M. (2003). Abnormalities of basement membrane on blood vessels and endothelial sprouts in tumors. Am.J.Pathol. 163:1801-1815

Barber, A. J. and Antonetti, D. A. (2003). Mapping the blood vessels with paracellular permeability in the retinas of diabetic rats. Invest Ophthalmol.Vis.Sci. 44:5410-5416

Barber, A. J., Antonetti, D. A., and Gardner, T. W. (2000). Altered expression of retinal occludin and glial fibrillary acidic protein in experimental diabetes. The Penn State Retina Research Group. Invest Ophthalmol.Vis.Sci. 41:3561-3568

Benedito, R., Roca, C., Sorensen, I., Adams, S., Gossler, A., Fruttiger, M., and Adams, R. H. (2009). The notch ligands Dll4 and Jagged1 have opposing effects on angiogenesis. Cell 137:1124-1135

Benjamin, L. E., Hemo, I., and Keshet, E. (1998). A plasticity window for blood vessel remodelling is defined by pericyte coverage of the preformed endothelial network and is regulated by PDGF-B and VEGF. Development 125:1591-1598

Berger, W. (1998). Molecular dissection of Norrie disease. Acta Anat.(Basel) 162:95-100

Berger, W., Kloeckener-Gruissem, B., and Neidhardt, J. (2010). The molecular basis of human retinal and vitreoretinal diseases. Prog.Retin.Eye Res.

Berger, W., van de Pol, D., Bachner, D., Oerlemans, F., Winkens, H., Hameister, H., Wieringa, B., Hendriks, W., and Ropers, H. H. (1996). An animal model for Norrie disease (ND): gene targeting of the mouse ND gene. Hum.Mol.Genet. 5:51-59

Berger, W., van de Pol, D., Warburg, M., Gal, A., Bleeker-Wagemakers, L., de, Silva H., Meindl, A., Meitinger, T., Cremers, F., and Ropers, H. H. (1992). Mutations in the candidate gene for Norrie disease. Hum.Mol.Genet. 1:461-465

Bergers, G. and Song, S. (2005). The role of pericytes in blood-vessel formation and maintenance. Neuro.Oncol. 7:452-464

Bernales, S., Papa, F. R., and Walter, P. (2006). Intracellular signaling by the unfolded protein response. Annu.Rev.Cell Dev.Biol. 22:487-508

Bertolino, P., Deckers, M., Lebrin, F., and ten, Dijke P. (2005). Transforming growth factor-beta signal transduction in angiogenesis and vascular disorders. Chest 128:585S-590S

Boucheix, C. and Rubinstein, E. (2001). Tetraspanins. Cell Mol.Life Sci. 58:1189-1205

Bratt, A., Birot, O., Sinha, I., Veitonmaki, N., Aase, K., Ernkvist, M., and Holmgren, L. (2005). Angiomotin regulates endothelial cell-cell junctions and cell motility. J.Biol.Chem. 280:34859-34869

Caprara, C., Thiersch, M., Lange, C., Joly, S., Samardzija, M., and Grimm, C. (2011). HIF1A is essential for the development of the intermediate plexus of the retinal vasculature. Invest Ophthalmol.Vis.Sci.

Carmeliet, P. and Tessier-Lavigne, M. (2005). Common mechanisms of nerve and blood vessel wiring. Nature 436:193-200

Chai, J., Jones, M. K., and Tarnawski, A. S. (2004). Serum response factor is a critical requirement for VEGF signaling in endothelial cells and VEGF-induced angiogenesis. FASEB J. 18:1264-1266

Chan-Ling, T., Page, M. P., Gardiner, T., Baxter, L., Rosinova, E., and Hughes, S. (2004). Desmin ensheathment ratio as an indicator of vessel stability: evidence in normal development and in retinopathy of prematurity. Am.J.Pathol. 165:1301-1313

Chang, B., Smith, R. S., Peters, M., Savinova, O. V., Hawes, N. L., Zabaleta, A., Nusinowitz, S., Martin, J. E., Davisson, M. L., Cepko, C. L., Hogan, B. L., and John, S. W. (2001). Haploinsufficient Bmp4 ocular phenotypes include anterior segment dysgenesis with elevated intraocular pressure. BMC.Genet. 2:18-

Checchin, D., Sennlaub, F., Levavasseur, E., Leduc, M., and Chemtob, S. (2006). Potential role of microglia in retinal blood vessel formation. Invest Ophthalmol.Vis.Sci. 47:3595-3602

Chen, S. and Lechleider, R. J. (2004). Transforming growth factor-beta-induced differentiation of smooth muscle from a neural crest stem cell line. Circ.Res. 94:1195-1202

Chen, Z. Y., Battinelli, E. M., Fielder, A., Bundey, S., Sims, K., Breakefield, X. O., and Craig, I. W. (1993). A mutation in the Norrie disease gene (NDP) associated with X-linked familial exudative vitreoretinopathy. Nat.Genet. 5:180-183

Chen, Z. Y., Sims, K. B., Coleman, M., Donnai, D., Monaco, A., Breakefield, X. O., Davies, K. E., and Craig, I. W. (1992). Characterization of a YAC containing part or all of the Norrie disease locus. Hum.Mol.Genet. 1:161-164

Chu, Y., Hughes, S., and Chan-Ling, T. (2001). Differentiation and migration of astrocyte precursor cells and astrocytes in human fetal retina: relevance to optic nerve coloboma. FASEB J. 15:2013-2015

Chynn, E. W., Walton, D. S., Hahn, L. B., and Dryja, T. P. (1996). Norrie disease. Diagnosis of a simplex case by DNA analysis. Arch.Ophthalmol. 114:1136-1138

Claxton, S. and Fruttiger, M. (2003). Role of arteries in oxygen induced vaso-obliteration. Exp.Eye Res. 77:305-311

Claxton, S. and Fruttiger, M. (2004). Periodic Delta-like 4 expression in developing retinal arteries. Gene Expr.Patterns. 5:123-127

Clevers, H. (2009). Eyeing up new Wnt pathway players. Cell 139:227-229

Connor, K. M., Krah, N. M., Dennison, R. J., Aderman, C. M., Chen, J., Guerin, K. I., Sapieha, P., Stahl, A., Willett, K. L., and Smith, L. E. (2009). Quantification of oxygen-induced retinopathy in the mouse: a model of vessel loss, vessel regrowth and pathological angiogenesis. Nat.Protoc. 4:1565-1573

Covassin, L. D., Villefranc, J. A., Kacergis, M. C., Weinstein, B. M., and Lawson, N. D. (2006). Distinct genetic interactions between multiple Vegf receptors are required for development of different blood vessel types in zebrafish. Proc.Natl.Acad.Sci.U.S.A 103:6554-6559

Darland, D. C. and D'Amore, P. A. (2001). TGF beta is required for the formation of capillary-like structures in three-dimensional cocultures of 10T1/2 and endothelial cells. Angiogenesis. 4:11-20

Davis, S., Aldrich, T. H., Jones, P. F., Acheson, A., Compton, D. L., Jain, V., Ryan, T. E., Bruno, J., Radziejewski, C., Maisonpierre, P. C., and Yancopoulos, G. D. (1996). Isolation of angiopoietin-1, a ligand for the TIE2 receptor, by secretion-trap expression cloning. Cell 87:1161-1169

De, Val S. and Black, B. L. (2009). Transcriptional control of endothelial cell development. Dev.Cell 16:180-195

Diez-Roux, G. and Lang, R. A. (1997). Macrophages induce apoptosis in normal cells in vivo. Development 124:3633-3638

Dorrell, M. I., Aguilar, E., and Friedlander, M. (2002). Retinal vascular development is mediated by endothelial filopodia, a preexisting astrocytic template and specific R-cadherin adhesion. Invest Ophthalmol.Vis.Sci. 43:3500-3510

Duarte, A., Hirashima, M., Benedito, R., Trindade, A., Diniz, P., Bekman, E., Costa, L., Henrique, D., and Rossant, J. (2004). Dosage-sensitive requirement for mouse Dll4 in artery development. Genes Dev. 18:2474-2478

Eichmann, A., Le, Noble F., Autiero, M., and Carmeliet, P. (2005). Guidance of vascular and neural network formation. Curr.Opin.Neurobiol. 15:108-115

Eilken, H. M. and Adams, R. H. (2010). Dynamics of endothelial cell behavior in sprouting angiogenesis. Curr.Opin.Cell Biol. 22:617-625

Ernkvist, M., Luna, Persson N., Audebert, S., Lecine, P., Sinha, I., Liu, M., Schlueter, M., Horowitz, A., Aase, K., Weide, T., Borg, J. P., Majumdar, A., and Holmgren, L. (2009). The Amot/Patj/Syx signaling complex spatially controls RhoA GTPase activity in migrating endothelial cells. Blood 113:244-253

Falcon, B. L., Hashizume, H., Koumoutsakos, P., Chou, J., Bready, J. V., Coxon, A., Oliner, J. D., and McDonald, D. M. (2009). Contrasting actions of selective inhibitors of angiopoietin-1 and angiopoietin-2 on the normalization of tumor blood vessels. Am.J.Pathol. 175:2159-2170

Fantin, A., Schwarz, Q., Davidson, K., Normando, E. M., Denti, L., and Ruhrberg, C. (2011). The cytoplasmic domain of neuropilin 1 is dispensable for angiogenesis, but promotes the spatial separation of retinal arteries and veins. Development 138:4185-4191

Figueroa, D. J., Hess, J. F., Ky, B., Brown, S. D., Sandig, V., Hermanowski-Vosatka, A., Twells, R. C., Todd, J. A., and Austin, C. P. (2000). Expression of the type I diabetes-associated gene LRP5 in macrophages, vitamin A system cells, and the Islets of Langerhans suggests multiple potential roles in diabetes. J.Histochem.Cytochem. 48:1357-1368

Fischer, A., Schumacher, N., Maier, M., Sendtner, M., and Gessler, M. (2004). The Notch target genes Hey1 and Hey2 are required for embryonic vascular development. Genes Dev. 18:901-911

Franco, C. A. and Li, Z. (2009). SRF in angiogenesis: branching the vascular system. Cell Adh.Migr. 3:264-267

Franco, C. A., Mericskay, M., Parlakian, A., Gary-Bobo, G., Gao-Li, J., Paulin, D., Gustafsson, E., and Li, Z. (2008). Serum response factor is required for sprouting angiogenesis and vascular integrity. Dev.Cell 15:448-461

Fruttiger, M. (2007). Development of the retinal vasculature. Angiogenesis. 10:77-88

Fruttiger, M., Calver, A. R., Kruger, W. H., Mudhar, H. S., Michalovich, D., Takakura, N., Nishikawa, S., and Richardson, W. D. (1996). PDGF mediates a neuron-astrocyte interaction in the developing retina. Neuron 17:1117-1131

Fruttiger, M., Calver, A. R., and Richardson, W. D. (2000). Platelet-derived growth factor is constitutively secreted from neuronal cell bodies but not from axons. Curr.Biol. 10:1283-1286

Gale, N. W., Dominguez, M. G., Noguera, I., Pan, L., Hughes, V., Valenzuela, D. M., Murphy, A. J., Adams, N. C., Lin, H. C., Holash, J., Thurston, G., and Yancopoulos, G. D. (2004). Haploinsufficiency of delta-like 4 ligand results in embryonic lethality due to major defects in arterial and vascular development. Proc.Natl.Acad.Sci.U.S.A 101:15949-15954

Gale, N. W., Thurston, G., Hackett, S. F., Renard, R., Wang, Q., McClain, J., Martin, C., Witte, C., Witte, M. H., Jackson, D., Suri, C., Campochiaro, P. A., Wiegand, S. J., and Yancopoulos, G. D. (2002). Angiopoietin-2 is required for postnatal angiogenesis and lymphatic patterning, and only the latter role is rescued by Angiopoietin-1. Dev.Cell 3:411-423

Gardner, T. W., Lieth, E., Khin, S. A., Barber, A. J., Bonsall, D. J., Lesher, T., Rice, K., and Brennan, W. A., Jr. (1997). Astrocytes increase barrier properties and ZO-1 expression in retinal vascular endothelial cells. Invest Ophthalmol.Vis.Sci. 38:2423-2427

Garnaas, M. K., Moodie, K. L., Liu, M. L., Samant, G. V., Li, K., Marx, R., Baraban, J. M., Horowitz, A., and Ramchandran, R. (2008). Syx, a RhoA guanine exchange factor, is essential for angiogenesis in Vivo. Circ.Res. 103:710-716

Gerhardt, H., Golding, M., Fruttiger, M., Ruhrberg, C., Lundkvist, A., Abramsson, A., Jeltsch, M., Mitchell, C., Alitalo, K., Shima, D., and Betsholtz, C. (2003). VEGF guides angiogenic sprouting utilizing endothelial tip cell filopodia. J.Cell Biol. 161:1163-1177

Goumans, M. J., Lebrin, F., and Valdimarsdottir, G. (2003). Controlling the angiogenic switch: a balance between two distinct TGF-b receptor signaling pathways. Trends Cardiovasc.Med. 13:301-307

Gu, X., El-Remessy, A. B., Brooks, S. E., Al-Shabrawey, M., Tsai, N. T., and Caldwell, R. B. (2003). Hyperoxia induces retinal vascular endothelial cell apoptosis through formation of peroxynitrite. Am.J.Physiol Cell Physiol 285:C546-C554

Gyllensten , L. J. and HELLSTROM, B. E. (1954a). Experimental approach to the pathogenesis of retrolental fibroplasia. I. Changes of the eye induced by exposure of newborn mice to concentrated oxygen. Acta Paediatr.Suppl 43:131-148

Gyllensten , L. J. and HELLSTROM, B. E. (1954b). Experimental approach to the pathogenesis of retrolental fibroplasia. I. Changes of the eye induced by exposure of newborn mice to concentrated oxygen. Acta Paediatr.Suppl 43:131-148

Hackett, S. F., Wiegand, S., Yancopoulos, G., and Campochiaro, P. A. (2002). Angiopoietin-2 plays an important role in retinal angiogenesis. J.Cell Physiol 192:182-187

Haigh, J. J., Morelli, P. I., Gerhardt, H., Haigh, K., Tsien, J., Damert, A., Miquerol, L., Muhlner, U., Klein, R., Ferrara, N., Wagner, E. F., Betsholtz, C., and Nagy, A. (2003). Cortical and retinal defects caused by dosage-dependent reductions in VEGF-A paracrine signaling. Dev.Biol. 262:225-241

Hartzer, M. K., Cheng, M., Liu, X., and Shastry, B. S. (1999). Localization of the Norrie disease gene mRNA by in situ hybridization. Brain Res.Bull. 49:355-358

Hellstrom, M., Kalen, M., Lindahl, P., Abramsson, A., and Betsholtz, C. (1999). Role of PDGF-B and PDGFR-beta in recruitment of vascular smooth muscle cells and pericytes during embryonic blood vessel formation in the mouse. Development 126:3047-3055

Hellstrom, M., Phng, L. K., and Gerhardt, H. (2007a). VEGF and Notch signaling: the yin and yang of angiogenic sprouting. Cell Adh.Migr. 1:133-136

Hellstrom, M., Phng, L. K., Hofmann, J. J., Wallgard, E., Coultas, L., Lindblom, P., Alva, J., Nilsson, A. K., Karlsson, L., Gaiano, N., Yoon, K., Rossant, J., Iruela-Arispe, M. L., Kalen, M., Gerhardt, H., and Betsholtz, C. (2007b). Dll4 signalling through Notch1 regulates formation of tip cells during angiogenesis. Nature 445:776-780

Hemler, M. E. (2005). Tetraspanin functions and associated microdomains. Nat.Rev.Mol.Cell Biol. 6:801-811

Herr, F., Baal, N., Widmer-Teske, R., McKinnon, T., and Zygmunt, M. (2010). How to study placental vascular development? Theriogenology 73:817-827

Hobson, B. and Denekamp, J. (1984). Endothelial proliferation in tumours and normal tissues: continuous labelling studies. Br.J.Cancer 49:405-413

Hofmann, C., Dunger, N., Scholmerich, J., Falk, W., and Obermeier, F. (2010). Glycogen synthase kinase 3-beta: a master regulator of toll-like receptor-mediated chronic intestinal inflammation. Inflamm.Bowel.Dis. 16:1850-1858

Hofmann, J. J. and Luisa Iruela-Arispe, M. (2007). Notch expression patterns in the retina: An eye on receptor-ligand distribution during angiogenesis. Gene Expr.Patterns. 7:461-470

Hong, C. C., Peterson, Q. P., Hong, J. Y., and Peterson, R. T. (2006). Artery/vein specification is governed by opposing phosphatidylinositol-3 kinase and MAP kinase/ERK signaling. Curr.Biol. 16:1366-1372

Hsieh, M., Boerboom, D., Shimada, M., Lo, Y., Parlow, A. F., Luhmann, U. F., Berger, W., and Richards, J. S. (2005). Mice null for Frizzled4 (Fzd4-/-) are infertile and exhibit impaired corpora lutea formation and function. Biol.Reprod. 73:1135-1146

Hughes, S. and Chang-Ling, T. (2000). Roles of endothelial cell migration and apoptosis in vascular remodeling during development of the central nervous system. Microcirculation. 7:317-333

Ishida, S., Yamashiro, K., Usui, T., Kaji, Y., Ogura, Y., Hida, T., Honda, Y., Oguchi, Y., and Adamis, A. P. (2003). Leukocytes mediate retinal vascular remodeling during development and vaso-obliteration in disease. Nat.Med. 9:781-788

Jakobsson, L., Bentley, K., and Gerhardt, H. (2009). VEGFRs and Notch: a dynamic collaboration in vascular patterning. Biochem.Soc.Trans. 37:1233-1236

Jakobsson, L., Franco, C. A., Bentley, K., Collins, R. T., Ponsioen, B., Aspalter, I. M., Rosewell, I., Busse, M., Thurston, G., Medvinsky, A., Schulte-Merker, S., and Gerhardt, H. (2010). Endothelial cells dynamically compete for the tip cell position during angiogenic sprouting. Nat.Cell Biol. 12:943-953

Jarray, R., Allain, B., Borriello, L., Biard, D., Loukaci, A., Larghero, J., Hadj-Slimane, R., Garbay, C., Lepelletier, Y., and Raynaud, F. (2011). Depletion of the novel protein PHACTR-1 from human endothelial cells abolishes tube formation and induces cell death receptor apoptosis. Biochimie 93:1668-1675

Jia, H., Bagherzadeh, A., Bicknell, R., Duchen, M. R., Liu, D., and Zachary, I. (2004). Vascular endothelial growth factor (VEGF)-D and VEGF-A differentially regulate KDR-mediated signaling and biological function in vascular endothelial cells. J.Biol.Chem. 279:36148-36157

Jin, Y. H., Kim, H., Oh, M., Ki, H., and Kim, K. (2009). Regulation of Notch1/NICD and Hes1 expressions by GSK-3alpha/beta. Mol.Cells 27:15-19

Jordan, M., Schallhorn, A., and Wurm, F. M. (1996). Transfecting mammalian cells: optimization of critical parameters affecting calcium-phosphate precipitate formation. Nucleic Acids Res. 24:596-601

Jordan, M. and Wurm, F. (2004). Transfection of adherent and suspended cells by calcium phosphate. Methods 33:136-143

Junge, H. J., Yang, S., Burton, J. B., Paes, K., Shu, X., French, D. M., Costa, M., Rice, D. S., and Ye, W. (2009). TSPAN12 regulates retinal vascular development by promoting Norrin- but not Wnt-induced FZD4/beta-catenin signaling. Cell 139:299-311

Kaloglu, C., Cesur, I., and Bulut, H. E. (2011). Norrin immunolocalization and its possible functions in rat endometrium during the estrus cycle and early pregnancy. Dev.Growth Differ.

Kertesz, N., Krasnoperov, V., Reddy, R., Leshanski, L., Kumar, S. R., Zozulya, S., and Gill, P. S. (2006). The soluble extracellular domain of EphB4 (sEphB4) antagonizes EphB4-EphrinB2 interaction, modulates angiogenesis, and inhibits tumor growth. Blood 107:2330-2338

Kevil, C. G., Okayama, N., Trocha, S. D., Kalogeris, T. J., Coe, L. L., Specian, R. D., Davis, C. P., and Alexander, J. S. (1998). Expression of zonula occludens and adherens junctional proteins in human venous and arterial endothelial cells: role of occludin in endothelial solute barriers. Microcirculation. 5:197-210

Kim, I., Ryu, Y. S., Kwak, H. J., Ahn, S. Y., Oh, J. L., Yancopoulos, G. D., Gale, N. W., and Koh, G. Y. (2002). EphB ligand, ephrinB2, suppresses the. FASEB J. 16:1126-1128

Kim, J., Oh, W. J., Gaiano, N., Yoshida, Y., and Gu, C. (2011). Semaphorin 3E-Plexin-D1 signaling regulates VEGF function in developmental angiogenesis via a feedback mechanism. Genes Dev. 25:1399-1411

Kogata, N., Tribe, R. M., Fassler, R., Way, M., and Adams, R. H. (2009). Integrin-linked kinase controls vascular wall formation by negatively regulating Rho/ROCK-mediated vascular smooth muscle cell contraction. Genes Dev. 23:2278-2283

Krebs, L. T., Shutter, J. R., Tanigaki, K., Honjo, T., Stark, K. L., and Gridley, T. (2004). Haploinsufficient lethality and formation of arteriovenous malformations in Notch pathway mutants. Genes Dev. 18:2469-2473

Krebs, L. T., Xue, Y., Norton, C. R., Shutter, J. R., Maguire, M., Sundberg, J. P., Gallahan, D., Closson, V., Kitajewski, J., Callahan, R., Smith, G. H., Stark, K. L., and Gridley, T. (2000). Notch signaling is essential for vascular morphogenesis in mice. Genes Dev. 14:1343-1352

Kubota, Y. and Suda, T. (2009a). Feedback mechanism between blood vessels and astrocytes in retinal vascular development. Trends Cardiovasc.Med. 19:38-43

Kubota, Y., Takubo, K., Shimizu, T., Ohno, H., Kishi, K., Shibuya, M., Saya, H., and Suda, T. (2009b). M-CSF inhibition selectively targets pathological angiogenesis and lymphangiogenesis. J.Exp.Med. 206:1089-1102

Kurz, H., Gartner, T., Eggli, P. S., and Christ, B. (1996). First blood vessels in the avian neural tube are formed by a combination of dorsal angioblast immigration and ventral sprouting of endothelial cells. Dev.Biol. 173:133-147

Ladomery, M. R., Harper, S. J., and Bates, D. O. (2007). Alternative splicing in angiogenesis: the vascular endothelial growth factor paradigm. Cancer Lett. 249:133-142

Lang, R. A. and Bishop, J. M. (1993). Macrophages are required for cell death and tissue remodeling in the developing mouse eye. Cell 74:453-462

Lawson, N. D., Mugford, J. W., Diamond, B. A., and Weinstein, B. M. (2003). Phospholipase C gamma-1 is required downstream of vascular endothelial growth factor during arterial development. Genes Dev. 17:1346-1351

Lawson, N. D., Scheer, N., Pham, V. N., Kim, C. H., Chitnis, A. B., Campos-Ortega, J. A., and Weinstein, B. M. (2001). Notch signaling is required for arterial-venous differentiation during embryonic vascular development. Development 128:3675-3683

Lawson, N. D., Vogel, A. M., and Weinstein, B. M. (2002). Sonic hedgehog and vascular endothelial growth factor act upstream of the Notch pathway during arterial endothelial differentiation. Dev.Cell 3:127-136

Lenzner, S., Prietz, S., Feil, S., Nuber, U. A., Ropers, H. H., and Berger, W. (2002). Global gene expression analysis in a mouse model for Norrie disease: late involvement of photoreceptor cells. Invest Ophthalmol.Vis.Sci. 43:2825-2833

Li, C., Hampson, I. N., Hampson, L., Kumar, P., Bernabeu, C., and Kumar, S. (2000). CD105 antagonizes the inhibitory signaling of transforming growth factor beta1 on human vascular endothelial cells. FASEB J. 14:55-64

Ling, T. L. and Stone, J. (1988). The development of astrocytes in the cat retina: evidence of migration from the optic nerve. Brain Res.Dev.Brain Res. 44:73-85

Liu, Z. J., Shirakawa, T., Li, Y., Soma, A., Oka, M., Dotto, G. P., Fairman, R. M., Velazquez, O. C., and Herlyn, M. (2003). Regulation of Notch1 and Dll4 by vascular endothelial growth factor in arterial endothelial cells: implications for modulating arteriogenesis and angiogenesis. Mol.Cell Biol. 23:14-25

Lobov, I. B., Rao, S., Carroll, T. J., Vallance, J. E., Ito, M., Ondr, J. K., Kurup, S., Glass, D. A., Patel, M. S., Shu, W., Morrisey, E. E., McMahon, A. P., Karsenty, G., and Lang, R. A. (2005). WNT7b mediates macrophage-induced programmed cell death in patterning of the vasculature. Nature 437:417-421

Lobov, I. B., Renard, R. A., Papadopoulos, N., Gale, N. W., Thurston, G., Yancopoulos, G. D., and Wiegand, S. J. (2007). Delta-like ligand 4 (Dll4) is induced by VEGF as a negative regulator of angiogenic sprouting. Proc.Natl.Acad.Sci.U.S.A 104:3219-3224

London, N. R., Smith, M. C., and Li, D. Y. (2009). Emerging mechanisms of vascular stabilization. J.Thromb.Haemost. 7 Suppl 1:57-60

Lu, X., Le, Noble F., Yuan, L., Jiang, Q., De, Lafarge B., Sugiyama, D., Breant, C., Claes, F., De, Smet F., Thomas, J. L., Autiero, M., Carmeliet, P., Tessier-Lavigne, M., and Eichmann, A. (2004). The netrin receptor UNC5B mediates guidance events controlling morphogenesis of the vascular system. Nature 432:179-186

Luhmann, U. F., Lin, J., Acar, N., Lammel, S., Feil, S., Grimm, C., Seeliger, M. W., Hammes, H. P., and Berger, W. (2005a). Role of the Norrie disease pseudoglioma gene in sprouting angiogenesis during development of the retinal vasculature. Invest Ophthalmol.Vis.Sci. 46:3372-3382

Luhmann, U. F., Meunier, D., Shi, W., Luttges, A., Pfarrer, C., Fundele, R., and Berger, W. (2005b). Fetal loss in homozygous mutant Norrie disease mice: a new role of Norrin in reproduction. Genesis. 42:253-262

Magnussen, A. L., Rennel, E. S., Hua, J., Bevan, H. S., Beazley, Long N., Lehrling, C., Gammons, M., Floege, J., Harper, S. J., Agostini, H. T., Bates, D. O., and Churchill, A. J. (2010). VEGF-A165b is cytoprotective and antiangiogenic in the retina. Invest Ophthalmol.Vis.Sci. 51:4273-4281

Marin-Padilla, M. and Amieva, M. R. (1989). Early neurogenesis of the mouse olfactory nerve: Golgi and electron microscopic studies. J.Comp Neurol. 288:339-352

Mazzone, M., Dettori, D., Leite de, Oliveira R., Loges, S., Schmidt, T., Jonckx, B., Tian, Y. M., Lanahan, A. A., Pollard, P., Ruiz de, Almodovar C., De, Smet F., Vinckier, S., Aragones, J., Debackere, K., Luttun, A., Wyns, S., Jordan, B., Pisacane, A., Gallez, B., Lampugnani, M. G., Dejana, E., Simons, M., Ratcliffe, P., Maxwell, P., and Carmeliet, P. (2009). Heterozygous deficiency of PHD2 restores tumor oxygenation and inhibits metastasis via endothelial normalization. Cell 136:839-851

McKenzie, J. A., Fruttiger, M., Abraham, S., Lange, C. A., Stone, J., Gandhi, P., Wang, X., Bainbridge, J., Moss, S. E., and Greenwood, J. (2012). Apelin is required for non-neovascular remodeling in the retina. Am.J.Pathol. 180:399-409

McKercher, S. R., Torbett, B. E., Anderson, K. L., Henkel, G. W., Vestal, D. J., Baribault, H., Klemsz, M., Feeney, A. J., Wu, G. E., Paige, C. J., and Maki, R. A. (1996). Targeted disruption of the PU.1 gene results in multiple hematopoietic abnormalities. EMBO J. 15:5647-5658

McLeod, D. S., Hasegawa, T., Prow, T., Merges, C., and Lutty, G. (2006). The initial fetal human retinal vasculature develops by vasculogenesis. Dev.Dyn. 235:3336-3347

Meindl, A., Berger, W., Meitinger, T., van de Pol, D., Achatz, H., Dorner, C., Haasemann, M., Hellebrand, H., Gal, A., Cremers, F., and . (1992). Norrie disease is caused by mutations in an extracellular protein resembling C-terminal globular domain of mucins. Nat.Genet. 2:139-143

Meitinger, T., Meindl, A., Bork, P., Rost, B., Sander, C., Haasemann, M., and Murken, J. (1993). Molecular modelling of the Norrie disease protein predicts a cystine knot growth factor tertiary structure. Nat.Genet. 5:376-380

Mi, H. and Barres, B. A. (1999). Purification and characterization of astrocyte precursor cells in the developing rat optic nerve. J.Neurosci. 19:1049-1061

Miano, J. M., Ramanan, N., Georger, M. A., de Mesy Bentley, K. L., Emerson, R. L., Balza, R. O., Jr., Xiao, Q., Weiler, H., Ginty, D. D., and Misra, R. P. (2004). Restricted inactivation of serum response factor to the cardiovascular system. Proc.Natl.Acad.Sci.U.S.A 101:17132-17137

Mitchell, C. A., Risau, W., and Drexler, H. C. (1998). Regression of vessels in the tunica vasculosa lentis is initiated by coordinated endothelial apoptosis: a role for vascular endothelial growth factor as a survival factor for endothelium. Dev.Dyn. 213:322-333

Miyawaki, T., Uemura, A., Dezawa, M., Yu, R. T., Ide, C., Nishikawa, S., Honda, Y., Tanabe, Y., and Tanabe, T. (2004). Tlx, an orphan nuclear receptor, regulates cell numbers and astrocyte development in the developing retina. J.Neurosci. 24:8124-8134

Mudhar, H. S., Pollock, R. A., Wang, C., Stiles, C. D., and Richardson, W. D. (1993). PDGF and its receptors in the developing rodent retina and optic nerve. Development 118:539-552

Mukouyama, Y. S., Gerber, H. P., Ferrara, N., Gu, C., and Anderson, D. J. (2005). Peripheral nerve-derived VEGF promotes arterial differentiation via neuropilin 1-mediated positive feedback. Development 132:941-952

Nakatsu, M. N., Sainson, R. C., Perez-del-Pulgar, S., Aoto, J. N., Aitkenhead, M., Taylor, K. L., Carpenter, P. M., and Hughes, C. C. (2003). VEGF(121) and VEGF(165) regulate blood vessel diameter

through vascular endothelial growth factor receptor 2 in an in vitro angiogenesis model. Lab Invest 83:1873-1885

Nikolic, I., Plate, K. H., and Schmidt, M. H. (2010). EGFL7 meets miRNA-126: an angiogenesis alliance. J.Angiogenes.Res. 2:9-

Nikopoulos, K., Gilissen, C., Hoischen, A., van Nouhuys, C. E., Boonstra, F. N., Blokland, E. A., Arts, P., Wieskamp, N., Strom, T. M., Ayuso, C., Tilanus, M. A., Bouwhuis, S., Mukhopadhyay, A., Scheffer, H., Hoefsloot, L. H., Veltman, J. A., Cremers, F. P., and Collin, R. W. (2010). Next-generation sequencing of a 40 Mb linkage interval reveals TSPAN12 mutations in patients with familial exudative vitreoretinopathy. Am.J.Hum.Genet. 86:240-247

Nishimura, G., Manabe, I., Tsushima, K., Fujiu, K., Oishi, Y., Imai, Y., Maemura, K., Miyagishi, M., Higashi, Y., Kondoh, H., and Nagai, R. (2006). DeltaEF1 mediates TGF-beta signaling in vascular smooth muscle cell differentiation. Dev.Cell 11:93-104

Nishishita, T. and Lin, P. C. (2004). Angiopoietin 1, PDGF-B, and TGF-beta gene regulation in endothelial cell and smooth muscle cell interaction. J.Cell Biochem. 91:584-593

Niu, Z., Yu, W., Zhang, S. X., Barron, M., Belaguli, N. S., Schneider, M. D., Parmacek, M., Nordheim, A., and Schwartz, R. J. (2005). Conditional mutagenesis of the murine serum response factor gene blocks cardiogenesis and the transcription of downstream gene targets. J.Biol.Chem. 280:32531-32538

Ohlmann, A., Scholz, M., Goldwich, A., Chauhan, B. K., Hudl, K., Ohlmann, A. V., Zrenner, E., Berger, W., Cvekl, A., Seeliger, M. W., and Tamm, E. R. (2005). Ectopic norrin induces growth of ocular capillaries and restores normal retinal angiogenesis in Norrie disease mutant mice. J.Neurosci. 25:1701-1710

Ota, T., Fujii, M., Sugizaki, T., Ishii, M., Miyazawa, K., Aburatani, H., and Miyazono, K. (2002). Targets of transcriptional regulation by two distinct type I receptors for transforming growth factor-beta in human umbilical vein endothelial cells. J.Cell Physiol 193:299-318

Outtz, H. H., Tattersall, I. W., Kofler, N. M., Steinbach, N., and Kitajewski, J. (2011). Notch1 controls macrophage recruitment and Notch signaling is activated at sites of endothelial cell anastomosis during retinal angiogenesis in mice. Blood

Paes, K. T., Wang, E., Henze, K., Vogel, P., Read, R., Suwanichkul, A., Kirkpatrick, L. L., Potter, D., Newhouse, M. M., and Rice, D. S. (2011). Frizzled 4 is required for retinal angiogenesis and maintenance of the blood-retina barrier. Invest Ophthalmol.Vis.Sci. 52:6452-6461

Parlakian, A., Tuil, D., Hamard, G., Tavernier, G., Hentzen, D., Concordet, J. P., Paulin, D., Li, Z., and Daegelen, D. (2004). Targeted inactivation of serum response factor in the developing heart results in myocardial defects and embryonic lethality. Mol.Cell Biol. 24:5281-5289

Perez-Vilar, J. and Hill, R. L. (1997). Norrie disease protein (norrin) forms disulfide-linked oligomers associated with the extracellular matrix. J.Biol.Chem. 272:33410-33415

Petrs-Silva, H., Dinculescu, A., Li, Q., Min, S. H., Chiodo, V., Pang, J. J., Zhong, L., Zolotukhin, S., Srivastava, A., Lewin, A. S., and Hauswirth, W. W. (2009). High-efficiency transduction of the mouse retina by tyrosine-mutant AAV serotype vectors. Mol.Ther. 17:463-471

Phng, L. K., Potente, M., Leslie, J. D., Babbage, J., Nyqvist, D., Lobov, I., Ondr, J. K., Rao, S., Lang, R. A., Thurston, G., and Gerhardt, H. (2009). Nrarp coordinates endothelial Notch and Wnt signaling to control vessel density in angiogenesis. Dev.Cell 16:70-82

Pierce, E. A., Foley, E. D., and Smith, L. E. (1996). Regulation of vascular endothelial growth factor by oxygen in a model of retinopathy of prematurity. Arch.Ophthalmol. 114:1219-1228

Pitulescu, M. E., Schmidt, I., Benedito, R., and Adams, R. H. (2010). Inducible gene targeting in the neonatal vasculature and analysis of retinal angiogenesis in mice. Nat.Protoc. 5:1518-1534

Potente, M., Gerhardt, H., and Carmeliet, P. (2011). Basic and therapeutic aspects of angiogenesis. Cell 146:873-887

Poulter, J. A., Ali, M., Gilmour, D. F., Rice, A., Kondo, H., Hayashi, K., Mackey, D. A., Kearns, L. S., Ruddle, J. B., Craig, J. E., Pierce, E. A., Downey, L. M., Mohamed, M. D., Markham, A. F., Inglehearn, C. F., and Toomes, C. (2010). Mutations in TSPAN12 cause autosomal-dominant familial exudative vitreoretinopathy. Am.J.Hum.Genet. 86:248-253

Rao, S., Lobov, I. B., Vallance, J. E., Tsujikawa, K., Shiojima, I., Akunuru, S., Walsh, K., Benjamin, L. E., and Lang, R. A. (2007). Obligatory participation of macrophages in an angiopoietin 2-mediated cell death switch. Development 134:4449-4458

Rehm, H. L., Gutierrez-Espeleta, G. A., Garcia, R., Jimenez, G., Khetarpal, U., Priest, J. M., Sims, K. B., Keats, B. J., and Morton, C. C. (1997). Norrie disease gene mutation in a large Costa Rican kindred with a novel phenotype including venous insufficiency. Hum.Mutat. 9:402-408

Rehm, H. L., Zhang, D. S., Brown, M. C., Burgess, B., Halpin, C., Berger, W., Morton, C. C., Corey, D. P., and Chen, Z. Y. (2002). Vascular defects and sensorineural deafness in a mouse model of Norrie disease. J.Neurosci. 22:4286-4292

Richter, M., Gottanka, J., May, C. A., Welge-Lussen, U., Berger, W., and Lutjen-Drecoll, E. (1998). Retinal vasculature changes in Norrie disease mice. Invest Ophthalmol.Vis.Sci. 39:2450-2457

Riva, C. E., Pournaras, C. J., and Tsacopoulos, M. (1986). Regulation of local oxygen tension and blood flow in the inner retina during hyperoxia. J.Appl.Physiol 61:592-598

Roca, C. and Adams, R. H. (2007). Regulation of vascular morphogenesis by Notch signaling. Genes Dev. 21:2511-2524

Rocha, S. F. and Adams, R. H. (2009). Molecular differentiation and specialization of vascular beds. Angiogenesis. 12:139-147

Ron, D. and Walter, P. (2007). Signal integration in the endoplasmic reticulum unfolded protein response. Nat.Rev.Mol.Cell Biol. 8:519-529

Rossant, J. and Cross, J. C. (2001). Placental development: lessons from mouse mutants. Nat.Rev.Genet. 2:538-548

Roukens, M. G., Alloul-Ramdhani, M., Baan, B., Kobayashi, K., Peterson-Maduro, J., van, Dam H., Schulte-Merker, S., and Baker, D. A. (2010). Control of endothelial sprouting by a Tel-CtBP complex. Nat.Cell Biol. 12:933-942

Ruether, K., van de Pol, D., Jaissle, G., Berger, W., Tornow, R. P., and Zrenner, E. (1997). Retinoschisislike alterations in the mouse eye caused by gene targeting of the Norrie disease gene. Invest Ophthalmol.Vis.Sci. 38:710-718

Ruhrberg, C., Gerhardt, H., Golding, M., Watson, R., Ioannidou, S., Fujisawa, H., Betsholtz, C., and Shima, D. T. (2002). Spatially restricted patterning cues provided by heparin-binding VEGF-A control blood vessel branching morphogenesis. Genes Dev. 16:2684-2698

Rymo, S. F., Gerhardt, H., Wolfhagen, Sand F., Lang, R., Uv, A., and Betsholtz, C. (2011). A two-way communication between microglial cells and angiogenic sprouts regulates angiogenesis in aortic ring cultures. PLoS.One. 6:e15846-

Saint-Geniez, M., Masri, B., Malecaze, F., Knibiehler, B., and Audigier, Y. (2002). Expression of the murine msr/apj receptor and its ligand apelin is upregulated during formation of the retinal vessels. Mech.Dev. 110:183-186

Sapieha, P., Sirinyan, M., Hamel, D., Zaniolo, K., Joyal, J. S., Cho, J. H., Honore, J. C., Kermorvant-Duchemin, E., Varma, D. R., Tremblay, S., Leduc, M., Rihakova, L., Hardy, P., Klein, W. H., Mu, X., Mamer, O., Lachapelle, P., Di, Polo A., Beausejour, C., Andelfinger, G., Mitchell, G., Sennlaub, F., and Chemtob, S. (2008). The succinate receptor GPR91 in neurons has a major role in retinal angiogenesis. Nat.Med. 14:1067-1076

Satchell, S. C., Harper, S. J., and Mathieson, P. W. (2001). Angiopoietin-1 is normally expressed by periendothelial cells. Thromb.Haemost. 86:1597-1598

Sato, T. N., Tozawa, Y., Deutsch, U., Wolburg-Buchholz, K., Fujiwara, Y., Gendron-Maguire, M., Gridley, T., Wolburg, H., Risau, W., and Qin, Y. (1995). Distinct roles of the receptor tyrosine kinases Tie-1 and Tie-2 in blood vessel formation. Nature 376:70-74

Schafer, N. F., Luhmann, U. F., Feil, S., and Berger, W. (2009). Differential gene expression in Ndph-knockout mice in retinal development. Invest Ophthalmol.Vis.Sci. 50:906-916

Schmidt, M., Paes, K., De, Maziere A., Smyczek, T., Yang, S., Gray, A., French, D., Kasman, I., Klumperman, J., Rice, D. S., and Ye, W. (2007). EGFL7 regulates the collective migration of endothelial cells by restricting their spatial distribution. Development 134:2913-2923

Schroder, M. (2006). The unfolded protein response. Mol.Biotechnol. 34:279-290

Scott, A., Powner, M. B., Gandhi, P., Clarkin, C., Gutmann, D. H., Johnson, R. S., Ferrara, N., and Fruttiger, M. (2010). Astrocyte-derived vascular endothelial growth factor stabilizes vessels in the developing retinal vasculature. PLoS.One. 5:e11863-

Seitz, R., Hackl, S., Seibuchner, T., Tamm, E. R., and Ohlmann, A. (2010). Norrin mediates neuroprotective effects on retinal ganglion cells via activation of the Wnt/beta-catenin signaling pathway and the induction of neuroprotective growth factors in Muller cells. J.Neurosci. 30:5998-6010

Sims, K. B., Lebo, R. V., Benson, G., Shalish, C., Schuback, D., Chen, Z. Y., Bruns, G., Craig, I. W., Golbus, M. S., and Breakefield, X. O. (1992). The Norrie disease gene maps to a 150 kb region on chromosome Xp11.3. Hum.Mol.Genet. 1:83-89

Smallwood, P. M., Williams, J., Xu, Q., Leahy, D. J., and Nathans, J. (2007). Mutational analysis of Norrin-Frizzled4 recognition. J.Biol.Chem. 282:4057-4068

Smith, D. F. (1978). Lithium chloride toxicity and pharmacodynamics in inbred mice. Acta Pharmacol.Toxicol.(Copenh) 43:51-54

Stahl, A., Connor, K. M., Sapieha, P., Chen, J., Dennison, R. J., Krah, N. M., Seaward, M. R., Willett, K. L., Aderman, C. M., Guerin, K. I., Hua, J., Lofqvist, C., Hellstrom, A., and Smith, L. E. (2010). The mouse retina as an angiogenesis model. Invest Ophthalmol.Vis.Sci. 51:2813-2826

Stalmans, I., Ng, Y. S., Rohan, R., Fruttiger, M., Bouche, A., Yuce, A., Fujisawa, H., Hermans, B., Shani, M., Jansen, S., Hicklin, D., Anderson, D. J., Gardiner, T., Hammes, H. P., Moons, L., Dewerchin, M., Collen, D., Carmeliet, P., and D'Amore, P. A. (2002). Arteriolar and venular patterning in retinas of mice selectively expressing VEGF isoforms. J.Clin.Invest 109:327-336

Stefater, J. A., Lewkowich, I., Rao, S., Mariggi, G., Carpenter, A. C., Burr, A. R., Fan, J., Ajima, R., Molkentin, J. D., Williams, B. O., Wills-Karp, M., Pollard, J. W., Yamaguchi, T., Ferrara, N., Gerhardt, H., and Lang, R. A. (2011). Regulation of angiogenesis by a non-canonical Wnt-Flt1 pathway in myeloid cells. Nature 474:511-515

Steinle, J. J., Meininger, C. J., Chowdhury, U., Wu, G., and Granger, H. J. (2003). Role of ephrin B2 in human retinal endothelial cell proliferation and migration. Cell Signal. 15:1011-1017

Steinle, J. J., Meininger, C. J., Forough, R., Wu, G., Wu, M. H., and Granger, H. J. (2002). Eph B4 receptor signaling mediates endothelial cell migration and proliferation via the phosphatidylinositol 3-kinase pathway. J.Biol.Chem. 277:43830-43835

Stone, J. and Dreher, Z. (1987). Relationship between astrocytes, ganglion cells and vasculature of the retina. J.Comp Neurol. 255:35-49

Stone, J., Itin, A., Alon, T., Pe'er, J., Gnessin, H., Chan-Ling, T., and Keshet, E. (1995). Development of retinal vasculature is mediated by hypoxia-induced vascular endothelial growth factor (VEGF) expression by neuroglia. J.Neurosci. 15:4738-4747

Suri, C., Jones, P. F., Patan, S., Bartunkova, S., Maisonpierre, P. C., Davis, S., Sato, T. N., and Yancopoulos, G. D. (1996). Requisite role of angiopoietin-1, a ligand for the TIE2 receptor, during embryonic angiogenesis. Cell 87:1171-1180

Takahashi, T., Yamaguchi, S., Chida, K., and Shibuya, M. (2001). A single autophosphorylation site on KDR/Flk-1 is essential for VEGF-A-dependent activation of PLC-gamma and DNA synthesis in vascular endothelial cells. EMBO J. 20:2768-2778

Tammela, T., Zarkada, G., Nurmi, H., Jakobsson, L., Heinolainen, K., Tvorogov, D., Zheng, W., Franco, C. A., Murtomaki, A., Aranda, E., Miura, N., Yla-Herttuala, S., Fruttiger, M., Makinen, T., Eichmann, A., Pollard, J. W., Gerhardt, H., and Alitalo, K. (2011). VEGFR-3 controls tip to stalk conversion at vessel fusion sites by reinforcing Notch signalling. Nat.Cell Biol.

Tammela, T., Zarkada, G., Wallgard, E., Murtomaki, A., Suchting, S., Wirzenius, M., Waltari, M., Hellstrom, M., Schomber, T., Peltonen, R., Freitas, C., Duarte, A., Isoniemi, H., Laakkonen, P., Christofori, G., Yla-Herttuala, S., Shibuya, M., Pytowski, B., Eichmann, A., Betsholtz, C., and Alitalo, K. (2008). Blocking VEGFR-3 suppresses angiogenic sprouting and vascular network formation. Nature 454:656-660

Thurston, G., Noguera-Troise, I., and Yancopoulos, G. D. (2007). The Delta paradox: DLL4 blockade leads to more tumour vessels but less tumour growth. Nat.Rev.Cancer 7:327-331

Tout, S., Chan-Ling, T., Hollander, H., and Stone, J. (1993). The role of Muller cells in the formation of the blood-retinal barrier. Neuroscience 55:291-301

Uemura, A., Ogawa, M., Hirashima, M., Fujiwara, T., Koyama, S., Takagi, H., Honda, Y., Wiegand, S. J., Yancopoulos, G. D., and Nishikawa, S. (2002). Recombinant angiopoietin-1 restores higher-order architecture of growing blood vessels in mice in the absence of mural cells. J.Clin.Invest 110:1619-1628

van Eys, G. J., Niessen, P. M., and Rensen, S. S. (2007). Smoothelin in vascular smooth muscle cells. Trends Cardiovasc.Med. 17:26-30

van Hinsbergh, V. W. and Koolwijk, P. (2008). Endothelial sprouting and angiogenesis: matrix metalloproteinases in the lead. Cardiovasc.Res. 78:203-212

Wang, H. U., Chen, Z. F., and Anderson, D. J. (1998). Molecular distinction and angiogenic interaction between embryonic arteries and veins revealed by ephrin-B2 and its receptor Eph-B4. Cell 93:741-753

Wang, Y., Huso, D., Cahill, H., Ryugo, D., and Nathans, J. (2001). Progressive cerebellar, auditory, and esophageal dysfunction caused by targeted disruption of the frizzled-4 gene. J.Neurosci. 21:4761-4771

Watanabe, T. and Raff, M. C. (1988). Retinal astrocytes are immigrants from the optic nerve. Nature 332:834-837

West, H., Richardson, W. D., and Fruttiger, M. (2005). Stabilization of the retinal vascular network by reciprocal feedback between blood vessels and astrocytes. Development 132:1855-1862

Wong, V. and Gumbiner, B. M. (1997). A synthetic peptide corresponding to the extracellular domain of occludin perturbs the tight junction permeability barrier. J.Cell Biol. 136:399-409

Xia, C. H., Liu, H., Cheung, D., Wang, M., Cheng, C., Du, X., Chang, B., Beutler, B., and Gong, X. (2008). A model for familial exudative vitreoretinopathy caused by LPR5 mutations. Hum.Mol.Genet. 17:1605-1612

Xia, C. H., Yablonka-Reuveni, Z., and Gong, X. (2010). LRP5 is required for vascular development in deeper layers of the retina. PLoS.One. 5:e11676-

Xu, Q., Wang, Y., Dabdoub, A., Smallwood, P. M., Williams, J., Woods, C., Kelley, M. W., Jiang, L., Tasman, W., Zhang, K., and Nathans, J. (2004). Vascular development in the retina and inner ear: control by Norrin and Frizzled-4, a high-affinity ligand-receptor pair. Cell 116:883-895

Xu, S., Cheng, F., Liang, J., Wu, W., and Zhang, J. (2012). Maternal xNorrin, a Canonical Wnt Signaling Agonist and TGF-beta Antagonist, Controls Early Neuroectoderm Specification in Xenopus. PLoS.Biol. 10:e1001286-

Yana, I., Sagara, H., Takaki, S., Takatsu, K., Nakamura, K., Nakao, K., Katsuki, M., Taniguchi, S., Aoki, T., Sato, H., Weiss, S. J., and Seiki, M. (2007). Crosstalk between neovessels and mural cells directs the site-specific expression of MT1-MMP to endothelial tip cells. J.Cell Sci. 120:1607-1614

Ye, X., Smallwood, P., and Nathans, J. (2011). Expression of the Norrie disease gene (Ndp) in developing and adult mouse eye, ear, and brain. Gene Expr.Patterns. 11:151-155

Ye, X., Wang, Y., Cahill, H., Yu, M., Badea, T. C., Smallwood, P. M., Peachey, N. S., and Nathans, J. (2009). Norrin, frizzled-4, and Lrp5 signaling in endothelial cells controls a genetic program for retinal vascularization. Cell 139:285-298

Ye, X., Wang, Y., and Nathans, J. (2010). The Norrin/Frizzled4 signaling pathway in retinal vascular development and disease. Trends Mol.Med.

You, L. R., Lin, F. J., Lee, C. T., Demayo, F. J., Tsai, M. J., and Tsai, S. Y. (2005). Suppression of Notch signalling by the COUP-TFII transcription factor regulates vein identity. Nature 435:98-104

Yu, D. Y. and Cringle, S. J. (2001). Oxygen distribution and consumption within the retina in vascularised and avascular retinas and in animal models of retinal disease. Prog.Retin.Eye Res. 20:175-208

Zuercher, J., Fritzsche, M., Feil, S., Mohn, L., and Berger, W. (2012). Norrin stimulates cell proliferation in the superficial retinal vascular plexus and is pivotal for the recruitment of mural cells. Hum.Mol.Genet.

Web links

Jackson Lab	www.jax.org
Webvision	http://webvision.med.utah.edu/

Appendix 1

Large Deletions including the *NDP* locus

Exon(s)	Mutation on DNA Level	Phenotype	References*
1-3	entire *NDP* deletion, as well as part of *MAOB*, 150 kb	ND	Berger, 1992
1-3	entire *NDP* deletion, as well as *MAOA* and *MAOB*; 2-2.5 Mb	ND	Suarez-Merino, 2001
2-3	partial *NDP* deletion, deletion of *MAOA* and *MAOB*, 340 kb	ND	Berger, 1992
2-3	partial *NDP* deletion, 15-20 kb	ND	Berger, 1992
2-3	partial *NDP* deletion	ND	Schuback, 1995
1	partial *NDP* deletion, 8-15 kb	ND	Berger, 1992
2	partial *NDP* deletion, 2-4 kb	ND	Berger, 1992
2	partial *NDP* deletion, 4kb	ND	Chen, 1993
2	partial *NDP* deletion, 5kb	ND	Chen, 1993
2	partial *NDP* deletion, 2-10kb	ND	Chen, 1993
2	partial *NDP* deletion	ND	Schuback, 1995
3	partial *NDP* deletion; *MAOA* and *MAOB* del >20kb	ND	Chen, 1993
3	partial *NDP* deletion; part of exon 3; 7 kb	ND	Chen, 1993
3	partial *NDP* deletion	ND	Schuback, 1995
3	partial *NDP* deletion	ND	Schuback, 1995
3	partial *NDP* deletion; 3'-UTR of exon 3 inclusive PAS	ND	Rivera-Vega, 2005
	4 different deletions (complete, partial, 4bp and single)	ND	Zhu, 1994
	Xp11.4invq22	ND	Pettenati, 1993

***NDP* mutations in Exons 1 to 3 and introns 1 and 2**

Exon / Intron	DNA Level**	Protein Level**	Phenotype	References*
Exon 1	c.-391_380delinsGTCTCTC	- (5´-UTR)	ROP (4 & 5)	Talks, 2001
Exon 1	c.-386_310del	- (5´-UTR)	ROP (3/5)	Talks, 2001
Exon 1	ins 12 bp (CT repeat)	- (5´-UTR)	ND, ROP (4B & 5)	Hiraoka, 2001; Wu, 2007
Exon 1	ins 10 bp (CT repeat)	- (5´-UTR)	ND	Schuback, 1995
Exon 1	del 14 bp (CT repeat)	- (5-´UTR)	ROP, RS	Hiraoka, 2001; Dickinson, 2006; Wu, 2007
Intron 1	c.-208+1G>A	- (splicing)	ND	Fuchs, 1996
Intron 1	c.-208+2T>G	- (splicing)	ND	Nikopoulos, 2010
Intron 1	c.-208+5G>A	- (splicing)	ND	Nikopoulos, 2010
Exon 2	c.1A>G	p.M1?	ND	Isashiki, 1995; Gal, 1996; Berger unpublished
Exon 2	c.2_3del	p.0?	ND	Caballero, 1996
Exon 2	c.2T>G	p.M1R	ND	Schuback, 1995
Exon 2	c.11_12del	p.H4RfsX21	ND	Nikopoulos, 2010
Exon 2	c.24_27dup	p.F10IfsX17	ND	Berger, 1992
Exon 2	c.25_40del	p.S9PfsX4	ND	Nikopoulos, 2010
Exon 2	c.38T>G	p.L13R	ND	Fuchs, 1994
Exon 2	c.44T>G	p.L15R	ND	Berger unpublished
Exon 2	c.47T>C	p.L16P	ND	Yamada, 2001

Exon 2	c.49delG	p.V17fsX1	ND	Waryah, 2011
Exon 2	c.50dup	p.I18DfsX8	ND	Gal, 1996
Exon 2	c.53T>A	p.I18K	ND, FEVR	Kondo, 2007; Shima, 2009
Exon 2	c.65del	p.T22KfsX10	ND	Schuback, 1995
Exon 2	c.86C>G	p.S29X	ND	Meindl, 1992
Exon 2	c.103del	p.D35TfsX6	ND	Chynn, 1996
Exon 2	c.109C>T	p.R37X	ND	Ott, 2000
Exon 2	c.112C>T	p.R38C	ND, FEVR, PHPV	Royer 2003; Riveiro-Alvarez, 2005
Exon 2	c.115T>C	p.C39R	ND	Joos, 1994; Wu, 2007
Exon 2	c.122G>A	p.R41K	EVR, sporadic	Shastry, 1997
Exon 2	c.123G>C	p.R41S	PFV	Wu, 2007
Exon 2	c.123G>?	p.R41T	ND	Pelcastre, 2010
Exon 2	c.123G>T	p.R41S	PFV	Dhingra, 2006
Exon 2	c.125A>G	p.H42R	FEVR, EVR (sporadic)	Shastry, 1997; Wu, 2007
Exon 2	c.128dup	p.H43QfsX14	ND	Caballero, 1996
Exon 2	c.128A>G	p.H43R	ND	Dickinson, 2006
Exon 2	c.129C>G	p.H43Q	ND	Royer, 2003
Exon 2	c.129delC	p.Y44MfsX60	ND	Nikopoulos, 2010
Exon 2	c.131A>G	p.Y44C	ND	Meindl, 1992
Exon 2	c.131dup	p.Y44X	ND, PHPV, sporadic	Hatsukawa, 2002
Exon 2	c.133G>A	p.V45M	ND	Royer, 2003
Exon 2	c.134T>A	p.V45E	ND, MR	Lev, 2007
Exon 2	c.136del	p.D46IfsX58	ND	Schuback, 1995
Exon 2	c.142_145del	p.I48VfsX55	ND	Zhu, 1994
Exon 2	c.162G>C	p.K54N	ND, FEVR	Hoefsloot, 2000; Kondo, 2007; Boonstra, 2009
Exon 2	c.163T>C	p.C55R	ND	Nikopoulos, 2010
Exon 2	c.170C>G	p.S57X	ND	Berger, 1992
Exon 2	c.174G>T	p.K58N	ND, EVR (sporadic)	Fuentes, 1993; Shastry, 1997
Intron 2	c.174+1G>T	- (splicing)	ND	Berger unpublished
Intron 2	c.174+1G>C	- (splicing)	ND	Fuchs, 1996
Intron 2	c.174+5G>C	- (splicing)	ND	Berger, 1992; Fuchs, 1996
Intron 2	c.175-1G>C	- (splicing)	ND	Royer, 2003
Intron 2	c.175-1G>A	- (splicing)	ND, FEVR	Kondo, 2007
Exon 3	c.179T>A	p.V60E	ND	Meindl, 1992
Exon 3	c.181C>T	p.L61F	ND, VI	Berger, 1992; Rehm, 1997
Exon 3	c.181C>A	p.L61I	FEVR	Wu, 2007
Exon 3	c.182T>C	p.L61P	ND	Schuback, 1995
Exon 3	c.185T>C	p.L62P	ND	Zhu, 1994
Exon 3	c.187G>T	p.A63S	ND	Novelli, 1999
Exon 3	c.188C>A	p.A63D	ND	Schuback, 1995
Exon 3	c.194G>A	p.C65Y	ND	Strasberg, 1995; Wu, 2007
Exon 3	c.195C>G	p.C65W	ND	Schuback, 1995

Exon 3	c.196G>A	p.E66K	PFV (unilateral)	Aponte, 2009
Exon 3	c.199G>A	p.G67R	ND	Nikopoulos, 2010
Exon 3	c.200G>A	p.G67E	ND	Nikopoulos, 2010
Exon 3	c.205del	p.C69AfsX35	ND	Schuback, 1995
Exon 3	c.206G>C	p.C69S	ND	Chen, 1993
Exon 3	c.218C>A	p.S73X	ND	Walker, 1997
Exon 3	c.220C>T	p.R74C	ND, FEVR	Berger, 1992; Fuchs, 1996; Allen, 2006
Exon 3	c.223T>C	p.S75P	ND	Yamada, 2001
Exon 3	c.224C>G	p.S75C	ND	Berger, 1992
Exon 3	c.226G>T	p.E76X	ND	Hutcheson, 2005
Exon 3	c.236_240del	p.S80QfsX67	ND	Riveiro-Alvarez, 2005
Exon 3	c.267C>A	p.F89L	ND	Nikopoulos, 2010
Exon 3	c.267_268insCTC	p.F89_R90insL	ND	Hutcheson, 2005
Exon 3	c.268del	p.R90VfsX14	ND	Lin, 2010
Exon 3	c.268C>T	p.R90C	ND	Royer, 2003
Exon 3	c.269G>C	p.R90P	ND	Berger, 1992
Exon 3	c.274T>C	p.S92P	ND	Nikopoulos, 2010
Exon 3	c.282_283ins8	p.C95MfsX12	ND	Schuback, 1995
Exon 3	c.283T>C	p.P.C95R	ND (severe)	Isashiki, 1995
Exon 3	c.284G>T	p.C95F	ND (severe)	Khan, 2004
Exon 3	c.285C>A	p.C95X	ND (severe)	Wu, 2007
Exon 3	c.287G>A	p.C96Y	ND, EVR (sporadic)	Berger, 1992; Meindl, 1992; Shastry, 1999
Exon 3	c.288C>G	p.C96W	CD	Black, 1999
Exon 3	c.290G>C	p.R97P	ND	Rivera-Vega, 2005; Kondo, 2007
Exon 3	c.291del	p.Q99RfsX5	ND	Berger, 1992
Exon 3	c.293C>T	p.P98L	ND	Nikopoulos, 2010
Exon 3	c.302C>T	p.S101F	ND, PHPV (mild)	Walker, 1997
Exon 3	c.307C>G	p.L103V	FEVR	Dickinson, 2006
Exon 3	c.310A>C	p.K104Q	ND (mild)	Meindl, 1995
Exon 3	c.312G>T	p.K104N	ND	Riveiro-Alvarez, 2006
Exon 3	c.313G>A	p.A105T	ND	Torrente, 1997
Exon 3	c.323T>C	p.L108P	ROP (4B/5)	Shastry, 1997
Exon 3	c.325C>T	p.R109X	ND	Schuback, 1995; Mintz-Hittner, 1996
Exon 3	c.328T>C	p.C110R	ND	Zhu, 1993; Fuchs, 1996
Exon 3	c.328T>G	p.C110G	FEVR	Torrente, 1997
Exon 3	c.328T>A	p.C110S	ND	Berger unpublished
Exon 3	c.330C>A	p.C110X	ND	Berger, 1992
Exon 3	c.332C>A	p.S111X	ND	Nikopoulos, 2010
Exon 3	c.333del	p.G113AfsX149	ND	Hutcheson, 2005
Exon 3	c.335G>A	p.G112E	FEVR (highly variable)	Allen, 2006
Exon 3	c.344G>T	p.R115L	FEVR	Kondo, 2007
Exon 3	c.343C>T	p.R115X	ND	Liu, 2010

Exon 3	c.353C>A	p.A118D	ND	Shastry, 1999
Exon 3	c.359A>G	p.Y120C	EVR (sporadic)	Shastry, 1997
Exon 3	c.360C>A	p.Y120X	ND	Riveiro-Alvarez, 2005
Exon 3	c.360_368del	p.R121_I123del	ND	Schuback, 1995
Exon 3	c.361C>G	p.R121G	ND, PRDX	Zhu, 1994
Exon 3	c.361C>T	p.R121W	ND, ND (mild), FEVR, ROP	Meindl, 1995; Shastry, 1995; Kellner, 1996; Shastry, 1997; Wu, 2007; Pelcastre, 2010
Exon 3	c.362G>A	p.R121Q	ND, ND (mild), FEVR	Fuentes, 1993; Meindl, 1995; Riveiro-Alvarez, 2005; Boonstra, 2009; Pelcastre, 2010
Exon 3	c.362G>T	p.R121L	FEVR (highly variable)	Johnson, 1996; Mintz-Hittner, 1996
Exon 3	c.365A>T	p.Y122W	FEVR	Lucas Mohn unpublished
Exon 3	c.368T>A	p.I123N	ND	Schuback, 1995
Exon 3	c.370C>T	p.L124F	FEVR	Chen, 1993
Exon 3	c.377G>C	p.C126S	ND	Gal, 1996
Exon 3	c.378T>A	p.C126X	ND	Fuchs, 1996; Keller, 1996
Exon 3	c.382T>C	p.C128R	ND	Royer, 2003
Exon 3	c.383_384del	p.C128X	ND	Wong, 1993; Hutcheson, 2005
Exon 3	c.384C>A	p.C128X	ND	Schuback, 1995
Exon 3	c.397del	p.S133PfsX129	ND	Berger, 1992
Exon 3	c.399del	p.X134EfsX128	ND	Riveiro-Alvarez, 2008
Exon 3	c.*716T>C	p.?	FEVR	Wu, 2007

* Most of the cited references have multiple authors. For lack of space, only the last name of the first author of the respective publication was included.

** Nomenclature was edited according to recommendations of the Human Genome Variation Society (http://www.hgvs.org/).

Appendix 2

Summary of the most prominent features of the syndromes described above

		ND	EVR	CD	ROP	OPPG	PHPV
affected gene	NDP	x	x	x	x		x
	FZD4		x				
	LRP5		x			x	
	TSPAN12		x				
mode of inheritance	X-linked recessive	x					
	autosomal dominant		x				x
	autosomal recessive		x			x	x
	sporadic		x	x			
affected organ	ear	x					
	brain	x				(x)	
	eye	x	x	x	x	x	x
	bone					x	
occurrence	unilateral			x			x
	bilateral	x	x	(x)	x	x	(x)
clinical symptoms	subretinal exudation	x	x	x			
	intraretinal exudation			x			
	retinal detachment	x	x	x	x		
	pseudoglioma	x				x	
	neovascularisation		x		x		
	vitreus hemorrhage	x	x				
	retinal folds	x	x		x		
	leukokoria	x	x				x
	phthisis bulbi	x					
	massed fractures					x	
	persistent tunica vasculosa lentis						x
	osteoporosis					x	
	muscular hypotonia					x	
	ligamentous lataxy					x	
	hyperplasia of vitreous					x	
	microphthalmos	x					x
	nystagmus	(x)					(x)
	corneal opacities	x				x	(x)
	cataract	x					x
	secondary glaucoma	x				x	x
clinical consequences	impaired vision	x	x	x	x	x	x
	progressive blindness		x	x	x		x
	congenital blindness	x	x				(x)
	progressive deafness	x					
	mental retardation	x				(x)	

CD = Coats' Disease, ND = Norrie Disease, EVR = Exudative Vitreoretinopathy, PHPV = Persistent Hyperplastic Primary Vitreous; OPPG = Osteoporosis-pseudoglioma syndrome; x = common feature in affected individuals; (x) = rarely observed; for references consider the respective chapter about the disease; (adapted from Masterthesis Jurian Zürcher, 2008).

Appendix 3

Descriptive Statistics of investigated C56BL/6J mouse population

		Frequency	Percent
all stages	male	167	48.7
	female	176	51.3
	wildtype	154	44.9
	heterozygous	102	29.7
	knockout	87	25.4
	total	343	100
P5	male	32	47.7
	female	35	52.3
	wildtype	25	37.3
	heterozygous	24	35.8
	knockout	18	26.9
	total	67	100
P7	male	32	47.7
	female	35	52.3
	wildtype	28	41.8
	heterozygous	19	28.4
	knockout	20	29.8
	total	67	100
P9	male	40	55.5
	female	32	44.5
	wildtype	38	52.8
	heterozygous	19	26.4
	knockout	15	20.8
	total	72	100
P12	male	34	47.9
	female	37	52.1
	wildtype	37	52.1
	heterozygous	21	29.6
	knockout	13	18.3
	total	71	100
P21	male	29	43.9
	female	37	56.1
	wildtype	26	39.4
	heterozygous	19	28.7
	knockout	21	31.9
	total	66	100

Weight differences depending on sex and stage

	male			female			
	AV	STDEV	CI	AV	STDEV	CI	p-value
P5	3.1	0.4	0.1	3.0	0.4	0.1	0.594
P7	4.0	0.6	0.2	3.9	0.6	0.2	0.546
P9	4.8	0.8	0.3	5.0	0.9	0.3	0.297
P12	6.2	1.0	0.3	5.8	0.9	0.3	0.12
P21	9.0	1.0	0.4	9.1	0.9	0.3	0.529

PX = Postnatal day X; AV = average; STDEV = standard deviation; CI = confidence interval (α=0.05)

Weight difference depending on genotype per stage

	wt			het			ko			p-values		
	AV	STDEV	CI	AV	STDEV	CI	AV	STDEV	CI	wt - het	wt - ko	het - ko
P5	3.1	0.3	0.1	3.0	0.5	0.2	3.0	0.4	0.2	0.587	0.454	0.866
P7	4.0	0.7	0.3	3.9	0.2	0.2	3.9	0.6	0.3	0.692	0.775	0.907
P9	4.8	0.7	0.2	5.0	1.0	0.4	5.0	1.0	0.6	0.313	0.458	0.859
P12	6.0	1.0	0.3	5.9	0.8	0.3	6.3	1.0	0.6	0.586	0.309	0.212
P21	8.8	0.9	0.4	9.1	0.9	0.4	9.2	1.0	0.4	0.340	0.136	0.613

PX = Postnatal day X; AV = average; STDEV = standard deviation; CI = confidence interval (α=0.05); wt = wildtype; het = heterozygous; ko = knockout

Weight differences between different mice litters

litter	AV	STDEV	CI	litter	AV	STDEV	CI
1	3.1	0.4	0.3	21	6.7	0.6	0.5
2	3.0	0.2	0.1	22	4.1	0.4	0.4
3	3.6	0.3	0.3	23	4.2	0.2	0.2
4	3.4	0.4	0.4	24	5.3	0.3	0.2
5	3.1	0.1	0.1	25	7.3	0.5	0.7
6	2.6	0.2	0.2	26	4.3	0.5	0.5
7	3.1	0.1	0.1	27	6.6	0.8	0.6
8	2.6	0.2	0.2	28	6.3	0.3	0.2
9	4.3	0.3	0.3	29	6.6	0.8	0.6
10	4.4	0.1	0.1	30	6.3	0.3	0.2
11	3.1	0.2	0.2	31	5.3	0.5	0.4
12	3.4	0.3	0.2	32	5.3	0.4	0.3
13	4.1	0.4	0.3	33	8.5	0.4	0.3
14	4.8	0.2	0.2	34	10.0	0.5	0.4
15	3.4	0.3	0.2	35	8.5	0.6	0.4
16	4.2	0.4	0.3	36	9.7	0.3	0.4
17	4.9	0.2	0.2	37	9.9	0.5	0.5
18	4.4	0.8	0.6	38	9.8	0.6	0.6
19	4.9	0.4	0.2	39	8.9	1.0	0.8
20	4.5	0.3	0.2	40	8.1	0.7	0.6

AV = average; STDEV = standard deviation; CI = confidence interval (α=0.05);

Average weight of mice dependent on stage

	AV	STDEV	CI
P5	3.1	0.4	0.1
P7	4.0	0.6	0.1
P9	4.9	0.9	0.2
P12	6.0	0.9	0.2
P21	9.0	0.9	0.2

PX = Postnatal day X; AV = average; STDEV = standard deviation; CI = confidence interval (α=0.05);

Appendix 4

Quantification by independent samples t-test of morphometric data from wildtype and *NDPh*$^{y/-}$ retinas

		wildtype retinas	*NDPh*$^{y/-}$ retinas
P5	Number of filopodia	23 ± 2 (n=5)	32 ± 5 (n=6; p-value = 0.001)
	Vascular density	42 ± 5 (n=5)	30 ± 4 (n=5; p-value = 0.002)
	Number of branchpoints	30 ± 1 (n=5)	14 ± 3 (n=5; p-value =0.0001)
P7	Number of filopodia	21 ± 3 (n=4)	29 ± 2 (n=7, p-value =0.0001)
	Vascular density	48 ± 4 (n=5)	32 ± 3 (n=7; p-value = 0.0006)
	Number of branchpoints	89 ± 7 (n=5)	47 ± 8 (n=7; p-value =0.0001)

average ± standard deviation are reported; n= number of retinas; P-values below α=0.05 are considered to be statistically significant.

Appendix 5

Zuercher J, Neidhardt J, Magyar I, Labs S, Moore AT, Tanner FC, Waseem N, Schorderet DF, Munier FL, Bhattacharya S, Berger W, Kloeckener-Gruissem B (2010). Alterations of the 5'untranslated leader region of *SLC16A12* lead to age-related cataract. *Invest Ophthalmol Vis Sci* 51:3354-3361

Own contributions: I cloned the constructs used in the luciferase reporter assay, conducted the luciferase reporter assay, did the RNA in silico analysis, designed the figures and wrote and edited the paper.

Curriculum vitae

Personal Data

Name	Jurian Zuercher
Address	Huendlerstrasse 57, 8406 Winterthur
Date of birth	February 14th 1978
Place of birth	Winterthur, Switzerland
Place of origin	Madiswil (BE), Switzerland
Nationality	Swiss

Academic Education

2008 - present	PhD in Biology Institute of Medical Molecular Genetics, University of Zurich, Switzerland; Prof. Dr. Wolfgang Berger *Molecular mechanisms of sprouting angiogenesis in the retina: crosstalk between Notch and Norrin signaling.*
2008 – present	International Ph.D. Program in Neuroscience Neuroscience Center Zurich, University and ETH Zurich, Switzerland
2007 - 2008	Master in Neurosciences Institute of Medical Molecular Genetics, University of Zurich, Switzerland; Prof. Dr. Wolfgang Berger *Part 1: Analysis of transcriptional regulatory elements of NDP, FZD4 and LRP5* *Part 2: FZD4 mutation screening in patients diagnosed with exudative vitreoretinopathies*
2004 - 2007	Bachelor in Biology, University of Zurich, Switzerland
1998 – 2001	Bachelor in Bioengineering (financed by F. Hoffmann – La Roche Foundation scholarship) Department of Biochemistry, University of Applied Science Winterthur, Switzerland; Prof. Dr. Christiane Zaborosch

Work Experience

2005	Hight-troughput DNA sequencing Synergene GmBH, Schlieren, Switzerland
2002 - 2004	Screening for tumor supressors and oncogenes in Drosophila melanogaster The Genetics Company, Schlieren, Switzerland Prof. Dr. Ernst Hafen, Prof. Dr. Konrad Basler
1997 – 1998	Parallel synthesis of organic compounds for Parkinson Disease screening program Pharma Division, F. Hoffmann – La Roche AG, Basel, Switzerland Dr. Alexander Alanine

Additional Qualification

2008	Labortierkundekurs Modul 1 Vet Suisse, Switzerland
2003	Strahlenschutz Sachverständigenkurs für B und C Labors Federal Office of Public Health, Switzerland

Vocational Education

1994 – 1997	Apprenticeship as lab assistant in organic chemistry (graduate with honors) Vitamin Division, F. Hoffmann – La Roche AG, Basel, Switzerland Mr. Bruno Burdet and Dr. August Rüttimann
1994 – 1997	Technische Berufsmatura (vocational matura) Allgemeine Gewerbeschule Basel, Switzerland

Awards

Retina Suisse Award for best presentation and project, Swiss Eye Research Meeting, Biel, 26.-27.01.2012

Publications

Jurian Zuercher, John Neidhardt, István Magyar, Stephan Labs, Anthony T Moore, Felix Tanner, Naushin H Waseem, Daniel Schorderet, Francis L Munier, Shomi S Bhattacharya, Wolfgang Berger, and Barbara Kloeckener-Gruissem (2010). Alterations of the 5'untranslated leader region of SLC16A12 lead to age-related cataract. *Invest Ophthalmol Vis Sci 51(7):3354-61*

Jurian Zuercher, Martin Fritzsche, Silke Feil, Lucas Mohn, Wolfgang Berger (2012). Norrin stimulates cell proliferation in the superficial retinal vascular plexus and is pivotal for the recruitment of mural cells. *Hum Mol Genet* (Epub ahead of print)

Conferences/Scientific meetings

Talks:

Jurian Zuercher, John Neidhardt, István Magyar, Stephan Labs, Anthony T Moore, Felix Tanner, Naushin H Waseem, Daniel Schorderet, Francis L Munier, Shomi S Bhattacharya, Wolfgang Berger, and Barbara Kloeckener-Gruissem. *Point Mutations in the Monocarboxylate Transporter SLC16A12 Lead to Juvenile and Age-related Cataract.* Young Researcher Vision Camp, Leibertingen, Germany, June 25th-27th 2010

Jurian Zuercher, Martin Fritzsche, Silke Feil, Lucas Mohn, Wolfgang Berger. *The Role of Norrin in Retinal Blood Vessel Development.* Retina Meeting, Zurich, Switzerland, October 27th 2010

Jurian Zuercher, Martin Fritzsche, Silke Feil, Lucas Mohn, Wolfgang Berger. *The Role of Norrin in Retinal Blood Vessel Development.* Swiss Eye Research Meeting, Biel, Switzerland, January 27th-28th 2011

Jurian Zuercher, Martin Fritzsche, Silke Feil, Lucas Mohn, Wolfgang Berger. *Norrin stimulates proliferation of the superficial retinal vascular plexus and is pivotal for the recruitment of mural cells.* Swiss Eye Research Meeting, Biel, Switzerland, January 26th-27th 2012

Poster presentations:

Jurian Zuercher, John Neidhardt, István Magyar, Stephan Labs, Anthony T Moore, Felix Tanner, Naushin H Waseem, Daniel Schorderet, Francis L Munier, Shomi S Bhattacharya, Wolfgang Berger, and Barbara Kloeckener-Gruissem. *Point Mutations in the Monocarboxylate Transporter SLC16A12 Lead to Juvenile and Age-related Cataract.* ZNZ PhD Retreat Valens, Switzerland, May 13th-15th 2010